TAMPERE UNIVERSITY OF TECHNOLOGY

JENNI KOSKELA

LIGHT-INDUCED BIOMATERIAL MICROFABRICATION FOR ADVANCED CELL CULTURING – A COMPARATIVE STUDY

Master of Science Thesis

Examiners: Professor Minna Kellomäki and Researcher Niina Ahola
Examiners and topic approved in the Faculty of Automation, Mechanical and Materials Engineering council meeting on November 4, 2009

ABSTRACT

TAMPERE UNIVERSITY OF TECHNOLOGY
Master's Degree Programme in Materials Science
KOSKELA, JENNI: Light-induced biomaterial microfabrication for advanced cell culturing – a comparative study
Master of Science Thesis, 101 pages, 2 Appendix pages
June 2010
Major: Biomaterials
Examiners: Researcher Niina Ahola, Professor Minna Kellomäki
Keywords: microfabrication, two-photon polymerization, photopolymer, photocrosslinking, poly(ethylene glycol) hydrogel, polycaprolactone

The integration of microfluidics, microfabrication technologies and biomaterials has established new means to mimic the natural microenvironment of cells. Using microfluidic culture devices, cells can be stimulated with both mechanical and chemical cues. Light, in the form of UV lamps and lasers, is a powerful microfabrication tool for biomedical applications, offering high resolution and fast production. Special photocurable materials have been developed to meet the needs of this technology. The first part of this thesis is a literature review on this research field, focusing especially on microfabrication using lasers and photosensitive hydrogels in cell-based applications.

Recently, photopolymerization by non-linear light absorption has been introduced to microfabrication, breaking the resolution boundaries set by classical optics. This phenomenon is utilized in two-photon polymerization (2PP), a method for the rapid freeform fabrication of 3D micro- and nanostructures. The basic theory of 2PP is provided in the literature review. Unfortunately, 2PP has mainly been studied with common photoresists and investigation of suitable synthetic biomaterials for the biomedical applications of 2PP has remained insufficient. The latter part of this thesis presents an innovative and scientifically original study that aims to widen the selection of 2PP processable biomaterials. In the experiments, 2PP was investigated with a commercial photoinitiator (PI) and two biomaterials: a novel polycaprolactone-based oligomer (PCL-o) and a poly(ethylene glycol) hydrogel (PEGda). PCL-o is a novel photopolymer synthesized for research purposes and has never been used in 2PP; moreover, 2PP of PEGda with the laser type used has not been reported previously.

In the study, the two materials were compared in terms of resolution and overall 2PP processability. Using a custom-built fabrication setup based on an affordable Nd:YAG laser, arbitrary microstructures were polymerized on glass substrates and subsequently characterized using SEM imaging. Additionally, the effect of PI concentration on resolution was investigated. Cytotoxicity of the sample materials was tested in order to estimate the applicability of the fabricated microstructures in cell-based applications.

The outcome of this study was a success, since 2PP of both PEGda and PCL-o was successfully demonstrated and the Nd:YAG laser proved adequate for the research of novel biomaterial microstructures; resolution in the order of one micrometer was achieved with PCL-o. Based on the cytotoxicity tests, both PEGda and PCL-o were found non-cytotoxic and suitable e.g. for use in guided cell growth. Despite some differences in the fabrication process, the processability of PEGda and PCL-o was found equally well suited for 2PP and research with these materials should definitely be continued in the future. The versatility of the current fabrication system could be improved by experimenting different new photocrosslinkable oligomers, more efficient PIs, optimized equipment, sterilization of the microstructures and cell culturing.

TIIVISTELMÄ

TAMPEREEN TEKNILLINEN YLIOPISTO
Materiaalitekniikan koulutusohjelma
KOSKELA, JENNI: Biomateriaalien valomikrovalmistus soluviljelysovelluksissa – vertaileva tutkimus
Diplomityö, 101 sivua, 2 liitesivua
Kesäkuu 2010
Pääaine: Biomateriaalitekniikka
Tarkastajat: Professori Minna Kellomäki ja tutkija Niina Ahola
Avainsanat: mikrovalmistus, kaksifotonipolymeraatio, valopolymeeri, valosillotus, polyetyleeniglykoli, hydrogeeli, polykaprolaktoni

Biomateriaalien mikrovalmistusmenetelmien kehittymisen myötä voidaan valmistaa yhä paremmin solujen luonnollista mikroympäristöä mimikoivia kasvatusalustoja, joissa soluja stimuloidaan sekä mekaanisin että kemiallisin signaalein mikrofluidistiikan avulla. UV-lamppuja ja lasereita hyödyntävä valoavusteinen mikrovalmistus on yksi kehittyneimmistä menetelmistä tällaisiin sovelluskohteisiin ja menetelmää varten on kehitetty myös uusia valokovettuvia biomateriaaleja. Tämän diplomityön ensimmäinen osa on laaja kirjallisuusselvitys, joka käsittelee mikrofluidistiikan, valoavusteisen mikrovalmistuksen ja biomateriaalien hyödyntämistä soluviljelysovelluksissa. Työssä syvennytään lasermikrovalmistukseen ja valosillottuvien hydrogeelien mikrokuvioitiin.

Uusi trendi mikrovalmistuksessa on valon epälineaariseen absorptioon perustuvat menetelmät, joissa päästään nanometriluokan resoluutioon. Yksi niistä on kaksifotonipolymeraatio (2PP), 3D-mikrovalmistukseen sopiva pikamallinnusmenetelmä, jolla voidaan valmistaa mielivaltaisia mikro- ja nanokuvioita. Menetelmän teorian pääpiirteet esitellään kirjallisuusselvityksessä. Biosovelluksissa 2PP:n suurin rajoite on se, että pääsääntöisesti menetelmää on tutkittu perinteisillä fotoresisteillä ja bioyhteensopivien synteettisten materiaalien tutkimus on ollut puutteellista. Tässä työssä tehdyn tieteellisen tutkimuksen tarkoitus oli kokeilla ja esitellä 2PP:oon sopivia biomateriaaleja, joista voidaan valmistaa soluyhteensopivia mikrorakenteita. 2PP-menetelmää tutkittiin polyetyleeniglykolihydrogeelillä (PEGda) sekä uudella polykaprolaktonipohjaisella oligomeerilla (PCL-o) käyttäen kaupallista fotoinitiaattoria. PCL-o on synteettinen biohajoava polymeerimateriaali, jota ei ole ennen testattu 2PP:ssa; myöskään PEGda:n 2PP-valmistusta käytetyllä lasertyypillä ei ole aiemmin raportoitu.

Tutkimuksessa vertailtiin PEGda:n ja PCL-o:n sopivuutta 2PP-valmistukseen resoluutio ja prosessoitavuus huomioon ottaen. Itsekoottua Nd:YAG-laseriin perustuvaa tietokoneohjattua laitteistoa käyttäen lasialustalle polymeroitiin mikrokuvioita, jotka karakterisoitiin pyyhkäisyelektronimikroskoopilla. Työssä tutkittiin myös initiaattorikonsentraation vaikutus resoluutioon. Näytemateriaaleille tehtiin sytotoksisuuskokeet, joiden avulla arvioitiin valmistettujen mikrorakenteiden sopivuus biosovelluksiin.

Onnistuneeksi osoittautuneen tutkimuksen mukaan sekä PEGda:n että PCL-o:n prosessoitavuus 2PP:ssa oli riittävä ja käytetty laserlaitteisto soveltui tarkoitukseen hyvin; PCL-o:lla saatiin jopa 1 µm:n resoluutio. Sytotoksisuustestien perusteella molemmat materiaalit ovat ei-toksisia ja siten soveltuvat erilaisiin soluviljelysovelluksiin. Vaikka materiaalien välillä ilmeni valmistusprosessissa joitakin eroja, tämän tutkimuksen perusteella molempien materiaalien testaamista 2PP:ssa tulee ehdottomasti jatkaa. Tulevaisuudessa menetelmän käytettävyyttä voisi parantaa mm. testaamalla useampia uusia materiaaleja, tehokkaampia fotoinitiaattoreita, optisesti laadukkaampaa laitteistoa, mikrorakenteiden sterilointia sekä soluviljelyä polymeroiduilla rakenteilla.

Preface

This Master of Science thesis was done in the Biomaterials research group at the Department of Biomedical Engineering at Tampere University of Technology. The work was associated with the STEMFUNC-project, which is a joint project of TUT and the Regea Institute for Regenerative Medicine, and is funded by Academy of Finland.

I would like to thank Professor Minna Kellomäki for examining my thesis. I am grateful for getting such an interesting thesis subject that also suits my studies exceptionally well. I also thank my supervisor M.Sc. (Eng.) Niina Ahola for constantly encouraging and supporting me during the project, as well as for giving constructive criticism on my thesis. Special thanks to M.Sc. (Eng.) Sanna Turunen for practical guidance and supporting companionship throughout the project.

I wish to give special thanks also to other people who took part in the project. I gratefully thank researchers at the Laboratory of Polymer Technology in TKK for providing me with raw material and useful comments. I acknowledge the essential help of Research Professor Jouko Viitanen at VTT for advice and laser equipment expertise. In addition, I thank B.Sc. Sanna Siljander for SEM imaging and help at the laboratory and M.Sc. Laura Ylä-Outinen for the cytotoxicity testing. Furthermore, I wish to thank everyone at the Biomaterials research facility in Hermia who gave me altruistic help at any situation and made my work enjoyable by their company and the pleasant discussions.

Finally, I would like to compliment my husband Seppo for his love and support during this work and my studies, and for encouraging me to always strive for better. I also express my gratitude to my parents and my grandmother, who have always believed in my success. Special thanks to my friends for support and for fulfilling my free time with fun and laughter.

20.5.2010, Tampere

Jenni Koskela

Tel. +358443742441

TABLE OF CONTENTS

TERMS AND ABBREVIATIONS

Δt	Laser pulse width
σ_2 or σ_{TPA}	Two-photon absorption cross-section
1PA	Single-photon absorption
1PP	Single-photon polymerization
2D	Two-dimensional
2PA	Two-photon absorption
2PP	Two-photon polymerization
3D	Three-dimensional
BSA	Bovine Serum Albumine, a natural protein
CAD	Computer-aided design
CCD	Charge-Coupled-Device
CLiPP	Contact lithographic photopolymerization
E	Laser pulse energy
f	Laser pulse frequency
GM	Göppert-Meyer, a commonly used unit for 2PA cross-section; 1 GM equals 10^{-50} cm^4 s $photon^{-1}$
IPG	Inorganic-organic polysiloxane polymer by RPO Inc.
Irgacure® 127	An α-hydroxyketone type UV photoinitiator, 2-hydroxy-1-{4-(2-hydroxy-2-methyl-1-phenyl-1-propanoyl)-phenyl}-2-methyl-1-propanone
UV	Ultraviolet; electromagnetic radiation at wavelengths within the range of 10–400 nm
UV-nil	UV-nanoimprint lithography
LIGA	A fabrication process that produces metallic molds of high aspect ratio microstructures for cast molding of polymers, for example. The abbreviation LIGA stands for German words for lithography, electroplating and molding (lithographie, galvanoformung, abformung)
LN1	Urethane acrylate based photoresist by Sartomer
MEMS	Microelectromechanical system
MMA	Methyl methacrylate
MPA	Multi-photon absorption

NA	Numerical aperture of an objective lens
NOA63	Mercapto-ester polyurethane material by Norland Products
Nopcocure 800	Acrylic acid ester material by San Nopco
Oligomer	Consists of a limited number of monomer units
Ormocer®	Organically modified ceramic; an inorganic-organic hybrid material by Fraunhofer Institute Silicatforschung
Ormodev®	50:50 mixture of 4-methyl-2-penthanone and 2-propanol
PAG	Photoacid generator; a molecule that produces acidic species upon light exposure
P_{avg}	Average laser power
PC	Polycarbonate
TMC	Trimethylenecarbonate
PCL	Polycaprolactone
PDMS	Poly(dimethyl siloxane)
PEGdma	Poly(ethylene glycol) dimethacrylate
PEGMA	Poly(ethylene glycol) methacrylate
PEN	Poly(ethylene naphthalene)
PEO	Poly(ethylene oxide)
PET	Poly(ethylene terephtalate)
PGS	Poly(glycerol sebacate)
PLA	Polylactide
PLGA	poly(lactide-co-glycolide)
PMMA	Poly(methyl methacrylate)
P_{peak}	Peak laser power
PS	Polystyrene
PVA	Poly(vinyl alcohol)
PVC	Poly(vinyl chloride)
SCR500	Urethane acrylate based photoresist by Japan Synthetic Rubber Co.
SEM	Scanning electron microscopy/microscope

SFF	Solid freefrom fabrication
Si	Silicon
SR348	Ethoxylated (2) bisphenol A dimethacrylate by Sartomer
SU-8	Epoxy-based negative-tone photoresist by MicroChem
T	Cycle time, the inverse value of laser pulse frequency *f*
TBNVP	3-(t-butoxycarbonyl)-N-vinyl-2-pyrrolidone
t-BOC	*t*-butoxycarbonyl group
TEGDA	Tri(ethyleneglycol) diacrylate
Ti	Titanium
Hydrogel	Highly crosslinked hydrophilic polymer network of high water content
Laser	Light amplification by the stimulated emission of radiation; a source of electromagnetic radiation at particular wavelengths produced by the stimulated emission of atoms or molecules
Microfabrication	Fabrication of small structures, parts or patterns of dimensions in the micrometer scale
Microfluidic biomaterial	A biomaterial with an embedded network of microfluidic channels
Microfluidics	A system, method or a device that manipulates very small (10^{-9} to 10^{-18} litres) amounts of fluids
Monomer	A small molecule that is capable of forming covalent bonds to other monomers to form a polymer
Photocleavage	Light-initiated breaking of chemical bonds
Photocrosslinking	A light-induced chemical process in which relatively large molecules become covalently bonded to produce a three-dimensional network structure
Photocuring	Light-induced solidification of a photosensitive polymer solution
Photodecomposition	Light-induced breaking of chemical bonds without thermal melting or vaporization
Photoinitiator	A low-molecular-weight chemical compound that forms reactive species upon exposure to light of a specific wavelength

Photolysis	see *Photocleavage*
Photomask	A thin patterned sheet that allows light to pass through only in desired regions
Photopolymerization	Polymerization initiated by light
Photoresist	A light-sensitive polymer, that either cures or undergoes photocleavage under exposure to light
Photosensitizer	A chemical compound that is readily capable of light absorption and subsequent energy transfer to another molecule, thus making the reaction mixture more sensitive to light
Polymerization	A chemical process in which monomers are covalently bonded to produce a large chainlike or network molecule, called a polymer
Quantum yield	In photoinitiation, the ratio between the amount of initiating species produced and the amount of photons absorbed
Rapid prototyping	Automatic construction of physical objects using solid freeform fabrication
Scaffold	In tissue engineering, a support structure for cells and tissues made of a biomaterial
Stereolithography	A laser-based SFF technique for rapid prototyping
Tissue engineering	Production and development of biological substitutes of either natural or synthetic origin, which restore, maintain, or improve tissue function or a whole organ
Two-photon absorption	Atom or a molecule is excited from a lower quantum state to an excited state of the same parity in a single step via simultaneous absorption of two photons
Two-photon absorption cross-section	The measure of a materials susceptibility to 2PA
Two-photon polymerization	Polymerization induced by two-photon absorption
Voxel	A volumetric pixel

1. INTRODUCTION

Macroscale cell culturing devices such as traditional Petri dishes have numerous drawbacks representing physiological systems, as their operating volumes, lengths and time scales are inordinately large. In reality, biological phenomena occur within micro- and nanometer scale. For example, most eukaryotic cells, when attached and spread, have dimensions of 10–100 μm. Novel microscale cell culturing technologies have been developed to overcome these fundamental problems. In particular, the incorporation of different microfabrication techniques and microfluidics is currently of main interest in many research groups in the field of biomedical engineering. [155]

Microfabricated microfluidic cell culture platforms can be used to create a biomimetic environment for cells and also to control and monitor events and parameters of the culture more precisely than with traditional culturing devices. The incorporation of microfluidic channels in the culture matrix is essential for providing cells with fresh medium and a waste disposal system on a steady-state basis. Additionally, it is possible to create chemical gradients by varying the composition of culture medium within the channel network. Furthermore, cells can be stimulated with mechanical and electrical cues. To date, many different cell types including endothelial cells, hepatocytes, neurons and stem cells have been successfully cultured long-term using microfluidic devices. [23, 45]

The lack of abundant source of viable and healthy cells remains a barrier in the field of regenerative medicine. As an alternative to traditional cell sources obtained from mature human or animal tissue, stem cells from both adult and embryonic tissue hold great potential for tissue engineering. Temporal and spatial manipulation of the chemical environment of the culture allows the behavior of stem cells, such as proliferation and differentiation, to be controlled. Thus, one of the main targets of microscale fabrication and microsystems technology is to engineer microenvironments for stem cell culturing. Current research is focused on developing microfabricated bioreactors that stimulate stem cells with both mechanical and biochemical cues. [12, 38]

When it comes to the methods of microfabrication, light-induced polymerization, crosslinking and molecule cleavage have been vastly utilized. Special polymers with optimal bonding or scission characteristics have been developed to meet the needs of special applications and fabrication technologies. With respect to microfluidic devices, photofabrication has many advantages over other technologies. These advantages include fast curing rates and high control spatially and temporally, as well as the important ability to encapsulate living cells within the material during *in situ*

polymerization. Photofabrication can be carried out in ambient conditions, physiological temperature and pH with minimal heat production. [106] For these interests, novel photosensitive biomaterials have been developed to meet the demands of both the biomedical application and the fabrication method [8].

The outline of this thesis consists of two parts: the first part is a literature review, and the second part presents an experimental study. The main objective of the literature review is to aggregate the advances in cell culturing from fields of microfluidics, microfabrication and photosensitive biomaterials. After a general introduction to these topics, special focus will be set on laser-based microfabrication by a novel technology called two-photon polymerization and microfabrication of photosensitive hydrogels. In the end of the literature review, outlook on future themes for research will be shortly discussed.

In the experimental study, the two-photon polymerization technology is used to study the polymerization of two photopolymers into variable microstructures. Introduction to this method is provided in the literature review, but a detailed discussion of all the theoretical aspects of two-photon polymerization is beyond the extent of this thesis. For those interested, extensive information can be found in the recent advisable reviews by Lee *et al.* [75, 76] and Wu *et al.* [159].

This thesis was done as part of a multi-disciplinary project, STEMFUNC, a joint project between Tampere University of Technology and Regea Institute of Regenerative Medicine, funded by Academy of Finland. The project aims to develop a biomimetic, multifunctional culturing platform for stem cell derived neurons and cardiomyocytes by combining engineering expertise in biomaterial technology, modeling, signal processing, microsensors, microfluidics and microactuator technology. The theoretical part of this thesis aims to suit the interests of the project, thus was not merely focused on the 2PP technology used in the experimental study. Another reason for this slight inconsistency between the two parts is that another Master of Science thesis previously written at the Department of Biomedical Engineering (*Käpylä, E. Two-photon polymerized hybrid polymer-ceramic microstructures*) already covered all aspects of 2PP, and re-writing the theory would not have been reasonable.

The goal of the experimental part is to study the adaptability of laser-induced polymerization to two specific photosensitive biomaterials: a novel methacrylated poly-ε-caprolactone-based oligomer and polyethylene glycol diacrylate (PEGda) hydrogel. Using a commercial photoinitiator, a comparison of processability between these materials will be made considering the whole microfabrication process. The study will consist of (1) determining the most important equipment-related parameters, (2) studying resolution and the effect of photoinitiator concentration on resolution, (3) polymerizing arbitrary microstructures with various geometries and (4) studying cell behavior on photopolymerized samples. Based on these results, the potential use of the polymerized structures in stem cell culturing and other biomedical applications will be discussed. In the end of the latter part of the thesis, conclusions will be drawn from the results gained, and suggestions for future research will be made.

LITERATURE REVIEW

2. MICROFABRICATION AND MICROFLUIDICS IN BIOMEDICAL APPLICATIONS

2.1. Microfluidics in general

The term microfluidics refers to a system, method or a device that manipulates very small (10^{-9} to 10^{-18} liters) amounts of fluids. In microfluidic devices, fluid flows are processed in microchannels having dimensions of tens to hundreds of micrometers. [79] Microfluidics is often related very closely to terms like lab-on-a-chip (LoC) and micro-total-analysis-system (μTAS). The explanations of these terms proposed by Lee and Lee [79] are presented in Table 2.1.

Table 2.1. *Terminology in microfluidics. Reproduced with modifications from [79].*

Microfluidics	Transporting and manipulating minute amounts of fluid through microchannels on the chips
Micro total analysis systems (μTAS)	Miniaturization of an overall analytical process from sample preparation through reaction and separation to detection
Lab-on-a-chip	A microfabricated device, integrating several laboratory processes on a single chip

Microfluidics technology has developed dramatically since the 1950's, when the first efforts to dispense small amounts of fluids in the nanometer range were made, enabling the development of today's ink-jet technology [49]. Terry *et al.* [148] set a milestone in 1979 realizing a miniaturized gas chromatograph on a silicon wafer. Since those days, the number of microfluidic applications has increased exponentially. In 2004, Ducrée and Zengerle published a comprehensive study, *Microfluidics Roadmap for the Life Sciences* [105], in which they estimated the economical aspects and technological trends related to microfluidics technologies for the life sciences. According to the writers, drug discovery, medical diagnostics, and therapeutic devices represent the most promising fields for future microfluidics economic-wise. Figure 2.1 illustrates the most important segments that offer business potential and emerging markets for microfluidic technologies. At present, microfluidic inkjet printing technology is the most mature and commercially most successful application of microfluidics, whereas life sciences present the most growth potential. [105] Figure 2.2 presents an example of a biomedical microfluidic device, a microchip developed for cell handling and analysis [40].

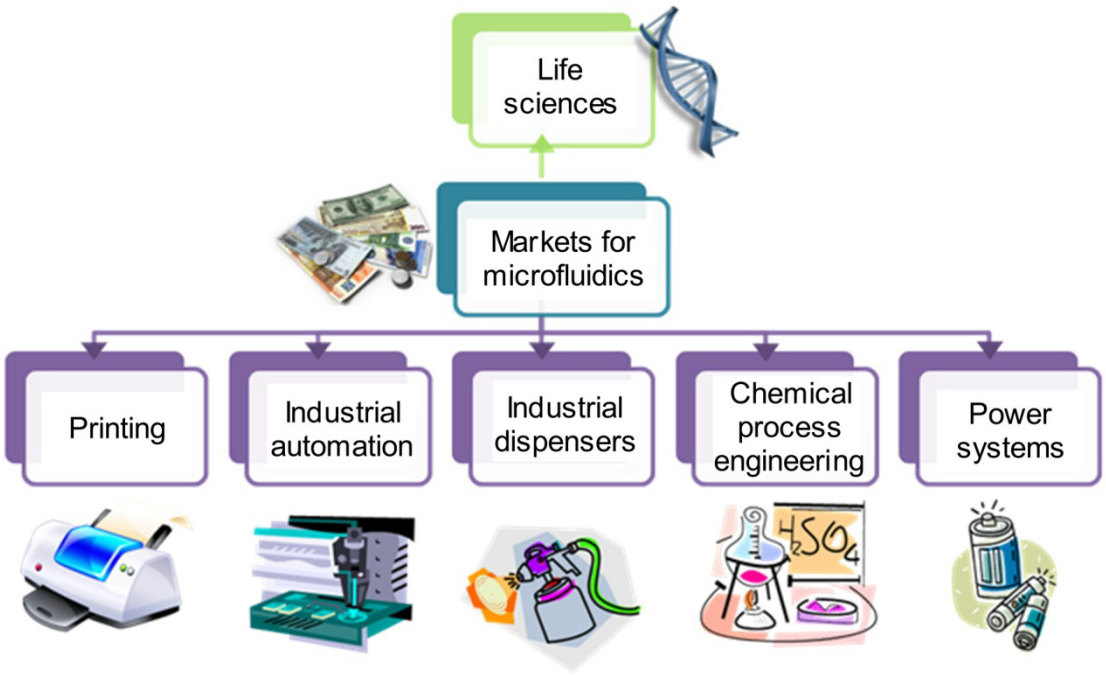

Figure 2.1. *The six major markets for microfluidics technology. Reproduced with modifications from [105].*

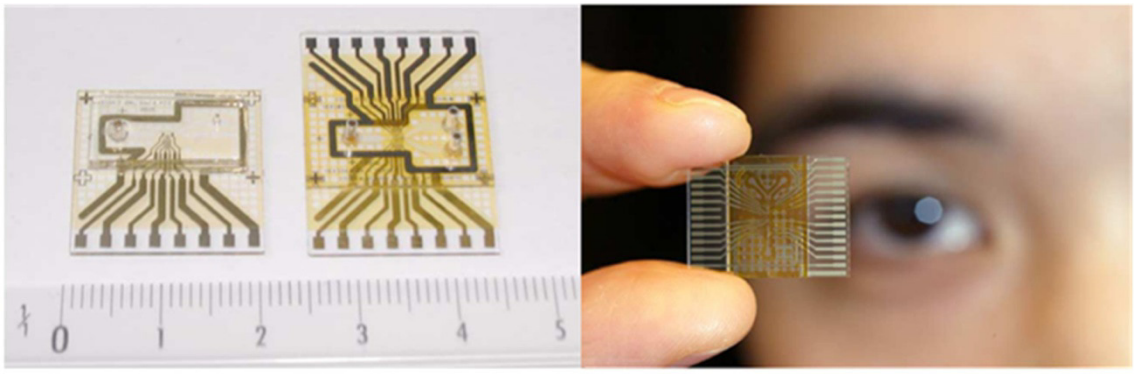

Figure 2.2. *An example of a microfluidic device; a cytological tool for cell counting and separation. Modified from [40].*

Review articles on microfluidics in several fields of biomedical sciences, such as chemical biology [150], cell culturing [38], microarrays for bioanalysis and diagnostics [122, 138, 162], and tissue engineering [4] have been written in recent years. For those interested in the general idea of microfluidics research, George Whitesides [155] has published an advisable review. Velve-Casquillas *et al.* [152], on the other hand, have recently written an excellent review on microfluidics in cell biological research in general. The great impact of microfluidic technologies has also been realized as a large number of recently published books [49, 81, 82], and journals (*Microfluidics and Nanofluidics,* Springer*, Lab on a Chip,* Royal Society of Chemistry*).*

2.2. Microfluidic cell culturing

The behavior of fluid flows within micrometer scale is fundamentally different than what can be observed in the macroscale world. A physical quantity commonly used in fluid mechanics, the Reynolds number (*Re)*, represents the ratio of inertial forces to viscous forces that affect a fluid particle. In microfluidic systems *Re* is low (<2000), which means that fluid flow in a channel is laminar, predictable and dominated by viscous forces. Flow patterns are also reversible because flows with low *Re* are time-independent. Laminarity of flows means that in a microchannel, adjacent streams of miscible fluids flow side-by-side, and mixing only occurs by diffusion at the interface of the streams. This phenomenon can be exploited in many ways, for example when producing temporally and spatially stable chemical gradients perpendicular to the fluid flow. [122, 150]

When considering cell-based biomedical applications, miniaturization by microfluidics offers fundamental improvements over traditional macroscopic devices. Firstly, the number of cells needed is reduced, and short transport distances enable cells to respond more quickly to chemical and environmental signals. Secondly, when reduced amounts of expensive fluids are needed, experiments become more cost-effective. [122, 155]

Microarray technologies have been addressed to study the effects of different immobilized factors on cells, but these studies do not give information on soluble factors. With microfluidic cell culturing platforms, on the other hand, it is possible to combine the benefits of (1) miniaturization, (2) optical real-time observation, (3) patterning the culture substrate, (4) continuous feed of fresh medium and waste disposal, (5) varying the composition of culture medium spatially and temporally, and (6) creating physiological culture conditions. [45]

The spatial microenvironment of cells is a critical factor for the structure and function of tissues in the body. Regulation of cell function by biomaterial surface chemistry and surface patterning with lithographic methods is a typical approach in microfluidic techniques developed for spatial control of cell behavior. [12] However, in an ideal culture device, the microfluidic channels would be fabricated into the matrix of a porous biomaterial scaffold that permits diffusion of smaller and larger biomolecules, whereas the matrix serves as mechanical support for the tissue in all three dimensions. Convective mass transfer along the microchannels allows for controlling the metabolic environment experienced by the cells in the scaffold matrix, serving as a waste disposal system for toxic waste products. [21]

In natural tissue, microvascular networks provide the basis for oxygen and nutrient transport. Microfabrication with photolithographic methods and polymer replica molding has been introduced to produce three-dimensional microfluidic vasculature for culturing of engineered tissue. The design principles for these artificial blood vessel networks originate from computational fluid dynamic models, which are based on morphometric analysis of natural microvasculature of vital organs. [12] An example of

such study is the work done by Fidkowski and co-workers [42] with a biodegradable elastomer, poly(glycerol sebacate) (PGS).

In addition to the function of microchannels as plain medium providers, they can be used to acquire chemical information about the condition of the cell population, and to produce chemical gradients for cell guiding and stimulation. [150] Especially for neuronal cells, introduction of chemical gradients is crucial for controlling neuronal behavior. As Dertinger *et al.* [32] demonstrated in their pioneering study, substrate interactions – such as contact with laminin – trigger axon formation and polarization in hippocampal neurons. In the absence of chemical gradients, axon formation does not occur and neurons do not become polarized. [12]

According to Borenstein [12], most of the work done within the field of microscale cell and tissue engineering has been targeted in liver tissue engineering and a larger number of microscale tools have been developed in investigations involving hepatocytes than any other cell type. For example, Kane *et al.* [66] and Power*s et al.* [125] have developed microfluidic bioreactors for culturing liver cells. Besides hepatocytes, microfabricated culturing devices for stem cell control and regulation present one the most important applications of microscale fabrication and microsystems technology [12].

2.3. Fabrication of microfluidic devices

2.3.1. Fabrication techniques

Microfabrication methods used for patterning microfluidic channels on substrates originate from the semiconductor industry, where layer-by-layer construction of transistors and its interconnections is done by photolithography. This fabrication method will be elaborated in Chapter 4.1. Generally speaking, thin layers of material are deposited on a planar substrate or etched from it, yielding a structure with dimensions of 0.1–5 μm. Using the same method, high aspect ratio microstructures for biomedical applications can be fabricated in the order of 20–200 μm by either bulk or surface micromachining. In bulk micromachining, material is selectively removed from the substrate, by a method such as *laser ablation* [91], whereas in surface micromachining the aim is to produce topology to the substrate by selectively adding thin films of material, as is the case in *nanoimprint lithography* [17]. [134]

Variable methods for producing high-resolution microstructures by replica molding of polymers have been well established since the late 1990's. These methods include the principal of generating polymeric structures with micron-scale precision by casting, micromolding or embossing the features from a photolithographically fabricated silicon master. As these techniques inherently create planar structures, also three-dimensional constructions can be realized by stacking and bonding multiple layers together. [12]

A generalized example of a typical manufacturing process for a planar two-dimensional (2D) microfluidic device for biomedical applications, as presented in Figure 2.3, can be described through the following steps: first, a master mold is designed and fabricated by conventional lithographic methods. The master is a negative replica of the designed structure. Secondly, using the master, a positive replica of the design is molded, embossed or imprinted to a selected polymer part, and the part is machined to the desired size. Thirdly, a cover sheet is bonded to the polymer to seal the channels. Finally, connections to an external fluidic reservoir system are fabricated. [99, 134]

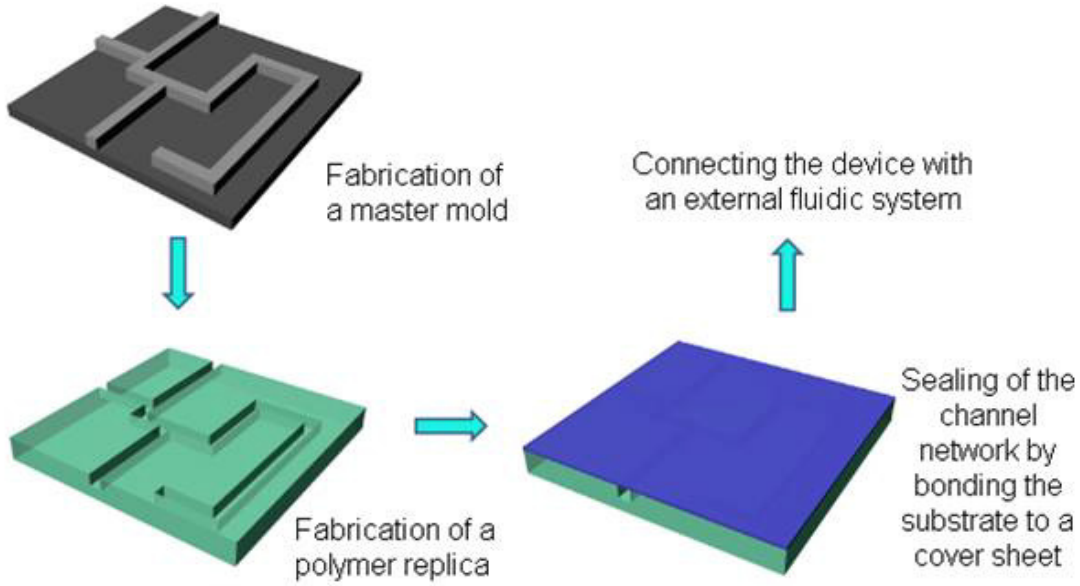

Figure 2.3. *A generalized example of the fabrication of a biomedical microfluidic device. Concept adapted from [134].*

Polymer replication from a sustainable master mold is very cost-effective especially for serial production of disposable biomedical devices. Once the master is fabricated, thousands of polymer replicas can be molded without reductions in resolution or quality. [134] Examples of the polymers used in microfluidic applications for biomedical applications will be presented in the next chapter.

2.3.2. Materials for microfluidics

Microfluidic platforms used in biomedical research stem from the microelectronics industry and traditional microfabrication techniques with silicon and glass [122]. Considering the benefits for cell culturing, glasses are transparent, relatively biocompatible and have controllable surface properties. In particular, microfabrication methods for glass materials are well-established. [12] Glass provides excellent isolation properties, but the machining of high aspect ratio 3D microstructures in glass is very difficult and expensive [134].

Silicon (Si) has been commonly used as a substrate material in microfluidics, exploiting its well-known fabrication methods. However, several silicon-related disadvantages exist. Silicon substrates have high electrical and thermal conductivities, thus a special insulation layer of an oxide, nitride or a polymer is needed to prevent heat and electricity transfer between chambers in the microfluidic device. Another trouble with silicon is interaction with biomolecules and fluids in the microchannels, which leads to adhesion, accumulation and fouling, preventing the device from functioning properly. These interactions can be eliminated by surface modification techniques such as silanization, which, however, raise the processing costs and the modified surface may degrade over time. [134]

Despite the many favorable properties of glass and silicon, fabrication costs for these materials are inordinate, and neither of them has optimal properties to work with living mammalian cells. Nevertheless, it is the development of fabrication methods that hinders the development new material solutions, and therefore silicon and glass are still used in fabricating specialized microfluidic systems as molds, supporting structures and whenever chemical and thermal stability are needed. [122, 155]

Special constraints from the implementation of microfluidic mass transfer set demand for the material to be (1) appropriate for the replication of microstructure with adequate resolution, (2) formable into pressure-tight fluidic structures, (3) highly permeable to small and large solutes and (4) able to be chemically modified to adjust the surface and adhesion characteristics. [15, 21] Polymer materials are easy to mold into complex geometries with small dimensions, and have insulation properties comparable to glass. Furthermore, polymers can be made inert to interaction with biomolecules and there are several modification techniques to manipulate the chemical character of the polymer surface. [134] The predominant polymer, or more precisely, an elastomer, used for microfluidic microfabrication is poly(dimethyl siloxane) (PDMS), a versatile, cheap and biocompatible material. [122, 155]

PDMS is a synthetic elastomer material belonging to the group of silicones, polymers containing a Si-O backbone. The repeating unit in the chemical structure of PDMS is $[(CH_3)_2\text{-Si-O}]_n$. PDMS can be synthesized in different rheological forms depending on the polymer chain length and crosslinking density. In microfluidic applications, PDMS is usually in elastomeric form, meaning the material is highly crosslinked and only little free fluid remains in the structure. The material is commercially sold as kits containing both the PDMS prepolymer solution and a curing agent (photoinitiator) for crosslinking. [134]

In the field of biomedicine, PDMS has been the predominant material for structuring microfluidic devices. For use with aqueous systems, biochemicals and cells, PDMS has an attractive combination of properties, which have been listed in Table 2.2. The primary disadvantages of PDMS for use in microfluidics include absorbance of a range of organic solvents and compounds, and the inability to covalently attach biomolecules on the material surface because of chemical inertness. [137, 150]

Table 2.2. *Properties and benefits of PDMS in biomedical applications.* [12, 95, 150]

property	benefit in biomedical applications
softness and flexibility	resembles natural soft tissue environment
transparency (UV-Vis)	can be optically investigated
biocompatible	essential properties when used in cell-based systems
withstands sterilization	
reversible deformation	keeps its shape after handling
inexpensive	useful in research and industrial scale applications
processability and low curing temperatures	fast, easy and reproducible fabrication of different geometries
permeable to gases	oxygen diffusion to cells
surface modificative	easy sealing with other surfaces

Other commonly used polymers in microfluidics include parylene, poly(methyl methacrylate) (PMMA), polycarbonate, polyesters, paraffin, polyimide and SU-8, a commonly used photoresist material presented later in Chapter 3.5.1 [97, 134, 164]. Figure 2.4 summarizes material properties of some of these polymers and those of silicon and glass.

Material property	Si (single-crystal)	Glass	SiO_2	PDMS
Coefficient of thermal expansion ($\times 10^{-6}\,°C^{-1}$)	2.6	0.55	0.55	310
Thermal conductivity at 300 K (W cm^{-1} K^{-1})	1.57	0.011	0.014	0.0018
>70% optical transmittance (nm)	>700	>350	>350	400~700
Maximum processing temperature (°C)	1415	550~600	1700	~150
Bulk resistivity ($\mu\Omega$ cm)	2.3×10^{11}	$>10^{10}$	$>10^{10}$	$>10^{20}$
Dielectric strength ($\times 10^6$ V cm^{-1})	3	5~10	2~3	2.1
Water contact angle, advancing (degree)	110	20~35	~30	~110

Material property	PMMA	Parylene C	Polycarbonate
Coefficient of thermal expansion ($\times 10^{-6}\,°C^{-1}$)	55	0.35	70.2
Thermal conductivity at 300 K (W cm^{-1} K^{-1})	0.002	8.3×10^{-4}	0.002
>70% optical transmittance (nm)	400~700	400~700	400~700
Maximum processing temperature (°C)	~100	290	~100
Bulk resistivity ($\mu\Omega$ cm)	$>10^{20}$	$>10^{20}$	$>10^{20}$
Dielectric strength ($\times 10^6$ V cm^{-1})	0.17~0.19	2.67	0.39
Water contact angle, advancing (degree)	60~75	87	78

Figure 2.4. *Properties of commonly used materials for microfluidic device fabrication. Modified from [164].*

Although traditionally microfluidics has only employed stable and inert polymers, there has been a growing trend of moving towards biodegradable and more

biocompatible materials, especially in the field of tissue engineering. [12] Biodegradable polymers earn the credit for most of the advances in tissue engineering applications, as well as in other biomedical applications including degradable surgical sutures and devices for controlled drug release. Most of these materials degrade via hydrolysis and the degradation process can be highly controlled. The most widely used biodegradable polymers are polyglycolide (PGA), polylactide (PLA), polycaprolactone (PCL) and poly(lactide-co-glycolide) (PLGA), which have adjustable degradation times varying from several months to years. [12, 134] Materials from this group have also been extensively studied at Tampere University of Technology [e.g. 2, 107, 116].

Biodegradable polymers are usually more difficult to process than traditional non-degradable polymers, since exposure to heat, oxygen or unsuitable solvents may lead to degradation and loss of mechanical properties. Conventionally, processing methods such as injection molding and extrusion have been used to shape biodegradable polymers. Nowadays there are also several suitable microfabrication methods for structuring these materials with micrometer precision. Some of these methods use a microfabricated master mold, such as imprinting, hot embossing and soft lithography, whereas others employ direct shaping of the polymer; these include direct writing, stereolithography and laser micromachining. [12, 134] Soft lithography is a method developed for molding of rigid polymers such as PLGA, and will be discussed in Chapter 4.2. This double-transfer method employs an elastic PDMS mold, since it would be difficult to peel off the rigid polymer part from a rigid silicon master. [12]

Several studies of microfluidic device fabrication using biodegrarable polymers, especially for tissue engineering scaffolds, have been published. For example, King *et al.* [69] fabricated a three-dimensional microfluidic network of thin PLGA films using soft lithography, hot embossing and thermal fusion bonding. The construct was designed to mimic natural tissue microvasculature, and aimed to be scalable for large-scale tissue engineering [69]. Mills *et al.* [98] have studied nanoimprint lithography and hot embossing methods for structuring microchannels in PLA in addition to experiments with poly(ethylene naphthalene) (PEN) and PMMA. A scheme of the fabrication method and scanning electron microscope (SEM) images of the imprinted microstructures on PLA are presented in Figure 2.5.

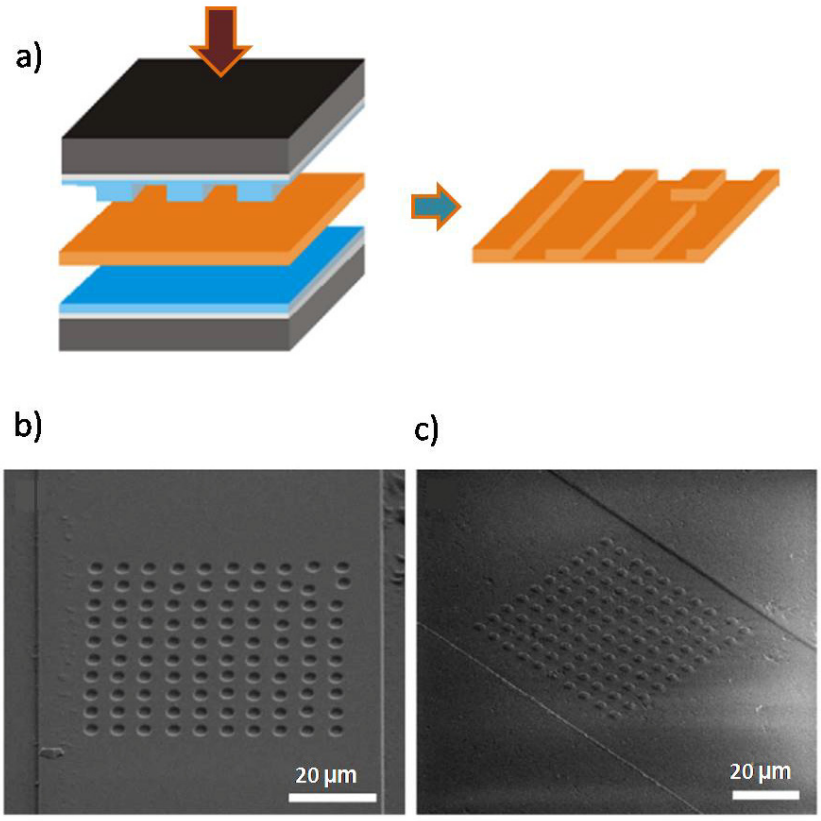

Figure 2.5. *Nanoimprint lithography of PLA. a) A schematic diagram of the imprinting technique, and b) and c) SEM-images of imprinted microstructures. Modified from [98].*

The group of Robert Langer [11, 42] has developed replica-molding techniques for fabricating microfluidic devices from poly(glycerol sebacate) (PGS), which is a synthetic biocompatible and biodegradable elastomer. Bettinger *et al.* [11] fabricated a microfluidic system using two layouts, one for a microvascular network and the other for hepatocytes culturing. PGS was molded into single-layer microfluidic networks, which were then stacked and bonded into a three-dimensional scaffold structure. Figure 2.6 presents the microstructure of the mold and the molded network. According to the writers, this technique is fast, efficient and scalable. As a special advantage, the polymer can be cured and bonded without using any cytotoxic solvents or adhesives. They also see that the microfluidic network described in the study could easily be incorporated into existing biomaterial systems and technologies such as drug delivery systems. [11]

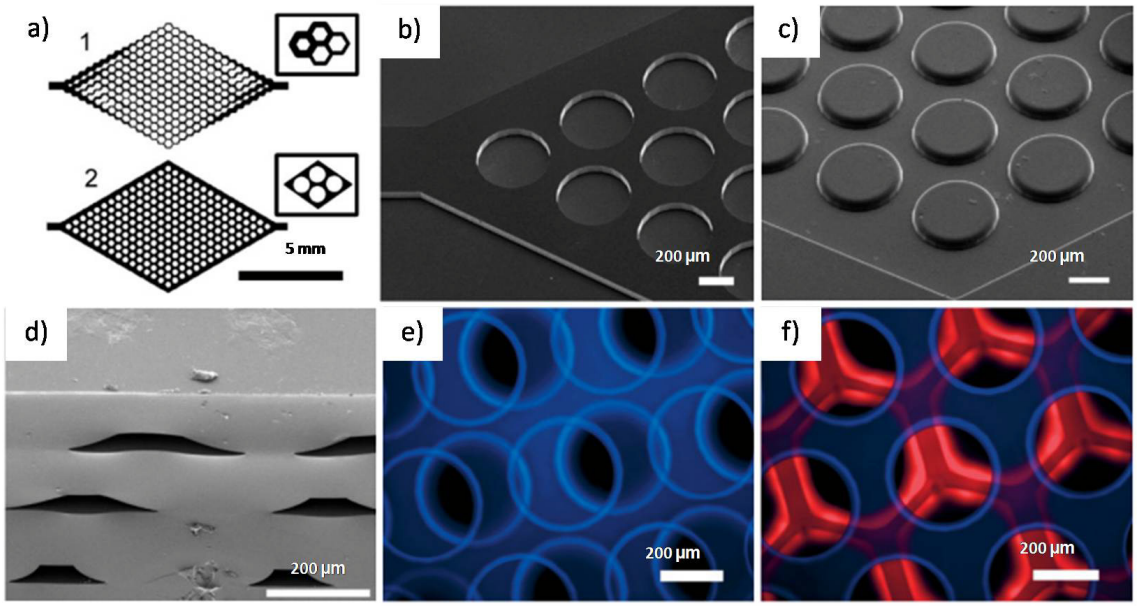

Figure 2.6. *Characterization of PGS microfluidic devices. a) Mask layout for (1) vascular and (2) hepatocyte networks, b) SEM-image of a silicon mold for polymer replica molding of microfluidic hepatocyte networks, c) replica-molded PGS layer of silicon master shown in (b), d) SEM-image of the cross-sections of a three-layer PGS device, e) and f) composite fluorescent micrographs of the devices after flowing rhodamine and 4,6-diamidino-2-phenylindole solutions to demonstrate the patency of multilayer hepatocyte devices. Modified from [11].*

Also biopolymers of natural origin have been employed in microfluidics for their inherent biocompatibility and mild fabrication conditions. Micropatterning and channel fabrication in natural hydrogels such as calcium alginate [143], and gelatin [117] have been studied. One of the advantages of using hydrogels in microfluidic cell culturing is the low fraction of solid material within the structure, so that the gel is permeable to diffusion of small and large molecules. Furthermore, the fabrication conditions for natural hydrogels are mild enough to allow pre-seeding of the gel with cells. [143]

3. LIGHT-INDUCED MICROFABRICATION OF POLYMERIC MATERIALS

3.1. Introduction to light-induced reactions in polymers

The interaction of electromagnetic radiation of suitable wavelength with monomer or polymer molecules can induce chemical bond formation or bond breakdown. The terms photopolymerization, photocrosslinking and photocuring refer to the former; the latter phenomenon is termed photoscission. In practice, the term photopolymerization means a polymerization process initiated by visible or ultraviolet (UV) light. Theoretically, polymerization can be initiated also by electromagnetic radiation of other wavelengths. [28]

The term *curing* is usually used to denote any kind of solidification of a polymeric solution. The interpretational difference between the terms *photopolymerization* and *photocrosslinking*, on the other hand, can be explained in reference to the size or length of the polymerizable species. When the term photopolymerization is used, polymerization occurs between molecules of short chain length or small molar mass (monomers) forming a polymer structure with greater molar mass and longer chains. Photocrosslinking, on the other hand, refers to the formation of covalent bonds between already polymerized molecule chains (oligomers) through double bond opening, for example. Another distinctive fact is that unlike photopolymerization, photocrosslinking involves the absorption of a photon in every chain propagation step. Photopolymerization and photocrosslinking can occur simultaneously if the monomer has more than one reactive functional units, and the overall result is a highly crosslinked polymer network as in photocrosslinking. [147]

In the field of biomedicine, light sources utilized in the fabrication of polymeric networks and devices include UV lamps, halogen lamps, plasma arc lamps, light emitting diodes (LED), titanium-sapphire lasers and other laser lamps. The light beam generated by these lamps differs in terms of emission wavelength, intensity and associated heat. Typically, UV and halogen lamps have been used for tissue engineering, drug delivery and cell encapsulation, whereas other light sources have been employed in other purposes such as dental applications and microfabrication. [8]

3.2. Photopolymerization reaction mechanism

Photopolymerization (or –crosslinking) in a photosensitive material is first initiated by small molecules called photoinitiators (PIs), which exhibit high absorption at the

specific wavelength of light used in the fabrication process. The primary reaction mechanism, dominated by free radicals, has four steps presented in Figure 3.1. [7]

In the initiation step, the PI molecule is excited (PI^*) by absorption of a photon (or more, as seen later) and forms one or more radicals ($R\bullet$), depending on the molecule. Usually only one of these radicals is active and can induce the convertion of monomer species (M) into a growing polymer ($P\bullet$) during the association step. In the propagation phase, the growing polymer is elongated by continuous addition of monomer units. Elongation occurs until two growing chains meet and react at their radical ends, terminating the propagation. [7, 43, 76] This termination mechanism is called *combination* [43]. The photopolymerization process is illustrated in Figure 3.2.

Initiation	$PI \xrightarrow{\lambda} PI^* \rightarrow R^\bullet$
Association	$R^\bullet + M \xrightarrow{k_1} P^\bullet$
Propagation	$P_n^\bullet + M \xrightarrow{k_p} P_{n+1}^\bullet$
Termination	$P_n^\bullet + P_m^\bullet \xrightarrow{k_t} P_{n+m}$

Figure 3.1. *The primary reaction mechanism of photopolymerization. The symbols λ and k with subscripts above the reaction arrow denote light energy absorbed by the PI and the reaction rate constants for each conversion reaction, respectively. Adapted from [7].*

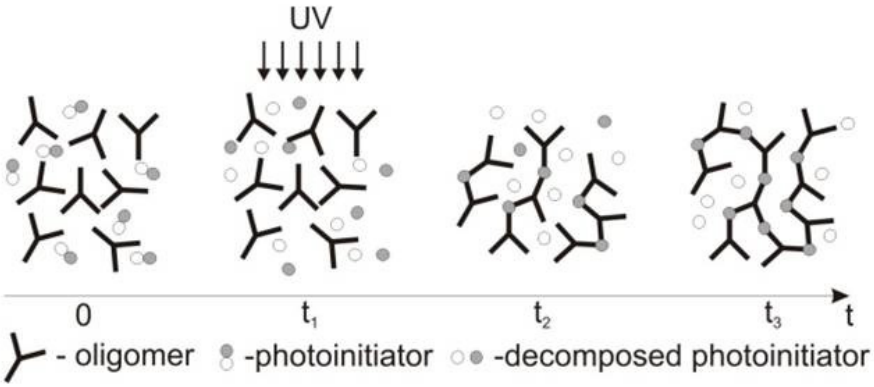

Figure 3.2. *A scheme of photopolymerization as a function of time. [7]*

The photoinitiation efficiency of a PI can be described in terms of *the quantum yield.* This quantity gives the ratio between the amount of initiating species produced and the amount of photons absorbed. [51] The photopolymerization mechanism presented above is greatly simplified and excludes all the side reactions related to PI excitation. Increase in the probability of these side reactions decrease the quantum yield of the PI, which of course is desired to be high. For example, instead of splitting into radicals, the excited PI molecule can decay back into the initial state and emit the absorbed energy as light and/or heat. Another possibility is a quenching reaction, where the excited PI reacts with an inhibitor molecule like oxygen and loses reactivity. [76]

Similarly, there are also other mechanisms for the chain termination reaction, including *disproportionation*, in which the terminated chains differ by their degree of saturation, and *chain transfer*, wherein the terminating chain abstracts hydrogen from a donor molecule. [43]

3.3. Photoscission

The term photoscission refers to light-induced cleavage of molecule chains in a polymer. Most polymers are susceptible to this type of degradation, and the harmful effects of this phenomenon are generally preferred to be minimized. Some microfabrication methods, however, take advantage of photoscission. These methods include photolithographic patterning of positive photoresists and laser ablation. [43, 51]

Photoscission of polymer chains produces units of smaller molecular weight. Scission can occur at the polymer backbone, leading to a dramatic decrease in molecular weight, or by non-chain scission, eliminating only small molecules from substituent groups. Theoretically any part of the polymer can undergo light-induced chemical reactions – if only the excitation energy is high enough. If the degradative effect of light can be focused to a small volume within the substrate, high-resolution patterns can be produced. The illuminated regions become more soluble compared to the parent polymer, and can be washed away leaving behind the unilluminated polymer regions with the desired pattern. [51]

3.4. Photoinitiators

PIs are molecules responsible for initiating the photopolymerization reaction by producing reactive species upon light absorption. Various types of PI molecules have been developed for better photopolymerization and optimal processing properties. Among the myriad of different molecules used for this purpose, worth mentioning are the ones that have been used for biomedical applications: eosin Y [70], 1-cyclohexyl phenyl ketone [39], 2,2-dimethoxy-2-phenylacetophenone (DMPA) [118], 2-hydroxy-1-[4-(hydroxyethoxy) phenyl]-2-methyl-1-propanone (Irgacure 2959; D2959; I2959) [5, 156], Irgacure 651 [5], and camphorquinone/amine [20, 29, 127]. PIs can be classified according to (1) the number of PI molecules needed for initiation, (2) polymerization type or (3) initiation mechanism. Furthermore, a PI can induce polymerization either directly or with the help of a photosensitizer (PS), which is a molecule that first absorbs light energy and then transfers it to the PI. [8]

When selecting a PI for a photofabrication process, the absorbance characteristics of the molecule should be considered first. Optimally, the PI should have an absorbance maximum at the wavelength of the light source used in the process. Although PIs utilized in biological applications exist in prepolymer solutions only at low concentrations (0.0125–2 % w/w), there are also other selection criteria to be considered

carefully. These include high quantum yield and initiation rate, biocompatibility, solubility in water, stability and a long shelf life. [8, 76, 106]

3.4.1. Photoinitiation mechanisms

Differing by the mechanism involved in the formation of reactive species (*photolysis)*, photoinitiation has three main classes: radical photopolymerization, hydrogen abstraction and cationic photopolymerization, of which the radical-induced mechanism is by far the most common. [8, 106] The schematic reactions of these three mechanisms are shown in Figure 3.3. Photoinitiators that produce radical species are usually aromatic carbonyl compounds like benzoin derivatives, benziketals, acetophenone derivatives and hydroxyalkylphenones. Under exposure to light of suitable wavelength, these photoinitiators form radicals by undergoing cleavage at C–C, C–Cl, C–O or C–S bonds. [106]

Initiation by radical species	$PI \xrightarrow{\lambda} PI^* \rightarrow PI^\bullet$
Initiation by cationic species	$PI \xrightarrow{\lambda} PI^* \rightarrow PI^\bullet$
Initiation by hydrogen abstraction	$PI \xrightarrow{\lambda} PI^* \rightarrow PI^\bullet$

Figure 3.3. *Photoinitiation mechanisms. Adapted from [106].*

The four basic steps of polymerization apply also to photopolymerization induced by cationic species. The difference is that instead of a radical, a carbocation ($C^{\oplus}$) is formed in the initiation process. The photolysis of a cationic photoinitiator, induced by absorption of light energy, yields acidic species (PI^+) that associate with the monomer and thus initiate the polymer propagation. [28, 43] Photoinititation by hydrogen abstraction occurs when the photoinitiator abstracts hydrogen from a H-donor molecule (DH) and two radicals are formed; usually only the H-donor radical ($D\bullet$) is involved in the initiation of the polymerization process. [106]

3.5. Photoresists

Photoresists are polymers that undergo chemical reactions leading to changes in the molecular structure due exposure to light, e.g. are photosensitive or imageable. When microscale devices are manufactured by means of photofabrication, photoresists play a key role. These materials can be divided into two categories: negative- and positive-tone photoresists. In negative resists light exposure leads to crosslinking and solidification of the resin, and the unexposed material can be dissolved and washed away. On the contrary, exposing positive resists to an adequate amount of light energy induces molecule chain scission leading to dissolvable shorter units. Positive-tone resists can be seen as more efficient, as most hollow structures can be manufactured by removing only a small fraction of the total material. [109, 165]

Negative-tone resists can be further divided according to whether the resin is solid or liquid before crosslinking. The solid ones are epoxy-based cationic photoresists that produce acidic radicals due to light exposure, which induces the polymerization during a so-called post-baking process. [109, 159] Epoxy-based photoresists usually have high mechanical strength and high chemical resistance [76]. Liquid negative-tone photoresists are commonly acrylate-based, but also organically modified ceramics (Ormocer®s) belong to the group of negative-tone photoresists. Before irradiation, a photoinitiator is added to the resin solution to form radicals during light exposure. In this method, the polymerization reaction is induced instantly. [109]

3.5.1. SU-8

SU-8 is a negative-tone photoresist first developed by IBM for the LIGA technology, which produces metallic molds of high aspect ratio microstructures for cast molding of polymers, for example. The abbreviation LIGA originates from German words for lithography electroplating and molding (lithographie, galvanoformung, abformung), which are the three major steps in this lithographic microfabrication technique. A photoresist film is deposited on a substrate and then exposed to x-rays or UV light through a photomask. A photomask is a thin patterned sheet that allows light to pass through only in desired regions. After the irradiated regions are washed away with a solvent, the remaining cavities are filled with metal by electroplating. The remaining polymer regions are then irradiated without a photomask, and subsequently washed away leaving behind the metallic microstructure. [12, 134]

The main constituent in SU-8 is the EPON® SU-8 epoxy resin. It is an aromatic hydrocarbon with an epoxide group at either end. In the conventional fabrication process of SU-8, the resin is first dissolved in γ-butyrolacton (an organic solvent), and 10 wt-% of a photoinitiator is added. Typically, the photoresist is spun on a silicon wafer as a thin layer, prebaked and then exposed to UV-light through a photomask to induce the crosslinking reaction by converting the resin molecules into reactive acidic species. The prebaking process determines the thickness of the layer, which can be varied from tens to hundreds of micrometers. After light exposure the structure is developed with a suitable solvent and post-baked to form the final crosslinks. [87, 134, 159]

The development of SU-8 set the start for using photoresists as structural layers in MEMSs and microfluidic devices, and since the resin has been widely used as sacrificial material for the fabrication of microfluidic channels and in semiconductor applications. [134] Although complex three-dimensional structures like networks of closed microchannels can be fabricated with SU-8, in biomedical applications and tissue engineering it is principally used as a master for replica molding of biopolymers. The biocompatibility of SU-8 has been widely investigated and proven acceptable. [12]

3.6. Photosensitive biomaterials

Besides the use as structural materials, photoresists have been employed to pattern substrates with biomolecules for directed cell growth. For example neural networks have been grown on polylysine patterns fabricated by a photolithographic "lift-off" process [25]. The problem with conventional photoresists such as SU-8 is the use of organic solvents in the development procedure. For example, microstructures fabricated in SU-8 have to be developed with non-biocompatible solvents like ethyl acetate or diacetone alcohol. The problem is that solvent residues can be toxic and lead to the denaturation of biomolecules, thus the process is not very biocompatible and suitable neither for patterning surfaces with biomolecules nor for any other biological application. Therefore, new photosensitive biopolymers have been developed to create patterned biocompatible surfaces by photolithography and other photopatterning techniques. [46]

A great number of photopolymerizable formulations of both synthetic and natural polymers have been studied for biomedical applications. A simple way of creating new photosensitive materials is to modify common monomers with photosensitive groups, usually with dimethacrylic or diacrylic moieties. In Finland, At Aalto University School of Science and Technology (TKK), crosslinked polyesters have been prepared from end functionalized PLA and PCL precursors by the group of Prof. Seppälä [53, 54]. The polyester networks have exhibited degradation characteristics similar to the corresponding thermoplastic polyesters. In a recent study, the group utilized these novel photocrosslinkable oligomers in a new selective leaching method for the fabrication of biodegradable tissue engineering scaffolds with predetermined pore structure [127]. As an example, the synthesis of the PCL-based biodegradable matrix material used in the study is presented in Figure 3.4. The oligomer synthesis begins with ring-opening polymerization of ε-caprolactone with 10 mol-% pentaerythritol, yielding a four-armed oligomer with molar mass of a little over 1000 g/mol. The oligomer is then functionalized with methacrylic anhydride, yielding crosslinkable acrylic moieties at the ends of the PCL-units. The overall synthesis is similar to what has been previously described by Seppälä and co-workers [53] for the fabrication of elastomeric poly(ε-caprolactone/D,L-lactide) copolymers.

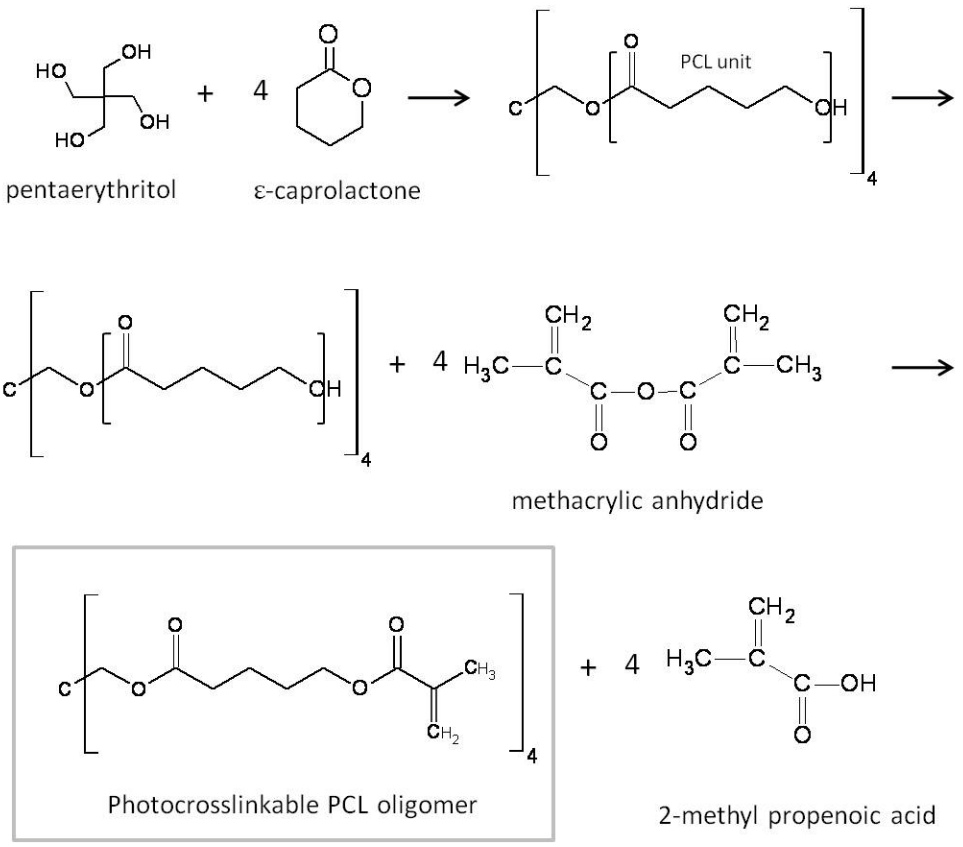

Figure 3.4. *Synthesis of a methacrylated four-armed PCL oligomer; the photocrosslinkable double bond is marked with red color. Adapted from [127].*

Matsuda and co-workers have also developed photocurable biodegradable polymers based on PCL and trimethylenecarbonate (TMC) [93, 94, 100, 101], whereas Grijpma and co-workers have synthesized photocurable derivatives of PDLA and PCL [47, 96]. Furthermore, acrylated poly(ethylene glycol) (PEG) and its derivatives count among the most investigated photopolymer systems; ethylene glycol has also been copolymerized with other monomers such as lactide and caprolactone to produce biodegradable photopolymers [29]. Other photocurable biomaterials studied for different biomedical applications include derivatives of poly(vinyl alcohol) (PVA) [131], chondroitin sulfate [83] and hyaluronic acid (HA) [118].

He *et al.* [52] have developed a photopatternable copolymer based on 3-(t-butoxycarbonyl)-N-vinyl-2-pyrrolidone (TBNVP) and methyl methacrylate (MMA), which has been proven biocompatible in fibroblast culture experiments. The researchers call it a *bioresist* as it is a "bioactive" photoresist; the bioactivity is a result of the chemical nature of the polymer – hydrophilicity and ability to bind biomolecules. Furthermore, the problem of using toxic solvents has been overcome with this bioresist as no solvent-based development procedure is needed. [52]

Groups of Diakoumakos *et al.* [33] and Douvas *et al.* [36] have also developed photoresists for more environmentally friendly and biocompatible photofabrication. Douvas and co-workers developed a bioresist based on poly(*t*-butyl acrylate) [36], which is processable in biocompatible conditions and used to pattern biomolecules on

different substrates for the use as biosensors. The photoresist itself is, however, used only as a processing material and removed at the end. The group has recently received a patent [119] for their photoresist synthesis and patterning technique. Diakoumakos *et al.* [33] have studied methacrylate-based photosensitive copolymers that can be developed in aqueous base solutions with low base concentration. The synthesized polymers were either negative- or positive-tone chemically amplified photoresists that were further functionalized to enable micropatterning with biomolecules. [33]

Both of the research groups mentioned above use the same chemistry: because of the *t*-butoxycarbonyl (*t*-BOC) groups, the copolymer can be used as chemically amplified photoresist in the precence of a photoacid generator (PAG). The *t*-BOC groups undergo photolysis upon exposure to UV light and become carboxylic groups, which turns the surface of the polymer to hydrophilic. As mentioned, in the study by He and co-workers, no further development process is needed, but if such a procedure is performed, it can be done with an aqueous solution because of increased hydrophilicity. Furthermore, the hydrophilic surface with COOH-groups favors the adsorption of peptides and proteins that promote cell attachment and migration. [46] Overall, it seems like these kinds of "bioresists" would be good candidates for photopatterning cell guiding microstructures also in cell culturing devices.

4. COMMON PHOTOFABRICATION METHODS

4.1. Photolithography

Primarily, photolithography is a planar technique used extensively in microelectronics in the fabrication of integrated circuits and not suitable for producing three-dimensional biomimetic structures. In biomedical applications it is, however, still widely used to create molds, from which the designed microstructure is subsequently transferred to another material. [12, 165] Thus, it is only appropriate to shortly present this fundamental microfabrication method in this thesis as well. A schematic diagram of the key procedures is presented in Figure 4.1.

The primary step is to create a computer-aided design (CAD) of the desired two-dimensional pattern and then use it to fabricate a photomask. Secondly, a thin film of the structural material is deposited on a substrate (a plate of glass or silicon), and after this yet another thin layer (0.5–2.5 μm) of a photoresist is spin-coated on the top. [165]

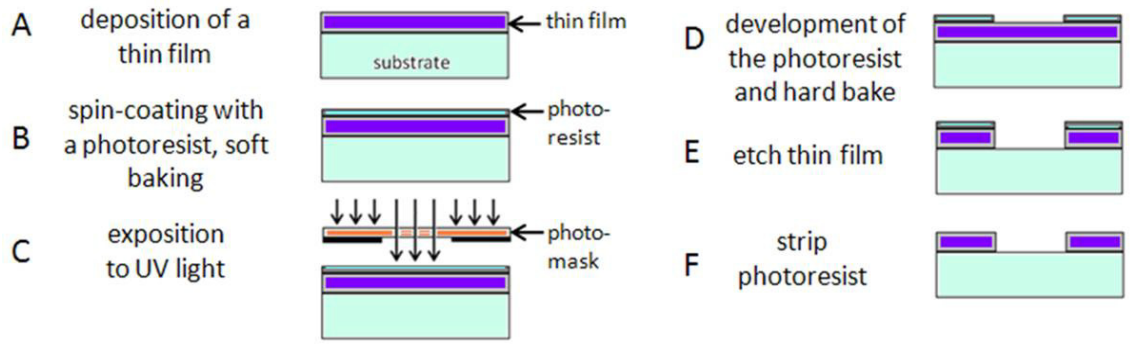

Figure 4.1. *A schematic presentation of photolithography. Note that the first step (A) is left out if the photoresist itself is used as the structural material. Reproduced with modifications from [165].*

In the next step, the substrate is soft-baked to remove solvents from the photoresist and to improve adhesion. Then, the photomask is aligned relative to the substrate and the photoresist is exposed to UV light through the mask. Due to the light-induced chemical changes in the photoresist, the illuminated regions become either crosslinked or degraded, and a replica of the design in the photoresist is developed with a suitable solvent. The substrate is then hard-baked to improve adhesion of the photoresist. Now, the microstructured photoresist can either be used as it is, as a mold, or to further modify the underlying material. In the latter case, etching techniques are used to transfer the pattern and finally, the photoresist layer is peeled off. [165]

4.2. Soft lithography

The name of this fabrication method includes the word *soft* because it uses elastomeric materials, most commonly PDMS. Other used elastomers include polyurethanes and polyimides. Soft lithography refers to a set of techniques that use a patterned elastomer as a stamp, mold or a mask to produce structures within nano- to micrometer length scale. These techniques were first developed by Xia and Whitesides [154] and include microcontact printing, replica molding, microtransfer molding, micromolding in capillaries, solvent-assisted micromolding, and phase-shift photolithography; also cast molding, embossing and injection molding also come under the term soft lithography.

Most of the research done in the field on microfluidics has used replica molding of PDMS. This microfabrication technique starts with the photolithographic fabrication of a master mold, on top of which the prepolymer solution of PDMS is casted. One advantage of using PDMS is that because of the low surface tension of the PDMS prepolymer solution, the mold fills up thoroughly thus providing high resolution replicas. [95, 134, 154]

After casting, the polymer is cured by crosslinking the solution thermally or with UV-light, and peeled off. Now a negative replica of the master – the original microchannel structure – is generated in PDMS. Soft lithography with PDMS is illustrated in Figure 4.2. [95, 134, 154]

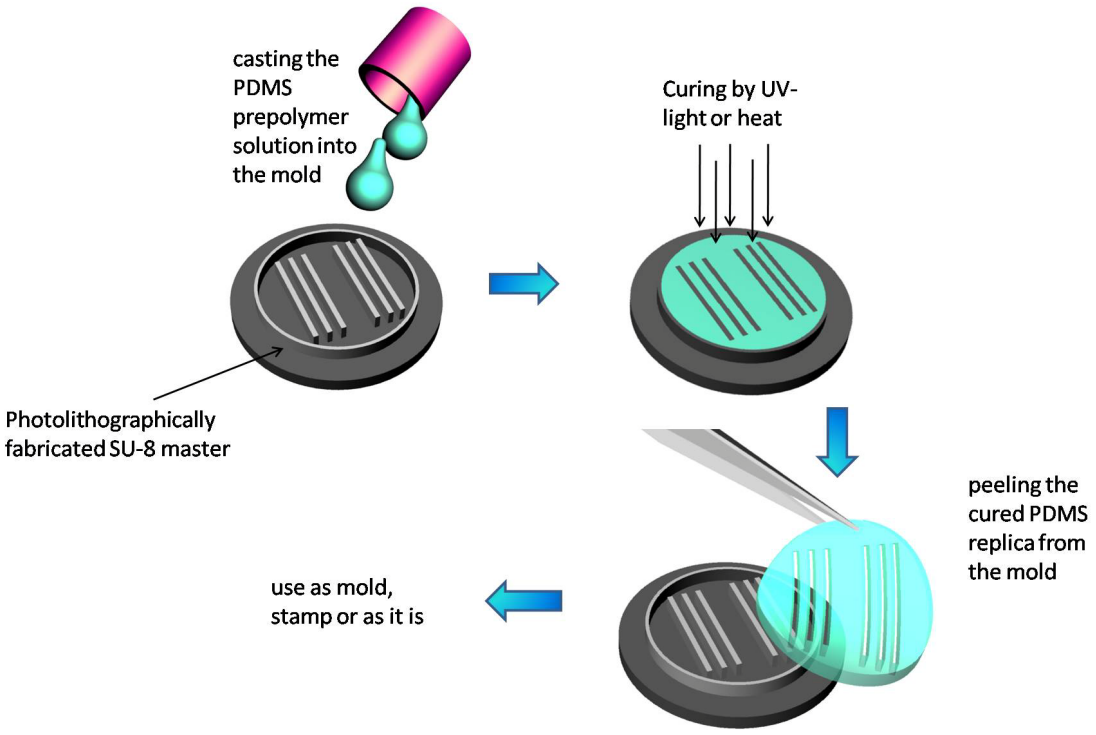

Figure 4.2. *Rapid prototyping of PDMS using a photolithographically fabricated master. Adapted from [134] and [154].*

PDMS also has some downsides in soft lithography because of its thermal and chemical properties. The material shrinks about one percent upon curing, so the cured

structure may not be the exact replica of the design. In addition, some nonpolar organic solvents such as toluene and hexane can make the cured PDMS swell. Because of the elastomeric softness of PDMS, the aspect ratio of the microstructure design has to be optimal to avoid deformation or distortion. With PDMS, the aspect ratio would have to be between 0.2 and 2 to obtain defect-free stamps and molds, as Delamarche *et al.* [31] have shown. [31, 154]

Replica molding of PDMS can be done in ambient conditions without the need of clean room facilities, and many replicas can be fabricated from a single master. Three-dimensional microfluidic devices can be manufactured by stacking together multiple microstructured PDMS sheets fabricated as described above. PDMS sheets can be readily bonded together or to other Si-based materials by treatment with oxygen plasma, which oxidizes the surface to silanol (Si-OH), thus enabling the formation of a covalent Si-O-Si bond. Hence, it is important to notice that in the first step of soft lithography, the master has to be treated with fluorinated silanes to prevent bonding between the casted polymer and the mold. [136]

Khademhosseini *et al.* [68] used PDMS in a soft lithographic technique to fabricate robust microchannels with precise control over the spatial properties of the substrate. In their study, microfluidic channels were patterned with a non-biofouling PEG-based copolymer or HA. These patterns were then used to fabricate arrays of fibronectin, bovine serum albumin or mammalian cells. According to the writers, the presented approach has potential use in various soft lithographic patterning techniques to design and fabricate more sophisticated microfluidic devices for analytical applications and microreactors. [68]

4.3. UV-nanoimprint lithography

UV-nanoimprint lithography (abbreviated as UV-NIL, also known as UV-nanoembossing) is somewhat similar with traditional photolithography, as it uses UV-light curing of a photoresist to create microstructures and predesigned patterns. In the UV-NIL method, a thin film of the photoresist prepolymer solution is coated on a substrate, which is then pressed against a prepatterned master. The substrate material has to be UV-transparent, because in the subsequent step the photoresist is exposed to UV-light through the substrate. Furthermore, it is supposed to be flexible to enable easy demolding after curing. Figure 4.3 (a) presents micropatterning with UV-NIL. [17]

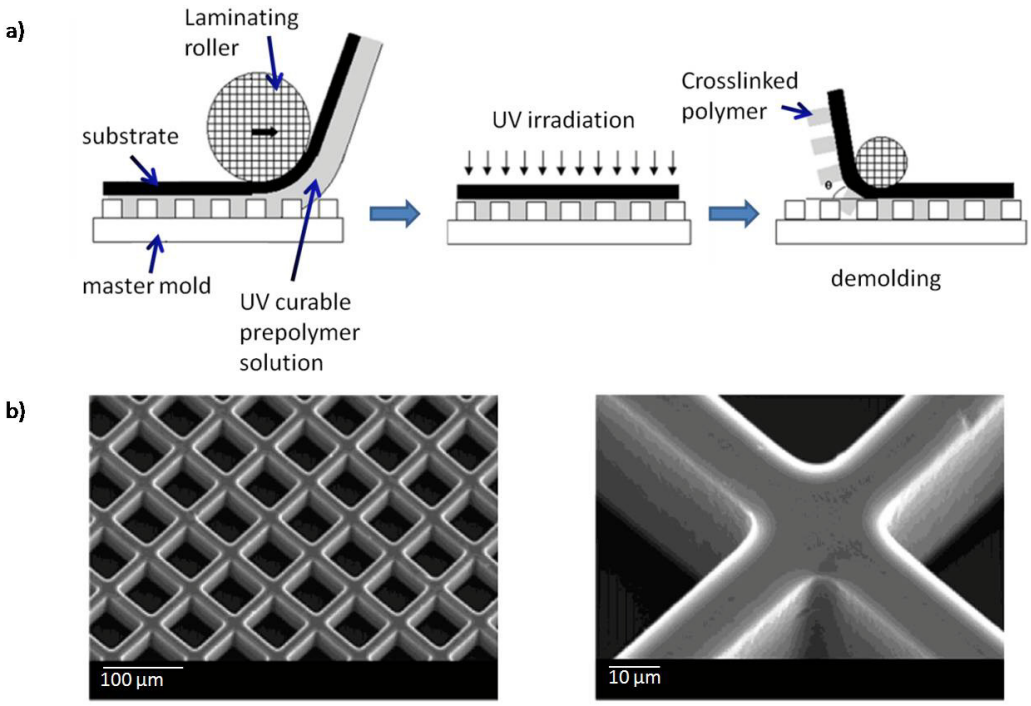

Figure 4.3. *Micropatterning using UV-nanoimprint lithography. a) Scheme of the patterning technique and b) SEM images of a UV-imprinted PEGda hydrogel microarray. Reproduced from [16].*

UV-NIL can be done in room temperature and low pressure, which is a major advantage when patterning hydrogels, protein-containing polymers, or other delicate biomaterials. [17] Chang-Park *et al.* [16] fabricated three-dimensional high aspect ratio microarrays of PEGda hydrogel by UV embossing, shown in Figure 4.3 (b), demonstrating faithful replication and the possibility of incorporating proteins within the array. These arrays were designed to find use in many biological applications such as protein and drug delivery.

4.4. Contact lithographic photopolymerization

Contact lithographic photopolymerization (CLiPP) is a microfabrication method that combines traditional silicon micromachining with polymeric materials and unique initiation chemistry. Microdevices with highly complex three-dimensional structures and versatile surface and bulk properties can be fabricated using CLiPP. In microfluidics, the advantage of CLiPP is the possibility for parallel fabrication of multilayered devices. Furthermore, the method is well suited for both rapid prototyping and large scale fabrication. [55]

CliPP employs living radical photopolymerization, exploiting specific initiator chemistries that continuously reactivate under exposure to UV light. As a result the propagating polymer chains are never completely terminated or deactivated. This phenomenon can be utilized for initiation and covalent adhesion of new polymer chains or films to the surfaces of previously photopolymerized films. Specifically, different

photopolymerizable material formulations can be incorporated within individual layers which are covalently adhered, and the surface chemical properties can be spatially modified via tethered polymer chains. [55]

Simms *et al.* [137] reported a fabrication method for a multilayer microfluidic cell culture device by contact lithographic photopolymerization (CLiPP), which enabled the incorporation of three-dimensional cell culturing sites and the surface modification of the microchannels to prevent unwanted protein or cell adsorption. The device framework was built on a glass coverslip by photopolymerizing a mixture of two acrylates using the living radical polymerization method, and the microchannel structure was created by stacking individually polymerized layers to form a multilayer structure. The main advantage was that the surface of the device remains chemically reactive and enables covalent bonding with other polymers or functional materials to enhance the biological features of the device. Studied materials were hexanedioldiacrylate and fluorinated diacrylate (Polyfox) for the microfluidic device, and an aromatic urethane diacrylate and tri(ethylene glycol) diacrylate (TEGDA) for the macroporous rigid scaffold. Lastly, channel surfaces were modified with poly(ethlyne glycol) methacrylate (PEGMA). [137]

Sebra *et al.* [132] also reported a study on the surface modification of a CLiPP-fabricated microfluidic device. According to the article, the functionality of a polymeric microfluidic device can dramatically improved via different surface modification chemistries while bulk material properties are retained. The surface properties of the microchannels such as adhesiveness, hydrophobicity, biocompatibility, antifouling, surface hardness, and surface roughness can be adjusted. [132]

5. LASER-BASED MICROFABRICATION IN BIOMEDICAL APPLICATIONS

5.1. Introduction to laser-based microfabrication

The term *laser* is an acronym from "light amplification by the stimulated emission of radiation". In other words, *laser* means a source of electromagnetic radiation at particular wavelengths produced by the stimulated emission of atoms or molecules. Stimulated emission produces photons of the same energy and phase. Thus, the laser beam is monochromatic and coherent, and can be brought to a fine focus. [74, 91]

Many different types of lasers with diverse characteristics have been developed and widely employed in industrial production from product development to finishing. Although laser machining is many times more expensive than manufacturing with traditional tools, lasers are outstanding instruments especially for microfabrication. Lasers can be used as energy sources with several advantages including spectral purity, spatial and temporal coherence, and high peak intensity. There are multiple choices for selecting a laser source, with a broad wavelength spectrum varying from deep UV (157 nm) to IR (10 μm). Also the duration of the laser exposure can be selected among a wide range varying from continuously generated beams to different pulse durations from microseconds to femtoseconds. [74, 91]

Laser fabrication is based on the interaction between laser energy and matter. Photons from the laser beam are absorbed by the sample material, which induces chemical changes in the material such as radical-initiated polymerization or molecule chain scission. These light-generated phenomena only occur above a certain threshold, which is material-, wavelength-, and pulse-duration-dependent. Therefore, the wavelength of the laser has to be chosen carefully to obtain maximal absorption. [91]

The introduction of ultrafast lasers has enabled machining of materials that normally are transparent to the laser wavelength, as simultaneous multi-photon absorption at high peak intensities can be obtained. Ultrafast lasers produce high-energy radiation concentrated into brief pulses at regular frequency; this can be used to focus the radiation into a very small volume. Consequently, microfabrication with ultrafast lasers offers superior resolution compared to other photofabrication methods. [74, 91]

5.2. Methods of laser-based microfabrication

In general, there are two ways of microfabrication with lasers: (1) a serial mode for direct writing, in which a computer is used to control the tool path for the laser beam,

and (2) a parallel mode for batch process using a mask-imaging technique. In rapid prototyping and for research purposes, the serial mode is preferred as there is no requirement for expensive photomasks and the design can be varied arbitrarily. For large-scale production the batch process is a better and more efficient choice. [91] Moreover, lasers can be employed in microfabrication by using either a constructing or a destructive approach. In the former one, lasers are used to generate light-induced polymerization or crosslinking. In the latter case, a tightly focused beam is used to remove fractions of material. This processing method is called *laser ablation*, and will be discussed in Chapter 5.4. Ablative techniques are beneficial when only small fragments of the substrate material are to be removed. Laser ablation has been utilized for patterning microchannels on a microfluidic chip, for example. [91] In the constructive approach of laser microfabrication, solid objects or structures are manufactured using a laser beam; this is called laser-based solid freeform fabrication (SFF). SFF techniques can be divided by their two- or three-dimensionality. For example, stereolithography, a SFF method presented in the following chapter, produces inherently two-dimensional microstructures. [77, 142]

Traditionally, the minimum feature size achievable with laser-based SFF is determined by the diffraction limit of the optical system used in the process. This limitation is due to the optical characteristics of one-photon absorption, which is the principal phenomenon behind conventional photofabrication methods. Usually the diffraction limit is in the order with the radiation wavelength. Also thermal diffusion limits the minimum feature size, which is, at best, a few hundreds of nanometers. However, with ultrafast lasers inducing multi-photon absorption, the restraint of the diffraction limit can be overcome and even smaller features can be fabricated. [77, 142]

Under appropriate conditions, basically any solid material can be laser-machined. Processes for various ceramics, metals and polymers have been developed and established. For example poly(ethylene terephtalate) (PET), polycarbonate (PC), PMMA, and poly(vinyl chloride) (PVC) have been used for laser-based fabrication of microfluidic channels. [91] For biomedical applications, laser machining processes of more biocompatible and biodegradable materials have been developed. Chen and co-workers [1, 19] have extensively investigated the effects laser ablation on poly(vinyl alcohol) (PVA), PDLA, PGA and PCL with different types of lasers and process parameters. Laser machining of different biomaterials has also been studied at Tampere University of Technology by Huttunen and co-workers [56, 57, 58].

5.3. Stereolithography

Stereolithography is a laser-based SFF technique for rapid prototyping, developed in the 1980's. It was first introduced for manufacturing prototypes for the needs of automotive and aeronautical industries. Stereolithography, illustrated in Figure 5.1, employs a UV laser for curing a photosensitive polymer resin; a layer-by-layer approach is used to fabricate freestanding three-dimensional microstructures from CAD models. [77, 142]

The designed structure is polymerized by moving the xyz-stage under a static laser beam focus. Each layer is individually cured on top of the previous one by lowering the stage after every layer. Another possibility is to use a movable laser beam, and only move the stage vertically. This process is repeated until the whole design is finished, and the structure is developed with a suitable solvent. Selective exposure to the UV light with a computer-controlled laser beam enables creating arbitrary and complex structures. [77, 88, 142] An example of a scaffold structure fabricated by stereolithography is presented in Figure 5.2.

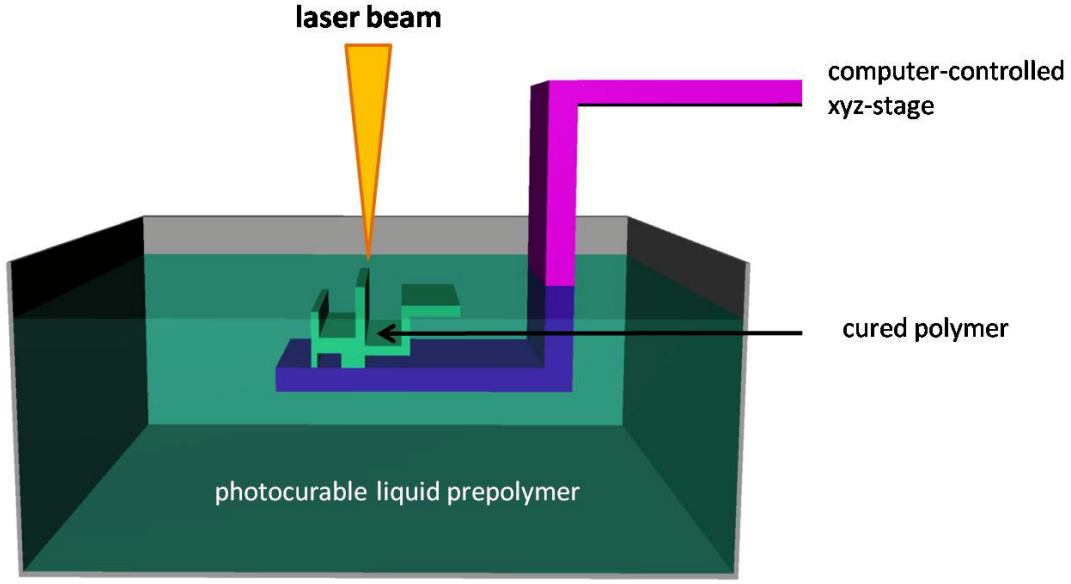

Figure 5.1. *Microfabrication by stereolithography. A photocurable polymer is selectively exposed to UV laser light in a layer-by-layer fashion to create complex microstructures. Adapted from [134].*

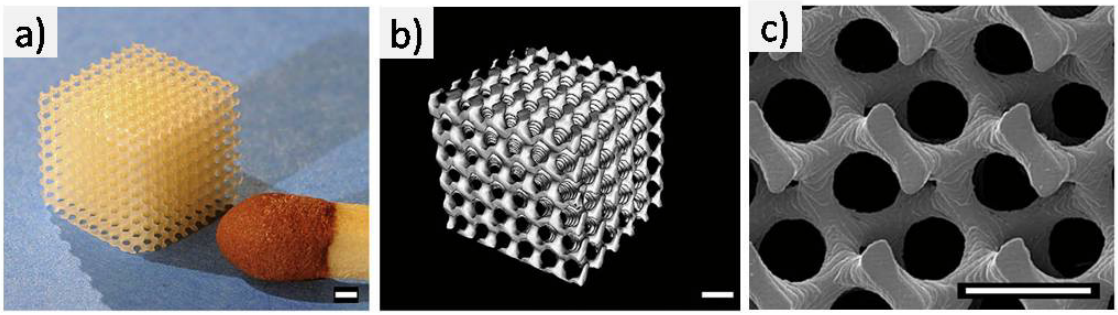

Figure 5.2. *Laser-based microfabrication using stereolithography. a) Photographic, b) μCT visualization and c) SEM images of PDLLA scaffolds built by stereolithography. All scale bars represent 500 μm. Modified from [96].*

Stereolithography can also be done by varying the photopolymer resin during the process. A precise spatial distribution of proteins, other biomolecules or microparticles can be introduced into the structure if a prepolymer solution of different concentration is deposited on top of the previous layer in each step. This is a unique advantage of stereolithography. [88]

When a photosensitive hydrogel is used in stereolithography, it is possible to encapsulate living cells within the cured microstructure. Arcaute and co-workers [6] reported a stereolithographic method of fabricating poly(ethylene glycol) dimethacrylate (PEGdma) hydrogel microconstructs with embedded fibroblasts. Although their work aimed for creating functional tissue engineering scaffolds, it would also be feasible to use these kinds of hydrogel structures in microfluidic cell culturing.

Despite the many advantages of stereolithography, a number of drawbacks can be listed. The additive one-layer-at-a-time approach for creating three-dimensional tructures is laborious and time-consuming. Moreover, since stereolithography is based on simple single-photon absorption, only shallow surfaces or adequately thin layers can be processed. To date, the minimum distance between two layers is 50 micrometers, which gives quite a poor resolution in the z-dimension. [142] Typical resolution in stereolithography is in the order of 150–200 μm in all three dimensions [134].

5.4. Laser ablation

Laser ablation is a microfabrication method, in which the interaction between the laser beam photons and the sample leads to removal of material. The interaction mechanism is complexly dependent on the particular system and its chemical and thermal processes, laser characteristics and material properties. Generally speaking, the mechanism involves absorption of the high-energy photons at the wavelength of the laser emission by the sample material. This absorption induces direct bond breaking without thermal melting or vaporization, a phenomenon also known as *photodecomposition*. Decomposition by thermal energy is induced at longer wavelengths, and in microfabrication processes, any thermal damage is to be minimized in order to achieve better resolution and shape accuracy. [91]

Conventionally, laser ablation has been a method for producing topographic features only on material surfaces due to the optical characteristics of single-photon absorption. Patterning is done by exposing the sample to ablative laser beam through a photomask. The illuminated regions become soluble and can be washed away with a suitable solvent. [25, 91]

The ablation method described above has been used to pattern microfluidic channels on various polymer substrates such as PET and polystyrene (PS) [91]. Also biomolecule-coated surfaces can be micropatterned by laser ablation; Stenger *et al.* [141] studied the neuronal polarity of hippocampal neurons cultured on laser-patterned adhesive materials, whereas Corey *et al.* [26] used polylysine surfaces patterned with laser ablation as substrates for neuron culturing. In addition to topographical patterning, laser ablation can be employed to modify the surface properties of the ablated substrates. [91]

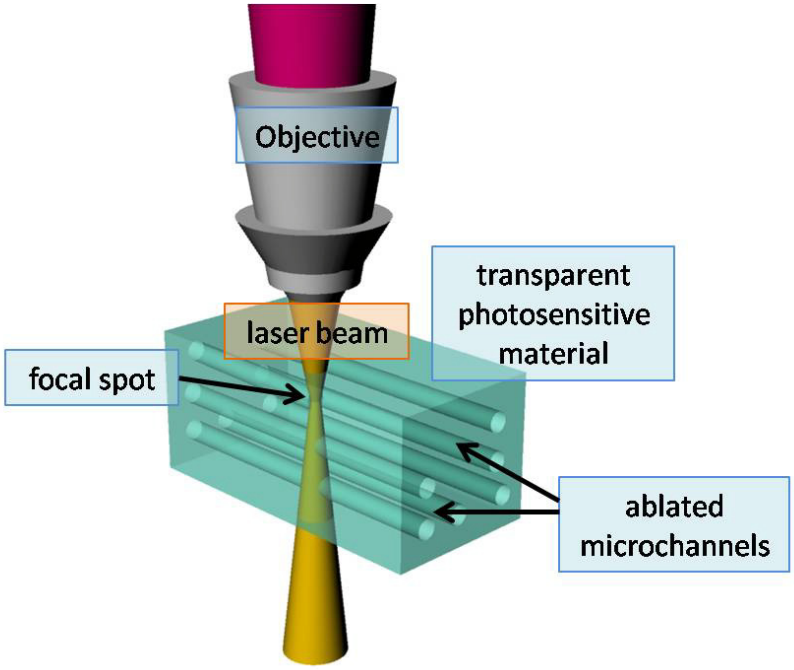

Figure 5.3. *Multi-photon laser ablation of microchannels in the bulk of a transparent material. Adapted from* [128].

Laser ablation based on single-photon absorption can only be used for two-dimensional patterning. For more complex structures, ultrafast lasers have to be employed. Through non-linear absorption caused by ultrashort laser pulses, photodecomposition can be induced even in a size scale smaller than the diffraction limit of the focusing optics. Moreover, the phenomenon can be stretched out into the bulk volume of the sample. [91] In a recent study, Sarig-Nadir *et al.* [128] used PEGylated fibrinogen hydrogels patterned with multi-photon laser ablation to guide the directional growth of neurites from dorsal root ganglia (DRG). Using two different lasers and varying process parameters, they ablated microchannels of arbitrary geometries within the bulk of the hydrogel, in which DRG cells were embedded. The cells preferred to migrate into the microchannels regardless of the channel type. Illustration of the method used is presented in Figure 5.3.

6. TWO-PHOTON POLYMERIZATION IN MICROFABRICATION

6.1. Introduction to two-photon polymerization

Two-photon polymerization (2PP) is an exciting photofabrication method, which can be used to create three-dimensional microstructures in a simple and fast manner from CAD models with a laser. Having a relatively short history in microfabrication, the technology has been described also with other terms such as *3D laser non-linear lithography* [24] and *two-photon microstereolithography* [7]. Even though the physical phenomenon behind this technology was first predicted already in the 1930's and experimentally confirmed thirty years later along the invention of lasers, the most vigorous development around 2PP has been done within the past two decades. [159] The novelty of the technology is highlighted by the fact that most the 2PP references used for this review have been written within the past ten years.

The primary application of 2PP was in the fabrication of three-dimensional photonic crystals, first proposed and demonstrated by Maruo *et al.* [92] in 1997. To date, application areas of 2PP include micromechanical systems, microfluidic devices, micro-optical components and plasmonic components. In addition to its vast success in these areas, 2PP has also shown great promise for biological applications including tissue engineering, drug delivery, medical implants and medical sensors. [7, 109, 110, 159]

Microfabrication with 2PP offers several advantages in biomedical applications. Especially for the fabrication of tissue engineering scaffolds, 2PP offers state-of-the-art resolution, high reproducibility, and a possibility to fabricated true three-dimensional structures. Also implants and prostheses can be fabricated using 2PP. [110] Even though the best achievable resolution of 2PP is in the order of nanometers, resolution can be decreased to speed up the fabrication of micro- to millimeter-scale features [111].

6.2. Basic theoretical principals

Traditional photofabrication methods, such as photolithography and stereolithography, utilize the phenomenon of single-photon absorption (1PA), in which polymerization (1PP) is initiated by absorption of one photon of a short wavelength through linear absorption. The problem with 1PA is that absorption can only occur at the surface of the photopolymerizable resin within the first few micrometers. In 2PP, on the other hand, the light beam can be focused into the volume of the photosensitive material. [159] The difference of principle between 1PP and 2PP is illustrated in Figure 6.1.

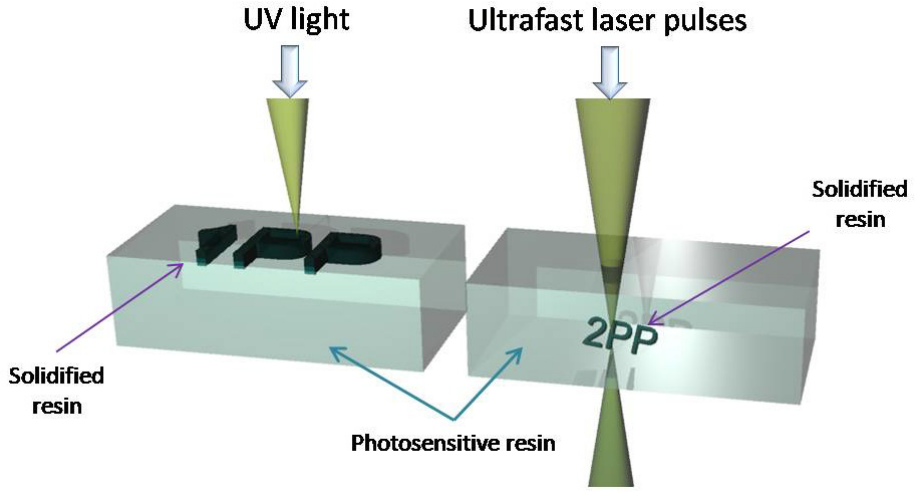

Figure 6.1. *The principal difference of 1PP and 2PP. Single-photon absorption, in the left, can only occur at the material surface. Two-photon absorption, on the right, on the other hand, only occurs at the focal point of the beam, and can thus be tightly focused into the volume of the material. Adapted from [159].*

In general, 2PP is based on radiation-matter interaction called multiphoton absorption (MPA). More precisely, in the case of 2PP, the phenomenon is two-photon absorption (2PA), in which an atom or a molecule is excited from a lower quantum state to an excited state by absorption of two photons instead of just one. The energy of each of the photons is equal to half the energy of the gap between the ground state and the excited state. 2PA can occur by two different mechanisms, which are sequential absorption and simultaneous absorption, as illustrated in Figure 6.2. In sequential absorption, a real intermediate state is produced by absorption of the first photon; this excited state has a well-defined lifetime of 10^{-4}–10^{-9} s, after which the second photon is absorbed. Simultaneous absorption only has a virtual intermediate state that is created by absorption of the first photon and characterized by lifetime of 10^{-15} s. Only if the second photon arrives within the virtual state lifetime, can it be absorbed, and thus higher intensities are required for this mechanism of 2PA. [76]

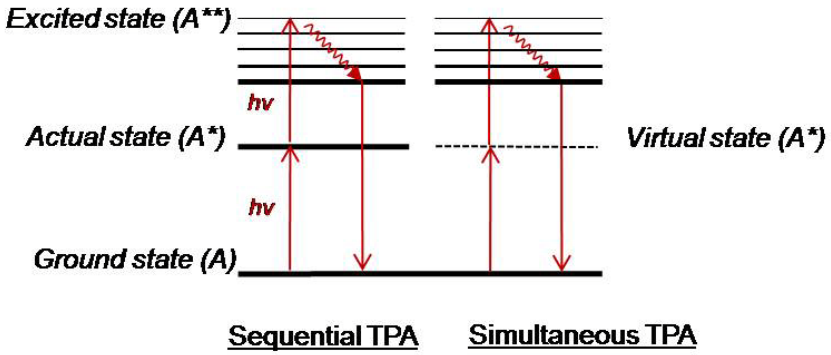

Figure 6.2. *Mechanisms of 2PA. Reproduced with modifications from [76].*

The MPA process is optically non-linear; due to a quadratic dependence of the absorption rate to the laser intensity, initiation of PI molecules only occurs in the

confined focal volume of the beam. Furthermore, polymerization does not occur unless the intensity of light at the laser focus exceeds a certain threshold value for 2PA and subsequent photoinitiation. Polymerization is thus limited to a very small volume in the photosensitive prepolymer solution, which, in turn, enables the fabrication of microstructures with resolution well beyond the diffraction limit of the focusing optics. [73, 76, 109, 159]

6.3. Microfabrication process

MPA is commonly driven by ultrafast lasers such as the Titanium:sapphire (Ti:sapphire) laser, which produces pulses of a few tens of femtoseconds in duration with high frequency (approx. 80MHz). High pulse intensity enables MPA, but the average power needed is low because the pulses are five to six orders of magnitude shorter than the repetition rate of the laser. Typically, the wavelength of the Ti:sapphire laser beam is 800 nm. [73]

As a usual fabrication set-up, the laser beam is directed into the polymerizable resin through a microscope objective with high numerical aperture to create photon density high enough. Furthermore, if an objective lens with a high numerical aperture is used, resolution of less than 100 or 200 nanometers can be obtained. The microscope is generally applied because of the more convenient sample positioning and viewing, and for being able to switch objectives easily. There are two alternate systems to manipulate the fabrication system in three dimensions: either the sample can be placed on a computer-controlled stage that can be moved in three dimensions relative to the laser beam focus – or – scanning mirrors can be used to move the focal point relative to the sample. The fabrication process can be monitored in real time with a Charge-Coupled-Device (CCD) camera and a screen using transmitted light. [73, 159]

After polymerizing the desired pattern, the cured polymer structure is developed by washing away the unpolymerized regions with an appropriate solvent. The sample is then ready to be examined and analyzed using, for example, a scanning electron microscope (SEM). [159]

6.3.1. Process characterization

Resolution in photopolymerization is determined by the longitudinal and lateral dimensions of a voxel (volumetric pixel), the smallest achievable feature size. In 2PP, voxel is the solidified volume of the prepolymer solution at the focal spot of the laser beam. The intensity distribution of the laser beam is assumed to possess a Gaussian profile, as presented in Figure 6.3. Due to a well-defined polymerization threshold, no polymerization occurs if the laser pulse intensity is not high enough. On the other hand, intensity too high will result in laser induced damage, observed as microboiling of the polymer solution during processing. The area of operation for suitable laser intensities is found between these two threshold values. [7, 76]

Resolution in 2PP is not limited by the diffraction limit of the focusing optics; theoretically, resolution depends only on the size of the monomer molecules. However, additional limits arise from the precision of approaching the polymerization threshold, which, in turn, depends on the laser system and the photosensitive material used. To date, feature sizes as small as 100 nm and below have been reported with 2PP fabrication systems. [109, 114]

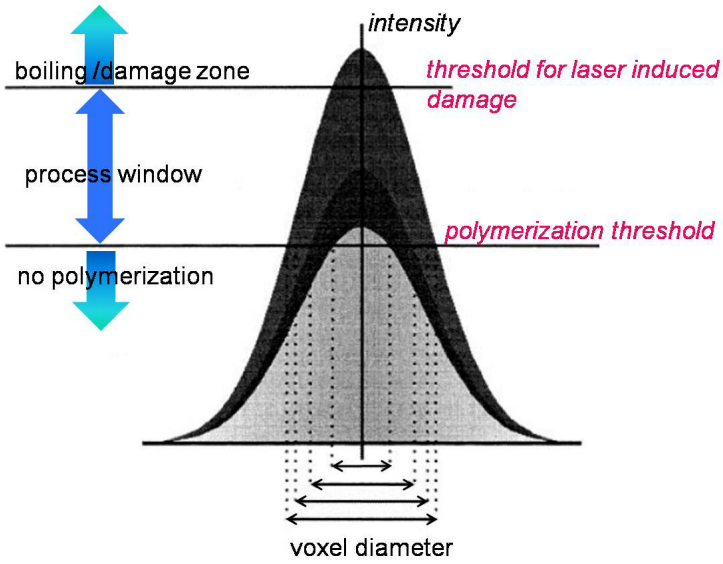

Figure 6.3. *Light intensity distribution of a Gaussian laser pulse and its contribution to voxel diameter. Reproduced with modifications from [114].*

The theoretical voxel dimensions for a certain fabrication set-up can be calculated using the processing parameters and the polymerization threshold value. Different mathematical models have been proposed for this purpose and can be found for example in refs. [7], [75] and [135]. Presentation of the equations for these calculations is excluded from this review. However, some of the main points will shortly be discussed qualitatively.

To maximize resolution in 2PP, the focusing optics should be carefully optimized. Especially the numerical aperture of the objective lens should be high enough; according to Bąk [7], optical lenses with numerical aperture of 1.3 and working distance of 200 μm are typically used in microstereolithography set-ups. Besides the focusing optics, resolution in 2PP is mostly dominated by laser power (P) and exposure time (Δt), which contribute to the laser dose ($P \cdot \Delta t$). High resolution can be achieved using low power and short exposure times. Furthermore, the voxel length is more sensitive to the power than to the exposure time. Hence, low aspect ratio voxels can be achieved by minimizing the laser power to the threshold level. In addition it should be noted that the height to diameter ratio of a voxel is mainly dependent on the NA of the microscope objective lens, and is independent on the applied laser dose. [7, 76]

The rate of polymerization in 2PP is dependent on the laser light intensity, the PI concentration, quantum yield and the initiation efficiency of the PI radicals. Additionally, any oxygen or additives can inhibit initiation leading to decreased

polymerization rate. In general, the polymerization reaction becomes faster when light intensity increases. Increasing the initiator concentration will not, however, increase polymerization rate in the same manner. A high initiator concentration may result in inefficient energy transfer and decrease the polymerization rate. Initiator molecules should be homogenously distributed within the prepolymer solution to prevent variation in the molecular weight and subsequent variation of mechanical properties in the final polymer. [159]

6.4. Selection of photoinitiator and materials

The material demands for 2PP are similar to other microfabrication methods using photopolymerization. At least two components are needed to enable the fabrication: a monomer and a photoinitiator (PI). These two constitute the prepolymer solution, which can also include additional components such as polymerization inhibitors, solvents or filler polymers. [73]

Among the photoinitiation mechanisms introduced in Chapter 3.4.1, radical photoinitiation is the most used in 2PP. Reason for this is the advantageous combination of high reaction rates, ease of processing and accessibility to wide range of suitable PI molecules and monomers for this type of chemistry. [73]

6.4.1. Photoinitiators for two-photon polymerization

When selecting an initiator molecule for 2PP, the wavelength of the light source used should be considered first. Ideally, for 2PP, the maximum absorption wavelength of the initiator should be approximately half of the wavelength of the laser beam. Commercial PIs originally indented for 1PA-induced polymerization using UV light often have a suitable absorption spectrum and thus are commonly used in 2PP. [159]

Other important characteristics of the PI are the ones that contribute to the polymerization efficiency; a large 2PA cross-section, high quantum yield, and high initiation velocity are desired [73]. The 2PA cross-section, (σ_2 *or* σ_{TPA}) is the measure of a materials susceptibility to 2PA, and widely used for comparison of 2PA activity between initiators. The σ_2 values are usually presented as units of GM (Göppert-Meyer). One GM is 10^{-50} cm^4 s $photon^{-1}$. Typical values for commercial UV initiators range from 1 to 10 GM. [159]

Due to the increasing utilization of 2PA in many research areas, special highly active initiators optimized for 2PA have been developed. A detailed discussion of the molecular design or recent research of these initiators unfortunately extends beyond the scope of this thesis, but for anyone interested, a comprehensive review on the subject is provided by Lee *et al.* [76]. In general, the use of a special two-photon initiator increases the photo-sensitivity of the whole system. Furthermore, it can lower the polymerization threshold and increase the polymerization rate. [159]

Much of the work on 2PA initiators has focused on molecules with a π-conjugated central region flanked by electron-donating (D) or -accepting (A) groups. Type I

initiators are symmetrical by structure, for example D–π–D, D–π–A–π–D, A–π–D–π–A. Type II, on the other hand, consist of asymmetrical structures such as D–π–A. By using initiators with the molecular structure described above, the 2PA cross-section can be a hundred times greater than with normal UV initiators. (E)-stilbene, bis(stryl)benzene, naphthalene, biphenyl, and fluorine count among the large group of organic molecules used in 2PA initiators. It should be noted, however, that it is not straightforward to adjust the absorption wavelength region of a PI, and much of the research has focused only on wavelengths around 800 nm, specially designed for Ti:sapphire femtosecond lasers. [73, 76, 159]

6.4.2. Materials for two-photon polymerization

As Wu *et al.* [159] describe the demands for a monomer solution to be used in 2PP, it must (1) be photocurable, (2) be transparent in the visible and near-IR region to prevent any single-photon interaction, (3) have a fast curing speed and the polymerized area should be confined to the focal spot to minimize scattering, (4) be resistant to dissolution after crosslinking and (5) not swell or be deformed by any solvent.

Both negative- and positive-tone photoresists, described earlier in Chapter 3.5, can be used in 2PP [159]. When using positive-tone resists, two-photon induced *polymerization* is not actually the case, and the technology should rather be called two-photon activated *processing*. Exposing positive photoresists to laser irradiation causes dissociation of molecules, and the irradiated regions will be washed away in the development process, as opposite to negative-tone resists. [113] Figure 6.4 shows a woodpile structure fabricated with a) SU-8 and b) a positive photoresist, S1813.

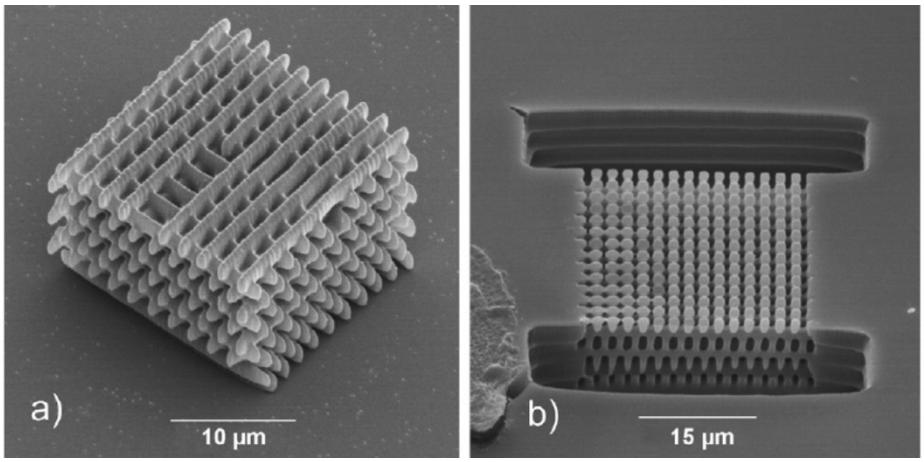

Figure 6.4. *Two-photon polymerized woodpile structures fabricated from a) a negative photoresist SU-8 and b) a positive photoresist S1813. Modified from [113].*

Many photosensitive resins have a tendency to shrink a little during the polymerization process, and therefore the mechanical properties of the material should be good enough to withstand the distortion. 2PP of solid-state negative-tone photoresists has the advantage that the absence of change in the refractive index due to liquid-to-solid transition minimizes shrinkage and defects usually seen with liquid resists. It also

creates stable recording conditions and permits the fabrication of areas behind the already crosslinked features thus enabling the fabrication of self-supporting structures. [159]

The viscosity of the prepolymer solution has a major effect on the outcome of the fabricated structure in 2PP. Usually a viscous liquid is used, but the prepolymer solution can also be an amorphous solid or a gel. Liquid samples are simple to prepare and process, which is more difficult with solids and gels. On the other hand, undesired motion and flow can occur in liquid prepolymer solutions during processing leading to distorted structures. Due to the greater viscosity of solids and gels, undesired motion is restricted in the prepolymer solution and complex structures, even with free-moving parts, can be fabricated. [73]

Photosensitive polymer solutions based on acrylate moieties are especially attractive for 2PP. Acrylates, especially as UV-curable resins, have a wide range of succesfull applications in industry and thus are commercially available in different functionalities, sizes and compositions. Photopolymerization of polyfunctional acrylates results in highly crosslinked transparent solids with high optical quality and dimensional stability. The main advantages of acrylate-based resins are their high activity and fast polymerization rate, which are especially beneficial in 2PP where fast scanning speeds are needed. [30, 73]

6.4.3. Commercially available materials

Table 6.1 lists some of the commercially available photoresists used in 2PP. One of the most utilized commercial photoresist in 2PP applications is epoxy-based SU-8. Like with other solid negative-tone photoresists, the 2PP process of SU-8 involves two steps: the creation of the reactive species upon light exposure and the post-baking step for crosslinking. Other commercially available photoresists polymerize by single-step radical polymerization due to laser light-induced PI radical formation. [159]

Table 6.1. *Commercially available photoresists used in 2PP. Modified from [159].*

Resin	Type of material	Manufacturer
SU-8	Epoxy (two-step reaction)	MicroChem
SCR500	Urethane acrylate	Japan Synthetic Rubber Co.
Ormocer®	Inorganic-organic hybrid	Fraunhofer Institute Silicatforschung
IPG	Inorganic-organic polysiloxane polymer	RPO Inc.
LN1	Urethane acrylate	Sartomer
SR348	Ethoxylated (2) bisphenol A dimethacrylate	Sartomer
Nopcocure 800	Acrylic acid ester	San Nopco
NOA63	Mercapto-ester polyurethane	Norland Products

The photopolymers listed in Table 6.1 have not been designed for biological applications and thus most of them are not very biocompatible. Furthermore, processing of these polymers involves the use of toxic solvents. To current knowledge, SU-8 and Ormocer®s have been the only commercial materials used in 2PP studies indented for biological applications. [159]

Ormocer®s (Organically modified ceramics) are inorganic-organic hybrid copolymers that consists of inorganic and organic units connected via covalent bonding. The inorganic network is synthesized by sol-gel processing and consists of oxidic species such as silicon alkoxides or metal alkoxides. The organic units, for example methacrylate groups, are crosslinked into a solid network by means of light, heat or redox-initiation. Together these networks form a solid three-dimensional structure, which contributes to the exceptional chemical and thermal stability of the Ormocer®s. [35, 48] The biocompatibility of Ormocer®s has been investigated and demonstrated in several studies, for example by Ovsianikov *et al.* [115] and Schlie *et al.* [130]. Among the wide family of Ormocer® materials, Ormocomp® has mainly been the photosensitive material used in 2PP studies, at least for biomedical purposes [35, 111, 112, 130]. It is marketed as a UV-curable material for lithographic microfabrication for applications in optics [108].

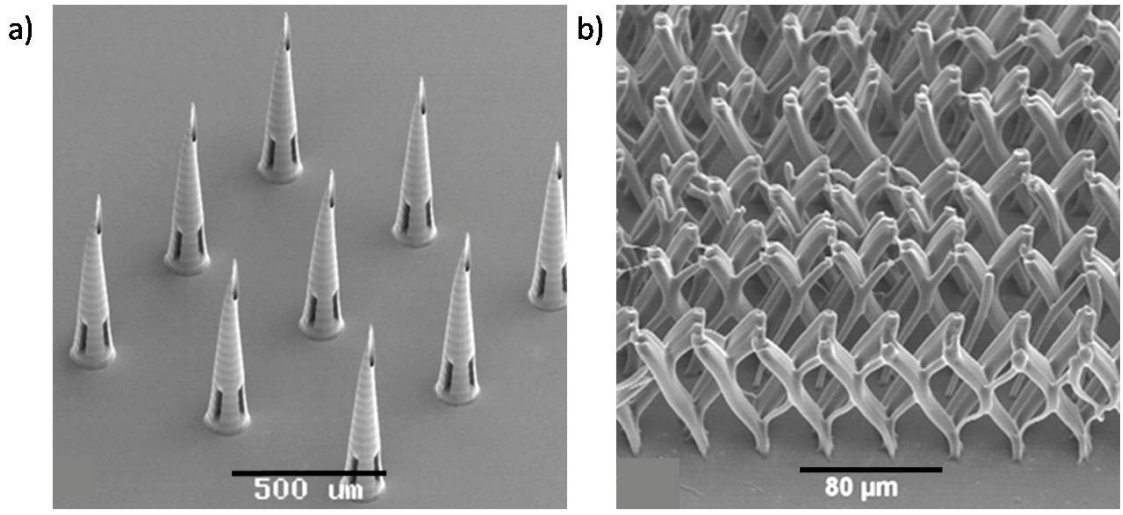

Figure 6.5. *Biomedical Ormocomp® microstructures fabricated by 2PP. a) Microneedles for drug delivery [modified from 112] and b) a porous scaffold structure for tissue engineering [modified from 113].*

Several biomedical studies of 2PP applications for Ormocer®s have been reported. Figure 6.5 presents SEM images of biomedical microstructures fabricated using Ormocomp®; an array of microneedles for drug delivery is shown in image (a), whereas image (b) presents a porous scaffold for tissue engineering purposes. In a study by Ovsianikov *et al.* [111], the applicability of 2PP in implant fabrication was demonstrated as the group managed to fabricate a robust middle ear bone replacement prosthesis in Ormocomp®, using a Ti:sapphire femtosecond laser. The fabricated part had dimensions of several millimeters; voxel size used in polymerization was more than 30 µm in length and 5 µm in width. This study did not include any *in vivo* testing. [111]

6.4.4. Proteins and other biomaterials

Due to the lack of synthetic biocompatible photopolymers available, natural proteins have been introduced to 2PP research as suitable materials for biological applications. Shear and co-workers have demonstrated the ability to fabricate biologically active protein microstructures by means of 2PP [3, 65], and reported studies of guided nerve cell growth on Bovine Serum Albumin (BSA) and avidin micropatterns [64]. Furthermore, the group has reported the 2PP microfabrication of chemically responsive hydrogels from avidin, BSA and lysozyme [63]. Campagnola and co-workers have also reported several 2PP studies on proteins, such as BSA [27, 123], fibrinogen [123] and collagen [10]. Finally, two-photon induced crosslinking of protein microstructures have also been studied at the Department of Biomedical Engineering by Turunen *et al.* [120].

Multiphoton crosslinking of proteins can be done using commercial photoinitiators; Campagnola's group has used Rose Bengal [10, 27, 123] but also synthesized new photoinitiators for two-photon crosslinking of type I collagen [124]. On the other hand, the group of Shear has placed effort on replacing the use of Rose Bengal and other cytotoxic initiators with more environmental-friendly two-photon absorbing molecules. A number of biologically based molecules were found suitable for multiphoton crosslinking of natural proteins, for example flavins (often referred to as FAD, flavin adenine dinucleotide). [64, 65]

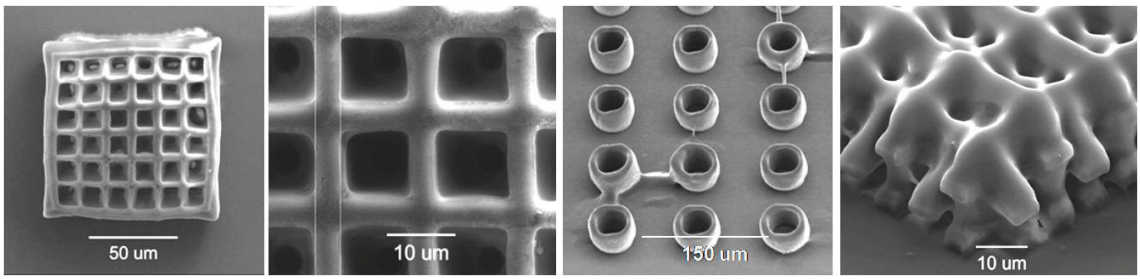

Figure 6.6. *Two-photon polymerized biodegradable microstructures fabricated from a polycaprolactone-based copolymer. Modified from [24].*

To overcome the biocompatibility issues concerning commercial photopolymers, 2PP with custom-synthesized photosensitive materials has been demonstrated. In a recent paper by Clayessens *et al.* [24], 2PP-based microfabrication of a PCL-based biopolymer with a Ti:sapphire femtosecond laser was reported. The SEM images of the fabricated structures are presented in Figure 6.6. According to the writers, the photosensitive copolymer used in the studies, poly(ε-caprolactone-co-trimethylene-carbonate)-b-poly(ethylene glycol)-b-poly(ε-caprolactone-co-trimethylenecarbonate), is both biocompatible and biodegradable. The aim of the study was to fabricate three-dimensional tissue engineering scaffolds with different structures. The structures were fabricated in a layer-by-layer fashion with the last layer on the surface of the coverslip, and despite slight distortion of the structures due polymer shrinkage, stable hollow structures could be manufactured. [24]

6.5. Applications in cell culturing and microfluidics

As is well known, cells sense and respond to their surroundings on the scale of one micron or less. Moreover, anchorage-dependent cells stay viable on adhesive surfaces, on which to exert forces and spread. Therefore, especially in tissue engineering and other cell-based applications, it is advantageous to be able to produce arbitrary scaffold structures that mimic the architecture of natural cellular microenvironments. [163]

Surface patterning with adhesion permissive and unpermissive areas has been the dominant technique for patterning neuronal networks, performed by a number of different techniques and using a wide range of different molecules. The study of neuronal patterning by Kleinfeld *et al.* in the 1980's was among the first reported. They used photolithography to pattern amines for neuronal attachment onto a cell-repellent background. Since those days, a number microfabrication techniques including photolithographic methods [126, 139], laser ablation, self-assembled monolayers [40, 103] and microcontact printing [13] have been used for creating micron-scale patterns of adhesive molecules against a non-adhesive background. [157]

Recently, 2PP has proven to be an efficient method for producing three-dimensional material constructs with subcellular resolution. Micron-scale topographies and three-dimensional structures of proteins and other biomaterials fabricated via 2PP can be utilized in the cell culture dishes to guide the attachment, growth and differentiation of the cells. There are different ways of using these microstructures: as adhesive and non-adhesive biomaterial patterns on cell culture platforms, or as cell-trapping matrices to localize cell bodies to specific substrate areas such as over recording sites on electrode arrays. [109, 159, 163]

In a recent study by Weiss *et al.* [151], three-dimensional microscaffolds with different pore sizes for chondrocyte culturing were fabricated using 2PP of Ormocomp®. As the polymerized scaffolds were seeded with bovine chondrocytes, mesh size-dependent spreading of the cells was observed, mesh holes of 60–70 μm being optimal for cell ingrowth. With smaller mesh sizes, from 10 to 30 μm, the cells oriented along the microstructures but did not infiltrate the scaffold. The results of this study demonstrate that the submicron resolution achievable with 2PP is not necessarily needed for cell-based applications, yet the true three-dimensional nature of the method is highly exploitable. [151]

Microfabrication of microfluidic structures with 2PP has been reported by Venkatakrishnan *et al.* [153] and Liu *et al.* [85, 86]. In these studies, both groups have used SU-8 as the photopolymerizable resin, which has produced stable and high-resolution microstructures. The group of Venkatakrishnan has also studied fabrication microfluidic structures by two-photon induced ablation using Ormocer® material [60]. However, among the large amount of 2PP studies published to date, none of the articles present 2PP microfabrication of microfluidic structures for biomimetic cell culturing applications.

7. MICROFABRICATION OF PHOTOSENSITIVE HYDROGELS

7.1. Photocrosslinked hydrogels

Hydrogels are highly crosslinked hydrophilic polymer networks with high water content. Due to intermolecular crosslinking, these gels are flexible and soft yet have quite good form stability – similar to soft tissues in the body. The type of crosslinking greatly affects the properties of the hydrogel. There are two classes of hydrogels, divided by the type of the crosslinks: physically and chemically crosslinked networks, depending on whether the polymer chains are linked covalently or non-covalently. Non-covalent crosslinking can be caused by several factors such as entanglement, hydrogen bonding, ionic bonding, and formation of crystallites. Another way to characterize hydrogels is to divide them by origin to synthetic, biological and hybrid hydrogels. [41, 106, 121]

Because of the numerous techniques to manipulate their properties, biocompatible hydrogels have found extensive use in biomedicine. The wide choice of hydrogels for mammalian cell culture applications includes various types ranging from purely natural to purely synthetic materials with each hydrogel possessing its own advantages and limitations. [67, 121, 149] Most hydrogels are intrinsically cell non-adhesive, but can be tailored to allow adhesion of a certain cell type [106]. For detailed discussion about hydrogels in biomedicine and biotechnology, the reader is referred to reviews [67, 121] written by Robert Langer and co-workers.

In this review, a particular interest is set on photocrosslinked hydrogels, which can be obtained polymerizing a photosensitive polymer solution in the presence of a photoinitiator using visible or UV light. Hydrogels of this type are stable and mechanically strong as a result of the covalent crosslinks between the polymer chains. [41, 106, 149]

Photopolymerizable hydrogels have generally been formed from macromolecular hydrogel precursors, such as derivatives of PEG and PVA, and modified polysaccharides. One major advantage with hydrogels is the possibility to incorporate cells, growth factors and other bioactive compounds homogenously within the material during photopolymerization. Because of the high solvent content, material transport through the gel is similar to convective mass transport in a fluid, especially for molecules significantly smaller than the gel pore size. As a major benefit in cell-based biomedical applications, this means that hydrogels are highly permeable for oxygen, nutrients and other water-soluble metabolites. [46, 106]

7.2. Poly(ethylene glycol) hydrogels

PEG has been used in many kinds of medical devices and pharmaceutical formulations. It is highly hydrophilic and biocompatible, exhibiting little to no immunogenicity. [9] The chemical structure of the PEG monomer is fairly simple, as seen in Figure 7.1. The structure is also known as poly(ethylene oxide) or PEO; the name PEG is usually used with molecular weights less than 20 000 Da. Often these terms are, however, used interchangeably. [71]

PEG chains can be modified with crosslinkable moieties, such as acrylate or methacrylate groups, to form hydrogels. Acrylates are susceptible to free radical polymerization, which enables the use of photocrosslinking in hydrogel fabrication. The chemical structure of a diacrylated PEG derivative, PEGda, is presented in Figure 7.1. [9]

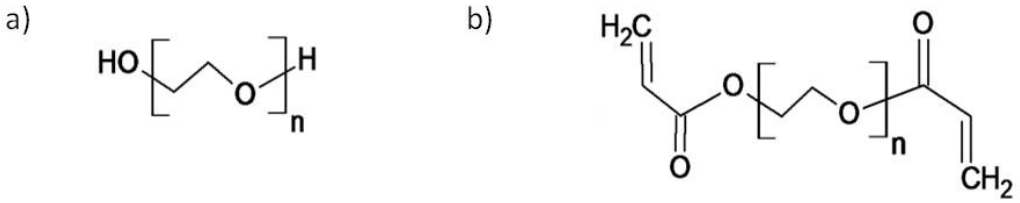

Figure 7.1. *The chemical structures of a) PEG and b) PEG diacrylate. In PEGda, the acrylate groups at either end enable crosslinking through radical polymerization. Adapted from [9].*

The PEG molecule can easily be modified and copolymerized with other monomers to introduce new polymer properties. Photopolymerizable and biodegradable hydrogels based on PEG-co-poly(α-hydroxy acid) diacrylate were developed by Sawhney *et al.* [129] In the hydrogel system developed by Sawhney and co-workers, degradation rates could be widely varied by changing the length and composition of the α-hydroxy acid segments of the block copolymers. On the other hand, the length of the PEG segment and the concentration of macromers in the hydrogel precursor solution influenced the permeability and mechanical properties of the hydrogels. A similar photocrosslinkable hydrogel material based on a copolymer of ethylene glycol and propylene fumarate has been synthesized by Suggs *et al.* [144, 145].

Like many other photocrosslinkable hydrogels, PEGs can be crosslinked in direct contact with living cells. For this reason, they have found use as post-operative adhesion preventing barriers, non-thrombogenic coatings, and immunoprotective coatings for transplanted cells, to name only a few applications for PEG hydrogels. To modify the cell adhesion characteristics of the material, peptide segments can be linked to the PEG hydrogel network by functionalizing the amine terminus of the peptide with an acrylate moiety. [9, 106]

As an example of a specific cell type, neural cells can be encapsulated within three-dimensional PEG hydrogels under physiological conditions by photopolymerizing a mixture of medium, isolated cells and the PEG macromer in the presence of a photoinitiator. The advantage of using biodegradable PEG hydrogels is that the matrix

can be remodeled and displaced by proliferating cells. Although these materials allow neural cells to grow processes into the bulk of the hydrogel, this only happens in a later stage of the matrix degradation. [90]

Recently, Namba *et al.* [104] published a novel method to enhance early process extension from primary neural cells using a porous degradable PEG hydrogel. According to Namba and co-workers, neurite outgrowth can be advanced by incorporating a continuous porous structure into the material instead of using a bulk hydrogel with mesh size too small. The researchers developed a fabrication protocol involving photopolymerization of PEG in the presence of neural cells and a fibrin network, which is then enzymatically degraded. After this a PEG hydrogel structure with interconnected pores of an appropriate size is created, thus permitting early neural process extensions and cell migration through the matrix. The dimensions of the fabricated cylindrical scaffolds were 4 mm in diameter and 3 mm wide, with the average pore size being approximately 1 μm. Additionally, Namba and co-workers showed in this study that the initial presence of fibrin in the material or its degradation do not influence cell viability of cell fate decision. The cell population used in their study contained differentiated neurons and multipotent neuronal and glial precursor cells, and is claimed by the writers to be fit for transplantation. [104]

7.3. Microfabrication techniques for hydrogels

Most of the common photofabrication methods can be applied to hydrogel materials. Liu and Bhatia [84] used a photolithography-based method to construct a three-dimensional PEG hydrogel scaffold with encapsulated cells. Living cells were suspended in an uncrosslinked polymer solution and localized using photolithographic patterning to create a high spatial organization of the cells; numerous layers could be patterned by a stepwise process. Minimum feature size achieved in the work of Liu and Bhatia was 50 μm. [12] Also stereolithography [6], UV-nanoimprint lithography [16], and laser ablation [128] have been used to create micropatterned hydrogel constructs for biomedical applications.

Studies of Shoichet and co-workers have exploited the phenomenon of light-induced molecule cleavage in the fabrication of chemically modified hydrogels. Anterior work by the group focused on neurite guidance in micropatterned three-dimensional matrices using S-2-nitrobenzyl cysteine-modified non-biodegradable agarose [89] and biodegradable HA [102] hydrogels. In these studies, focused UV laser light induced photocleavage of the 2-nitrobenzyl group, exposing the thiol groups in the hydrogel molecules. The thiols then reacted with an adhesive fibronectin peptide, glycine–arginine–glycine–aspartic acid–serine (GRGDS), exclusively within these laser-defined volumes. A chemical gradient of the immobilized peptide was created in the laser-irradiated regions due to a Gaussian light distribution; the laser patterning process is illustrated in Figure 7.2. When DRG cells were cultured on the peptide-modified

hydrogels, the GRGDS channels promoted neurite extension and cell migration despite the hydrogel material used. [89, 102]

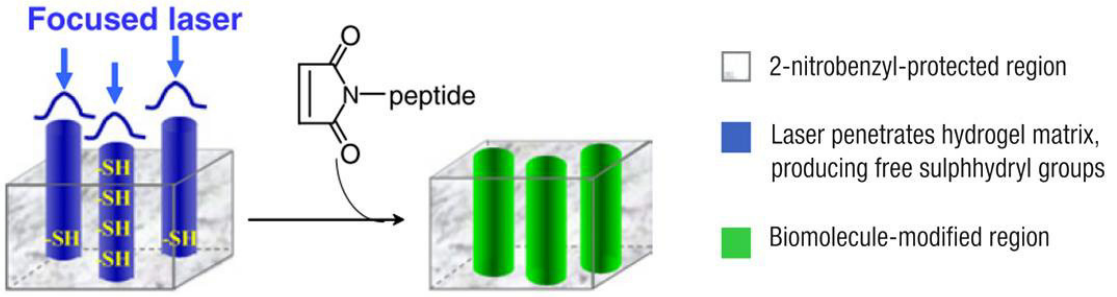

Figure 7.2. *A schematic presentation of the use of Gaussian laser light to create concentration gradients within the three-dimensional biochemical channels inside the hydrogel matrix. Modified from [89] and [102].*

More recently, the Shoichet group has employed MPA-induced molecule cleavage to produce more sophisticated three-dimensional chemical patterns in hydrogel matrices within the size scale of single cells using a Ti:sapphire laser. Wosnick and Shoichet [158] synthesized a new bromohydroxy-coumarin thiol derivative and used it for the preparation of a modfied agarose deriva tive yielding gel-bound thiols on multiphoton excitation. The thiol groups provide as sites for immobilization of complex biomolecule patterns within the hydrogel [158]. The MPA-induced chemical patterning process is illustrated in Figure 7.3. Using similar chemistry, Wylie and Shoichet [161] functionalized agarose hydrogel with primary amines. The three-dimensional amine patterns can be utilized as reactive sites for further water-based chemistry and cell adhesion.

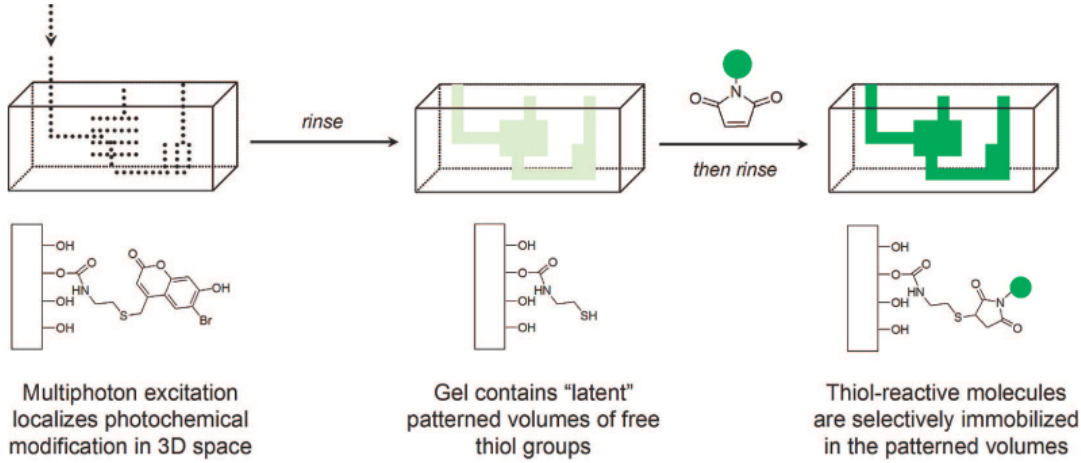

Figure 7.3. *A schematic representation of MPA-induced chemical patterning in hydrogels. [158]*

A very interesting approach to three-dimensional photofabrication of hydrogels is the combination of macroscopic photofabrication methods such as UV-curing with micropatterning using 2PP. Using this method, complex patterns of bioactive molecules or regions of altering crosslinking properties can be introduced into the bulk volume of a pre-photopolymerized hydrogel constructs. Hahn *et al.* [50] established the feasibility

of this technique for creating both biochemical and biomechanical patterns to be used in guided cell growth. The researchers used the concept of 2PP to create complex patterns of the cell adhesive peptide arginine–glycine–aspartic acid–serine (RGDS) within a pre-photopolymerized macroscopic hydrogel construct and demonstrated the ability to use these patterns for cell guiding. [50]

In the experiments of Hahn and co-workers, a precursor solution of fluorescently labeled acryloyl (ACRL)-PEG-peptide was first allowed to diffuse into a preswelled PEGda hydrogel. Computer-designed virtual masks were employed to crosslink different patterns using a Ti:sapphire laser induced 2PA (at wavelength of 720 nm). Also spatial gradients of immobilized ACRL-PEG-RGDS could be created by varying the exposure time used during crosslinking. In addition, alteration in the crosslinking density of the hydrogel could be introduced by crosslinking a PEGda prepolymer solution of lower molecular weight within the original hydrogel. The ability to spatially modify the mechanical and transport properties of the hydrogel at the cellular scale is desirable for many applications. In the final fabrication step, the patterned hydrogel was developed by immersing it in HBS and letting the unbound ACRL-PEG-RGDS solution to diffuse out of the gel. [50]

A similar study was recently published by Seidlits *et al.* [133] from the Shear group. The aim of their work was to produce a three-dimensional culturing environment for neural cells with the ability to guide cell localization and outgrowth with micrometer accuracy. Using femtosecond laser induced multiphoton excitation, pre-UV-cured HA hydrogels were spatially modified with biotinylated BSA. Micropatterns used in the study are shown in Figure 7.4. After development of the photocrosslinked patterns, they were functionalized with NeutrAvidin and coupled with laminin-derived peptides to provide chemical adhesion cues for neuronal guidance. It was demonstrated that the patterns effectively guided migration of DRG cells and embryonic neural progenitor cells cultured on the hydrogels. [133]

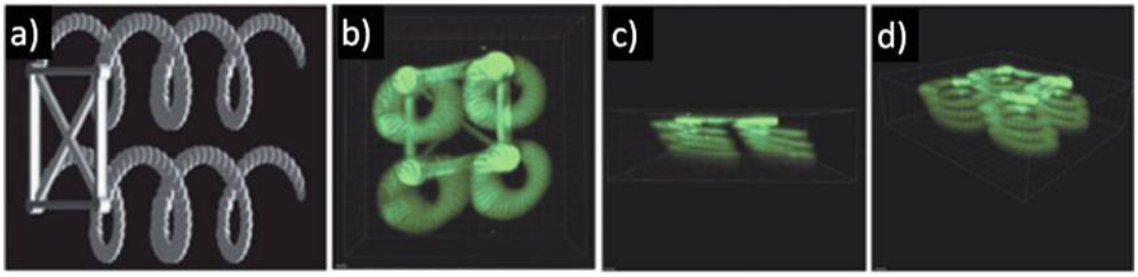

Figure 7.4. *a) The micropattern CAD design used in 2PA-induced protein crosslinking, b), c) and d) 3D reconstructions of confocal microscope images of BSA helices fabricated inside an HA hydrogel. The square pattern at the top of the pattern has side length of 40 µm, whereas the helices have diameter of 50 µm and length of 45 µm. Modified from [133].*

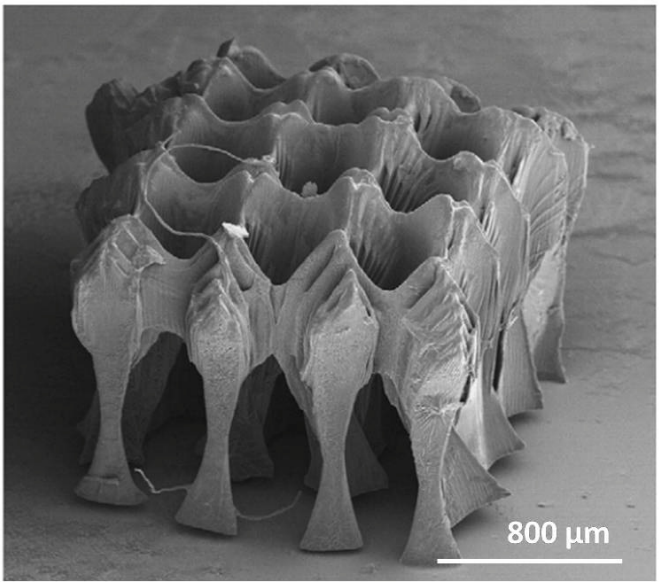

Figure 7.5. *A PEGda scaffold for cartilage tissue engineering fabricated by means of 2PP. Modified from [113].*

In addition to biomolecule patterning, multi-photon processes can be utilized for direct three-dimensional microfabrication of hydrogel materials. Especially PEGda has been used as a photoresist material in 2PP experiments. As Ovsianikov *et al.* [113] describe, using this material it is possible to bring together a very flexible microstructuring technology and a well-known material platform. A PEGda scaffold for cartilage tissue repair is presented in Figure 7.5. The scaffold provides free space for cell migration and flow of growth media in the lateral direction, whereas it is designed to sustain vertical loads [113].

7.4. Applications in microfluidics

An important class of hydrogel materials is stimulus-responsive hydrogels, which can be defined as "smart" polymers that change their degree of swelling according to changes in environmental conditions. Therefore these hydrogels can be classified to temperature, pH, electric, light, glucose, antigen and magnetic field sensitive according to the stimuli they respond to. Some hydrogels are capable of responding to multiple stimuli. For example pH sensitive hydrogels undergo volume transition due to change in molecular charge. Osmotic pressure exerted by mobile counter-ions neutralizing the hydrogel network causes expansion of the hydrogel. pH sensitive hydrogels are used to control the temporal release of pharmaceuticals, for instance. In the field of microfluidics, stimulus-responsive hydrogels have found use, for example, as valves, actuators and flow sorters. [18, 78]

The potential of using volume transition of hydrogels as "chemical muscles" was discovered already in 1950 by Kuhn *et al.* [72]. Today, stimulus-responsive hydrogels have been employed in microfluidic devices to replace some major components such as microsensors and microactuators that traditionally are driven by electricity. In a

hydrogel-regulated system, basically no external power source is needed and flow control is achieved by coupling the stimulus-induced volume expansion of the hydrogel to the microchannel width. [18, 78] A detailed discussion of hydrogelic microcomponents in microfluidics can be found in a review [37] by Eddington and Beebe.

One of the most efficient and easy ways to incorporate hydrogelic components within microfluidic channels is the use of *in situ* photopolymerization. Typically, a pre-polymer solution consisting of monomers, crosslinker molecules and photoinitiators is flowed into the microchannel, and patterned via UV-polymerization through a photomask. The method is illustrated in Figure 7.6. [37]

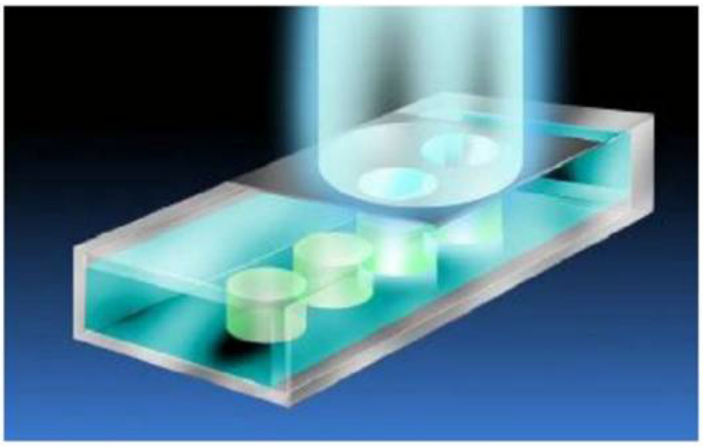

Figure 7.6. *In situ photopolymerization of hydrogelic microcomponents within a microchannel. [37]*

Using the photopolymerization method described above, Burdick *et al.* [14] fabricated gradient hydrogels using a PDMS microfluidic system. Controlling the injection flow rate, pre-polymer solution was injected into the channels and subsequently crosslinked with UV light. Flow rate control led to the formation of gradients of immobilized molecules incorporated to the prepolymer solution. Gradients of crosslinking density could be produced in a similar fashion. According to the writers, these gradient hydrogels could be used for photoencapsulation of cells and molecules to be used in tissue engineering applications. [14]

8. CONCLUSIONS AND FUTURE PERSPECTIVES

The power of microfabrication technologies in biomedical applications lies in the ability of replicating the cellular microenvironment. Compared to traditional cell culture techniques, microfabrication, combined with surface chemistry methods and microfluidics, provides means to control many parameters that affect cellular and subcellular events and signaling pathways. Micropatterned surfaces can be utilized to introduce mechanical and topographic cues into culture systems, enabling spatial control over cell behavior. Topography-induced contact guidance of various cell types, from fibroblasts to neurons, has been demonstrated with microfabricated substrates. Furthermore, microfluidic delivery of soluble factors provides chemical tools to regulate cell behavior such as neuronal growth and synaptic development. [12, 80]

In the former chapters, the convergence of microscale fabrication methods and biomaterial technology for the advance of biomedical applications was reviewed. As a special approach, the use of photofabrication methods in patterning microstructures for cell culturing devices was elaborated. It is clear that photofabrication has numerous advantages over other fabrication techniques that require elevated temperatures and pressures. However, utilization of light as driving force sets special demands for the substrate material and thus limits the range of biomaterials readily available for fabrication. Moreover, most photofabrication methods require multiple steps when three-dimensional structures are fabricated. Therefore the insintric three-dimensional nature of 2PP microfabrication makes it superior to other methods. Although 2PP has its advantages including high resolution and fast production rate, the incorporation of 2PP technology with biomedical research has just started and offers a wide-ranging field of work for researchers worldwide.

As the microfabrication technology develops complexly organized multiphenotype tissue constructs will be realized using advanced microfabrication methods. Further development in cell-based microscale systems will be realized through the integration of active microscale components such as micropumps and valves, which provide control over the flows and concentrations of culture media, oxygen, nutrients, and other biochemical factors. Integration of these elements into extracorporeal devices seems to be a natural development that will improve control and reliability, and lower the costs. A challenge for the future lies in the integration of these devices into fully implantable, biodegradable systems. [12]

EXPERIMENTAL STUDY

9. MATERIALS AND METHODS

9.1. Materials and characterization

Two photocurable polymer materials were used in the study. One of the materials was a commercial PEGda hydrogel (Sigma Aldrich, Steinheim, Germany). The chemical structure of PEGda was presented in Chapter 7.2, in which photocrosslinked PEG hydrogels were discussed in general. The PEGda prepolymer solution appeared as a colorless transparent liquid with viscosity of 57.000 cps (25 °C) and number-average molecular mass of 575 g/mol.

The other photosensitive material tested was a biodegradable PCL-based oligomer, custom-synthesized at the Laboratory of Polymer Technology in TKK (Aalto University School of Science and Technology). The synthesis reactions for the PCL oligomer, which was kindly donated for our experiments by TKK, were presented in Figure 3.4 (Chapter 3.6, Photosensitive biomaterials). The oligomer solution was a colorless liquid like PEGda, but opaque and much more viscous.

To initiate the photopolymerization reaction, a commercial UV photoinitiator, Irgacure® 127 (Ciba Specialty Chemicals, Basel, Switzerland) was added to the prepolymer solutions. Three different solvents were used for sample development, 2-propanol (99.8 %, Labscan Limited, Dublin, Ireland), dichloromethane (Sigma Aldrich, Steinheim, Germany) and Ormodev® (Micro Resist Technology, Berlin, Germany).

The absorbance of light energy in the UV range was measured for both the PCL oligomer and PEGda, in the prepolymer solutions with and without the initiator. The measurement was carried out with a UV-vis spectrofotometer (Unicam UV 540, Thermo Spectronic, Cambridge, England).

9.2. Methods

9.2.1. Laser equipment set-up

In the polymerization experiments, a diode-pumped passively Q-switched Nd:YAG microchip laser (PULSELAS-P-1064-300-FC, Alphalas, Göttingen, Germany) with the pulse duration of 800 ps and the maximum repetition rate of 15 kHz was used. The laser beam wavelength was 532 nm. The entire set-up of the laser equipment is presented in Figure 9.1. As seen in the picture, the laser source was placed on top. The beam was directed through a microscope (Nikon ECLIPSE ME 600, Nikon, Japan) to a 50x oil immersion objective. For controlling the laser exposure of the samples, a shutter and its controller (SH05 Beam Shutter and TSC001 T-Cube Shutter Controller, Thorlabs, Germany) were used. A motorized xyz-stage (SCAN 130x85, Märzhäuser Wetzlar,

Germany) with a controller (Corvus TT, ITK Dr.Kassen, Germany) was employed to enable accurate 3D fabrication. Two computer programs were used to control the movements of the sample stage: WinPos (ITK Dr.Kassen, Germany) and CorvusControl, a noncommercial program specially designed for this fabrication method. When simple two-dimensional structures were to be polymerized, the WinPos software was used, whereas all three-dimensional structures were fabricated with the CorvusControl program. The polymerization process could be monitored in real time with a CCD camera (CV-M10RS, JAI Corporation, Japan) and a commercial application program called Ulead DVD Movie Factory™ 4.0 (Ulead Systems, Inc., Taipei, Taiwan).

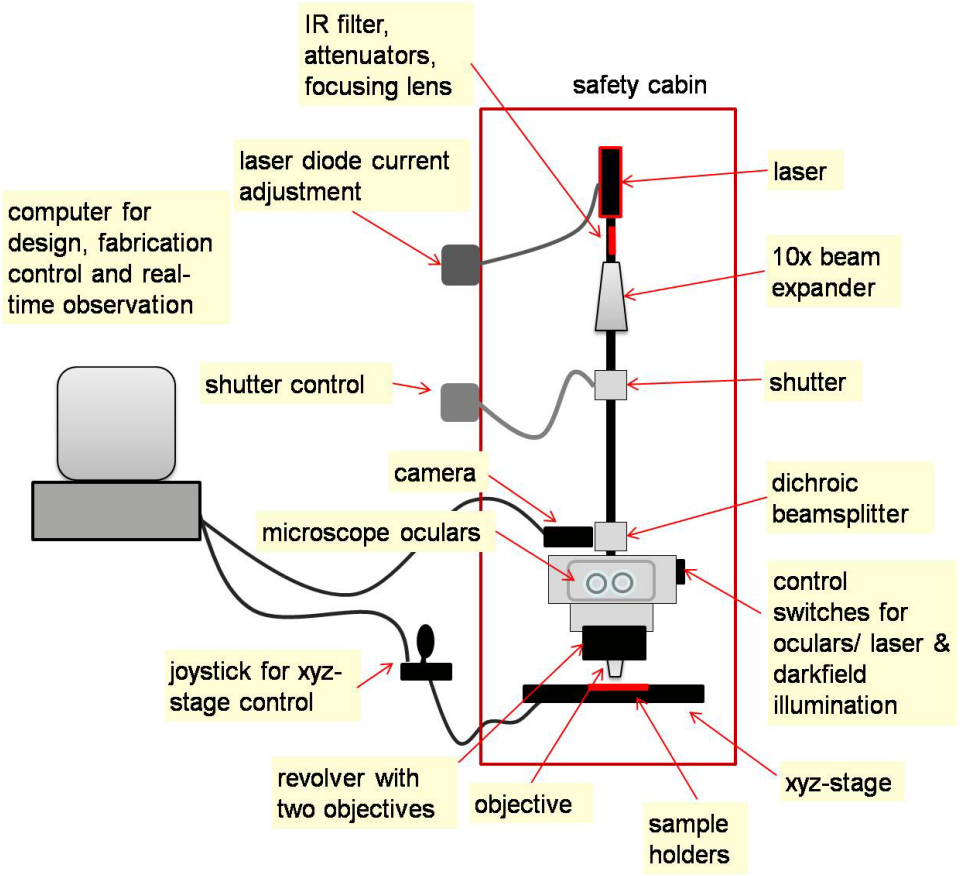

Figure 9.1. *A schematic drawing of the laser equipment set-up.*

The power range of the laser was roughly adjusted pre-fabrication using a suitable mass attenuator. There were five different mass attenuators available, allowing 0.3 %, 12.5 %, 25 %, 40 % or 50 % transmittance of the incident light. During the polymerization process, the laser power could not be directly adjusted. Instead, the laser diode current I could be varied from 1.75 A to 2.52 A. The diode current value was assumed to be directly related to the average laser power P_{avg}, and could thus be used to adjust the average power. Furthermore, in this laser system the laser pulse frequency f also changed along the laser current. The dependence was presumed linear, pulse frequency varying from 5 kHz to 15 kHz as the laser current value changed from 1.80 A

to the maximum of 2.52 A. The peak laser power P_{peak} and the pulse energy E for each pulse can be calculated using the following equation:

$$P_{peak} \cdot \Delta t = P_{avg} \cdot T = E \quad (9.1)$$

in which T is the inverse value of pulse frequency f, also known as *cycle time*. Δt is the laser pulse width, which, for this system, was kept constant at 800 ps. In Figure 9.2 the trend values drawn from measured average power and pulse frequency, as well as the calculated values of peak power and pulse energy are presented as functions of the laser current.

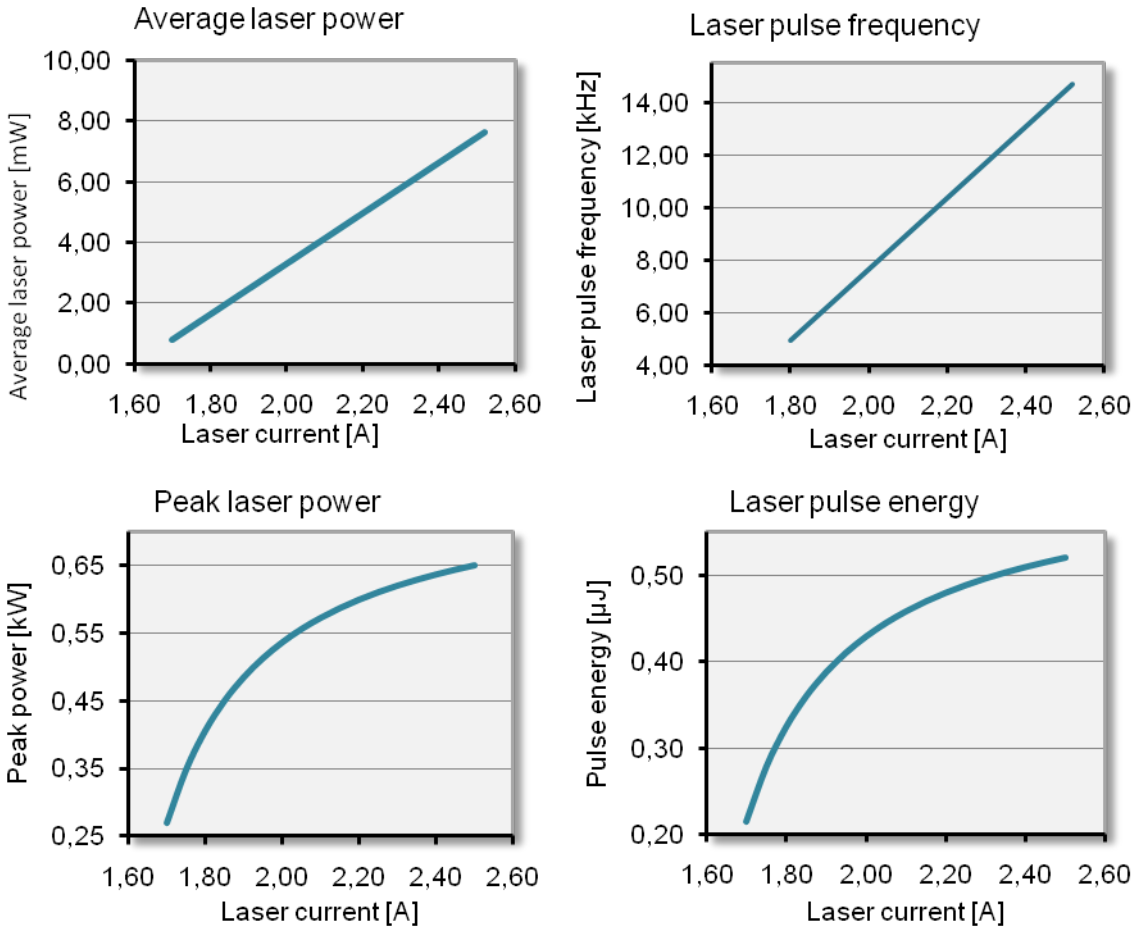

Figure 9.2. *The average power, pulse frequency, pulse energy and peak power are presented as functions of the laser current, the only accurately adjustable parameter in the laser system used in the experiments.*

The average laser power graph is based on measurements done with a hand-held laser power meter (LaserCheck, Coherent Inc., Santa Clara, CA, USA) using the 25 % attenuator and a 50x objective (NA = 0.90, Meiji Techno, Japan).

9.2.2. Fabrication of the prepolymer mixture

Fabrication of the prepolymer mixtures was simple and could be done in room temperature. All the prepolymer mixtures used in the experiments were fabricated using the following protocol: a spesific amount of the PI (Irgacure® 127) powder was

dissolved in a monomer sample by stirring the mixture with a magnetic stirrer for several hours in order to produce a homogenous solution. Different stirring times from 5 to 20 hours were used, although even the shortest time proved adequate and for each mixture the time was mainly determined by fabrication practicalities. During the process, care was taken to protect the mixture from light by covering the container with aluminum foil to prevent premature curing. Additionally, efforts were made to minimize the amount of any impurities in the final mixture. The proportioning process had some differences depending on whether PEGda or PCL oligomer was used due to the very different viscosity values of the materials.

The PCL oligomer (PCL-o) is highly viscous, hence could be pipetted. It was also very inconvenient to measure the solution by volume. Therefore, proportioning the PI according to weight percentages was chosen as the most expedient method. First, a fairly small amount – a couple of milligrams – of PCL-o was dispensed in a small container and weighted. Then the amount of PI needed was calculated with the following equation:

$$Weight\ percent = \frac{weight\ of\ solute}{weight\ of\ solution} \cdot 100\% = \frac{\boldsymbol{m_i}}{m_i + m_m} \cdot 100\% \qquad (9.2)$$

in which m_i and m_m denote the weights of the PI and the monomer solution, respectively. The proper amount of PI was then weighted, allowing a measuring error of ± 0.5 mg, and dispensed among the monomer solution. After stirring, the PCL-o prepolymer mixtures were stored in room temperature and protected from light.

For PEGda, proportioning could be done by pipetting due to the low viscosity of the material. Volumes of 2–4 ml were commonly used, and since the density of the solution was known (ρ_{PEGda}=1.12 g/ml), weighing was unnecessary. The suitable amount of PI could then be calculated, weighted and dispensed among the monomer solution. After stirring the PEGda prepolymer solutions were stored in a refrigerator in order to prolong the shelf life of the material.

From here on, the prepolymer mixtures will be abbreviated as PCL-o-α and PEGda-β, in which α and β denote the percentage of initiator per weight for each solution. PCL-o solutions of α = 2, 3, and 5, and PEGda solutions of $\beta = 0.5$, 1 and 1.5 were used in the experiments.

9.2.3. Substrate silanization

All the polymerizations were done using commercial microscope glass slides as substrates. To ensure that all polymerized structures would attach firmly to the substrate and not float away during development, the glass slide surfaces were treated with a coupling agent, 3-(trimethoxysilyl)propyl methacrylate (MAPTMS, Sigma Aldrich, Steinheim, Germany). The chemical structure of this silane coupling agent is presented in Figure 9.3. As seen in the picture, the molecule reacts with the glass surface by its silyl unit, leaving the functional methacrylate moieties pendant.

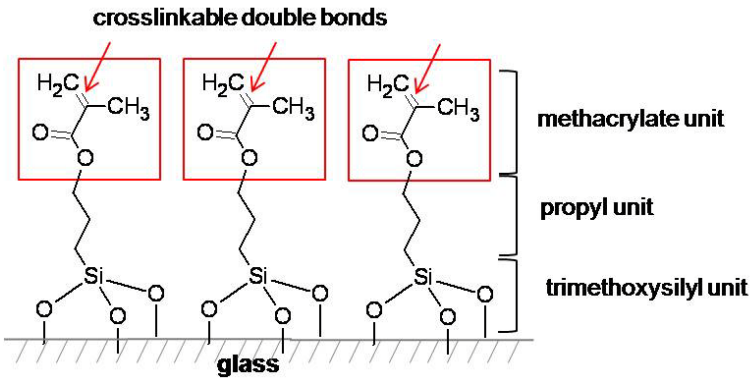

Figure 9.3. *The chemical structure of a glass surface silanized with 3-(trimethoxysilyl)propyl methacrylate (MAPTMS). Adapted from [62].*

The silanized surface is highly susceptible to moisture, and thus the silanized glass slides were stored in a desiccator to avoid denaturation and subsequent loss of functionality. A detailed description of the silanization procedure can be found in Appendix 1.

9.2.4. Sample preparation

Sample preparation for the polymerization procedure was simply done in room temperature, although only red light could be used for lightning to prevent premature curing. Furthermore, a green light filter was added in front of the microscope light source in order to provide suitable yellow light for the polymerization process.

First, a diamond blade was used to make a small scratch on the glass surface at one end of the glass slide; the scratch was needed for visual control to keep the same side of the slide up during processing. Even though the silanized microscope glasses were stored in a desiccator, they could be handled in room atmosphere during sample preparation. A 150 µm thick steel spacer was used to control the fluid on a microscope glass slide; spacer and glass slide dimensions are presented in Figure 9.4. As seen in the figure, the spacer has five equal circular holes, of which only one was used in these experiments to facilitate handling of the sample. The spacer was attached to the glass with a few spots of vaseline (Kløver® Vaseline, Chesebrough-Pond's Inc., USA).

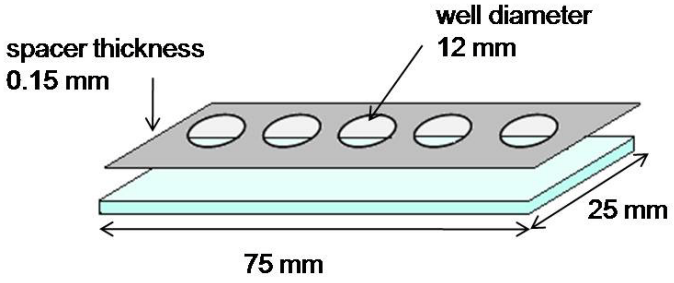

Figure 9.4. *Sample set-up for polymerization. A spacer with five circular wells was attached on a microscope glass of equal size to facilitate handling of liquid samples.*

Usually the middle well of the spacer was used, and a tiny scratch, or sometimes two, was made on the glass surface to enable setting the laser focus at the glass surface, and to ease locating the structures after development. The scratches were kept very narrow and small, since any shattered pieces of glass could not be rinsed away due to the delicate silane layer on the glass surface.

The PEGda prepolymer solutions were liquid enough to be pipetted into the spacer well using sample volumes of 20 to 30 microlitres. For all samples, any bubble formation was avoided. The fluid was then covered with a glass coverslip, which was also attached to the spacer with vaseline.

The PCL-o solutions were more viscous and would have blocked the jet of the pipette. Therefore a wooden stick was used to deliver small globs of solution into the well. Then again, a glass coverslip was attached to the spacer with vaseline. Since the PCL-o prepolymer solutions were in a crystallized stage at room temperature, the samples had to be slightly heated up before polymerization. Theoretically, temperature of 30 °C degrees was enough the melt the crystals and remove air bubbles from the sample. The heating was done with a hand-held fan heater by holding the sample above warm air flux for approximately five minutes. Measuring of the sample temperature could not be done strictly, but it was evaluated by sensing the heat flow on skin. Microscopic inspection was used to ensure that the heating was done successfully.

Once the sample was ready to be processed, it was placed on the microscope stage and a small droplet of immersion oil was applied on top of the coverslip to enable focusing of the light beam.

9.2.5. Computer-controlled manufacturing of microstructures

At first, a CAD model of the desired structure was made with either the WinPos program for two-dimensional structures or the Rhinoceros® (Robert McNeel & Associates, Seattle, USA) program for three-dimensional structures. With Rhinoceros®, a scanning contour method was used to slice the structure into layers; the required height of the contours depended on the photopolymer used and was experimentally adjusted.

For 3D models, the CAD data was then transferred from Rhinoceros® to the CorvusControl program, which converted this information into xyz-stage scanning coordinates. The 2D structures designed with WinPos could be directly fabricated with same program, which converted the entered data of coordinates into xyz-stage movements and simultaneously controlled the shutter as programmed. The polymerization process could be simultaneously monitored with the CCD camera and the Ulead program. This is possible, because the refractive index of the sample material changes slightly during polymerization and the illuminated structures become visible [24].

The optimal processing parameters such as xyz-stage scanning speed, laser current and light attenuation for each polymer-initiator-solution were studied first. The WinPos program was used to polymerize simple two-dimensional structures such as lines and

lattices by varying parameters. In addition, voxel arrays were polymerized with WinPos for resolution calculations.

After finding the suitable parameter combination for each sample material, more complicated structures such as three-dimensional cones, cylinders and miniature animals were polymerized.

9.2.6. Development procedure

When the polymerization process was finished, the sample was removed from the processing cabin and the coverslip and the spacer were stripped off in red light while keeping the room otherwise darkened. Vaseline surrounding the sample area was carefully wiped away and the remaining unpolymerized oligomer solution was then washed away with a suitable solvent.

For all PEGda samples the used solvent was water. The sample was held on decanter while rinsing the sample surface with ultrapure water using a plastic bottle with a straw. This was continued only until no monomer solution remained visible on the glass slide.

For PCL-o samples one of two solvents could be used: dichloromethane or Ormodev®, which is a 50:50 mixture of 4-methyl-2-penthanone and 2-propanol usually used in developing Ormocomp® samples. No differences in the solubility of PCL-o in these two solvents were observed, and the solvent choice was made randomly or based on availability. The sample was held over a Petri dish and rinsed using a Pasteur pipette to proportion the solvent. As with PEGda, rinsing was continued until all monomer solution had been washed away. The PCL-o samples were additionally rinsed with a less toxic solvent, 2-propanol. After adequate rinsing, the sample was examined with a 20x air objective to make sure the development was successful. Only when the development procedure was finished, the lights could be switched on again.

9.2.7. Imaging

The optical microscope included in the fabrication set-up was utilized for sample imaging and analysis before and after development. The 50x oil immersion objective used in polymerization was also used for pre-development sample imaging. After the development procedure, a 20x air objective was utilized for imaging and visual evaluation of sample quality.

Two scanning electron microscopes (Philips XL-30, Philips Electron Optics, Eindhoven, Holland; JEOL JSM – 6360 LV, JEOL Ltd., Tokyo, Japan) were employed for more precise sample characterization. Before imaging, the sample glass slides were cut smaller to fit the sample holders in the microscope. The cut pieces were sputtered with gold for 30 seconds three times in argon atmosphere (S 150 Sputter Coater, Edwards, UK).

9.2.8. Resolution calculations

For resolution studies, arrays of voxels and simple lines were polymerized by progressively varying exposure time and laser power by adjusting the xyz-stage scanning speed and the laser diode current, respectively. Other fabrication parameters were kept constant for each sample to obtain maximal comparability. SEM images of lines and voxels were then used for resolution characterization with the help of a free image processing software, GIMP 2.6 (GNU Image Manipulation Program) [44]. The dimension calculations were done by measuring the voxel or line height as pixels and then comparing the value to the scale bar length to obtain the dimensions in microns. An example of voxel dimension measurement is shown in Figure 9.5.

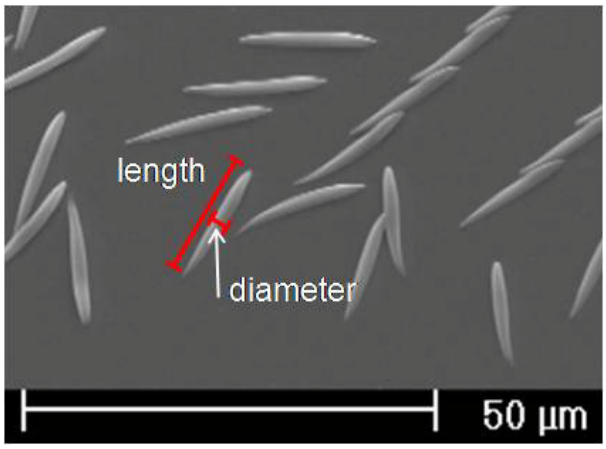

Figure 9.5. *SEM image of individual voxels, where the measured length and diameter of one of the voxels are indicated with red scale bars.*

Voxel arrays

The lateral and vertical resolution of the fabrication system was determined from SEM images of voxel arrays. Individual voxels were produced by programming the shutter to open and close periodically while the xyz-stage translated and descended between these commands. An ascending scan method was utilized to produce the voxel arrays, which means that initially, a certain number of voxels were polymerized in each row by lifting the laser focus progressively by 1 µm between every voxel. The ascending scan was used to find the optimal focus height for creating complete voxels, since the focus height could not be automatically determined. A schematic drawing of the ascending voxel scan is shown in Figure 9.6.

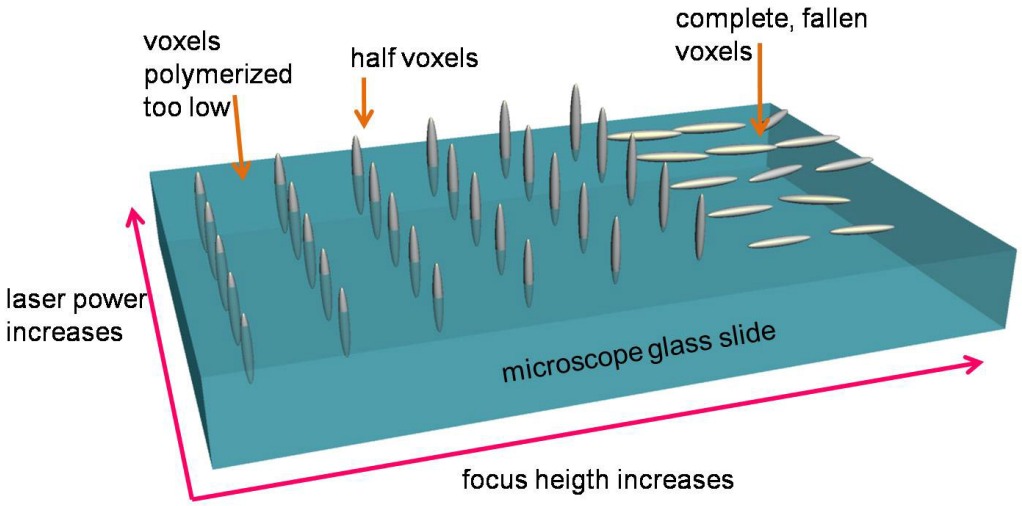

Figure 9.6. *A schematic view of the ascending voxel scan method.*

Figure 9.7 presents the five possible focus height positions for voxel fabrication. If the focus height is too low (voxel A), only the top of a voxel is polymerized on the substrate. In cases (B) and (C) the voxel is attached to the substrate by its bottom, but the geometry is clearly visible. These voxels can be used for diameter and height calculations. The optimal voxel for measurement is (D), which has almost been washed away during the development procedure, but it is still attached to the substrate. Both diameter and height are clearly visible and can easily be measured from the SEM image. In case (E), the focus height is too high, and the voxel will float away in the development process.

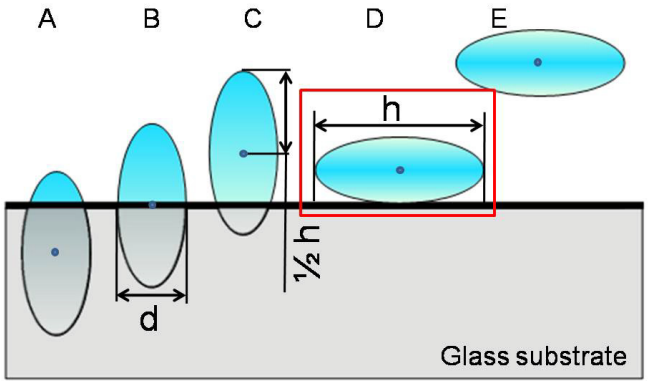

Figure 9.7. *Optimizing the focus height for fabrication of measurable voxels. The blue dots in the middle of the voxels symbolize the focus height. Voxels B, C and D can be used for dimension measurements, whereas voxels A and E are immeasurable.*

Figure 9.8 presents a PEGda-0.5 voxel array with close-ups of complete, measurable voxels (image b), and voxels that have been polymerized with a focus height too low (image c). In visual estimation, voxels possessing an ellipsoidal shape were selected for length calculations. This was repeated for all the voxel samples.

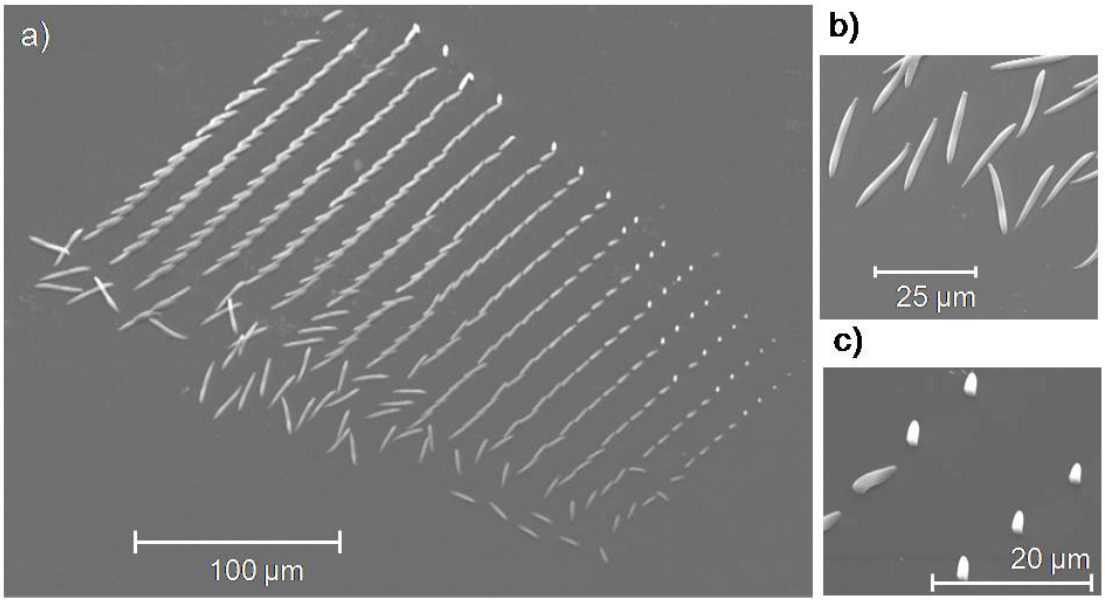

Figure 9.8. *a) SEM image of a voxel array and close-ups of voxels that have been polymerized with b) an optimal focus height and c) focus height too low.*

Two-dimensional lines

Two-dimensional lines were polymerized with varying scanning speeds and diode currents. Although resolution calculations were also done with voxels, continuously polymerized lines provide information on resolution dependence not only on the laser power but also on the exposure time.

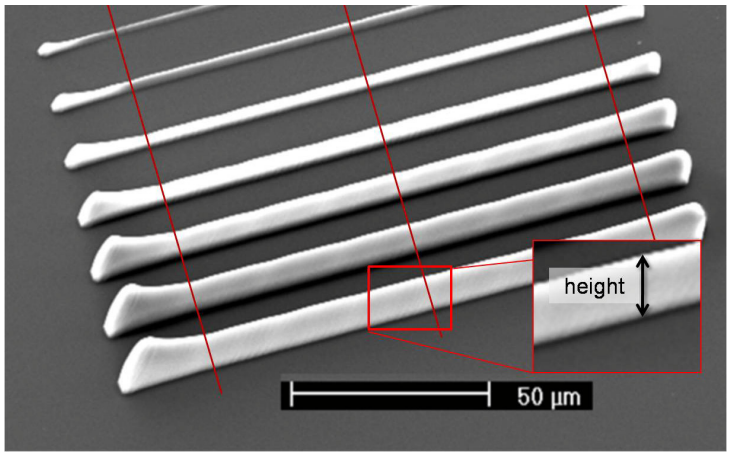

Figure 9.9. *SEM image of a line array for height calculations, with a close-up of the height measurement point.*

An example of a line array used for height calculation is presented in Figure 9.9. Three measurements were taken from each line at the points where the drawn lines intersect the polymerized lines. The close-up shows the direction of height measurement. The outermost lines drawn on the SEM images are placed so that in between the height of the polymerized line is nearly constant.

9.2.9. Initial cytotoxicity testing

Materials used in cytotoxicity testing were PEGda and PCL-o prepolymer solutions containing 1.5 wt-% and 3 wt-% of photoinitiator, respectively. Macroscopic samples were fabricated by curing thin films with a UV lamp (BlueWave™ 50, Dymax, Torrington, CT, USA). The sample set-up was similar to what was used in the 2PP experiments, employing a microscope glass and a spacer. The microscope glass was, however, coated with Teflon tape to ease peeling of the cured films, and no coverslip was used. The cured sample films had dimensions of 12 mm in diameter and approximately 150 μm in thickness. After curing, the samples were developed by immersing them into with water (PEGda) or dicloromethane (PCL-o). Furthermore, a careful disinfection procedure was carried out by washing the samples with ethanol in order to minimize contamination in cell testing. The disinfected samples were placed into a sterile 96-well plate, from which four wells of each material were used in the experiment. Sterile phosphate buffered solution (PBS) was poured onto the wells, the well plate was sealead and delivered for cell testing. Laminin (solution 10 μg/ml) coated polystyrene samples were used as control.

The cytotoxicity testing was done at Regea Institute of Regenerative Medicine. The experiment was done using human embryonic stem cell derived neural cells. These stem cells had been differentiated towards neurons during 8 weeks in neural differentiation medium in presence of FGF (fibroblast growth factor). In that time, the cell population consisted over 90 % young neurons, while a little amount astrocytes and non-neural, epithelial like flat cells were also present. Small cell aggregates were plated onto sample surfaces in NDM. Cells were let attach to surfaces and after 7 days the attachment and viability of cells was observed. Observation was done using a live-dead cell viability-kit (Sigma) to dye live cells green and dead cells red or yellowish.

10. RESULTS AND DISCUSSION

10.1. Objectives of the study

In the experimental part of this thesis, two-photon induced polymerization of two photosensitive materials, a novel custom-synthesized PCL-based oligomer and a commercial PEG hydrogel, was studied using a commercial photoinitiator. The aim was to make a comparison between these materials in terms of processability and resolution. As a special approach, the effect of photoinitiator concentration on resolution was investigated. The polymerization study was done using a microfabrication equipment based on a Nd:YAG laser. No previous reports on 2PP of PEG hydrogels with this type of a laser have been published. Furthermore, this was the first time that the biodegradable PCL-based photosensitive material was utilized as photoresist in 2PP. Consequently, the experimental study presented in this thesis is original and innovative in every aspect.

In addition to polymerization experiments, initial evaluation of the biocompatibility of the sample materials was done through cytotoxicity testing using stem cell derived neuronal cells. Based on the results from these tests, the suitability of the materials for cell culturing applications was deliberated.

10.2. Selection of photoinitiator

As in other photopolymerization systems, a photoinitiator molecule is usually utilized in 2PP to initiate the polymerization reaction. Selection of a PI for the photopolymerization starts with evaluating the wavelength of the light source used. Ideally, for 2PP, the maximum absorption wavelength of the initiator should be approximately half of the wavelength of the laser beam [159], which in our case is 532 nm. According to this, Irgacure® 127 was selected as the PI as it has maximum absorbance around 260 nm, estimated from Figure 10.1.

Irgacure® 127 is an α-hydroxyketone type catalyst for the radical photopolymerization of vinylic or acrylic based prepolymer formulations [22]. It is a difunctional derivative of the photoinitiator Irgacure® 1173. The chemical structures of both of the molecules are presented in Figure 10.2. Radical formation process in the parent molecule, Irgacure® 1173, is presented in Figure 10.3. When exposed to light, the molecule forms radicals by photolysis of the carbonyl groups [61].

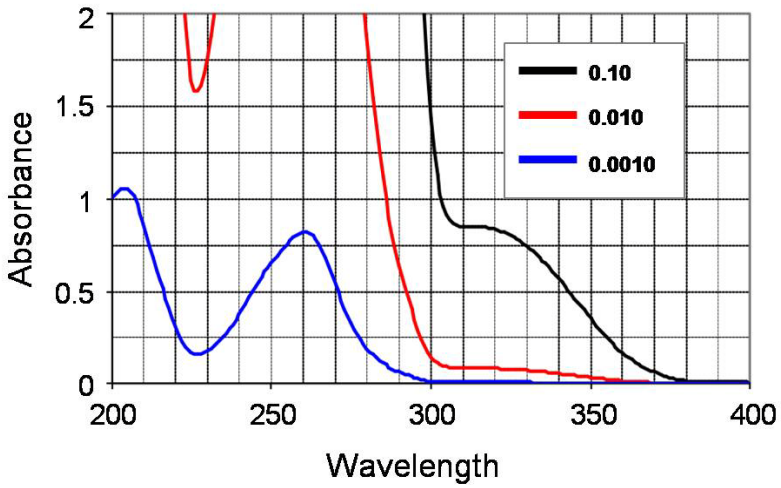

Figure 10.1. *Absorption spectrum of IRGACURE® 127 as % in acetonitrile. Modified from [22].*

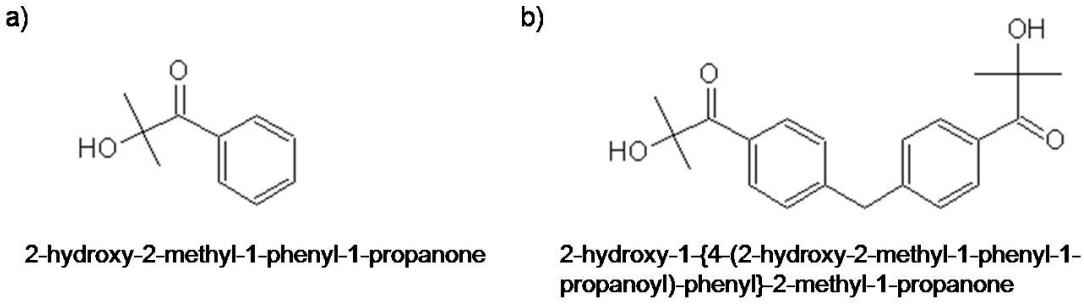

Figure 10.2. *The chemical structures of a) the photoinitiator Irgacure® 1173 and b) its derivative Irgacure® 127. Adapted from [34].*

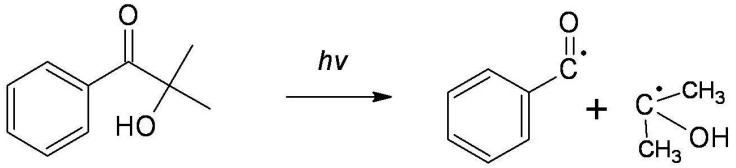

Figure 10.3. *Radical formation in Irgacure® 1173 due to absorption of light energy. Adapted from [61].*

In Irgacure® 127, the two identical chromophoric groups do not act as separate functional units, as Dietlin *et al.* [34] showed using spectroscopic methods and molecular modeling. In the excited state, the π-orbitals of the photoinitiator become "hyperconjugated" throughout the molecule, which is slightly twisted to allow coupling of the two π-systems. This enables higher absorption of light energy, although the polymerization activity itself is similar to what is observed with the parent molecule. The larger amount of absorbed energy increases the rate of the polymerization. [34] Figure 10.4 presents a simplified illustration of the most presumable reaction mechanism for the radical formation process in Irgacure® 127.

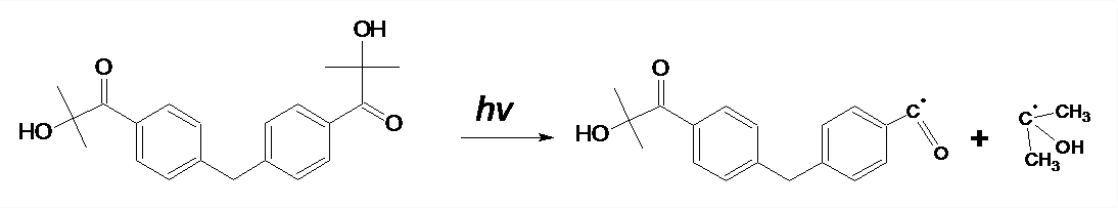

Figure 10.4. *Presumed reaction mechanism for radical formation of Irgacure® 127.*

The accurate photoinitiation efficiency of Irgacure® 127 is not known. Despite the fact that Irgacure® 127 has been effectively used for initiating polymerization in previous and current studies at TUT, it might not be the best alternative as it is originally designed to cure UV curing inks and coatings formulations by single-photon absorption of UV light [22].

Different weight-percentages of the PI were used for PEGda and PCL-o because of their differing molecular weights and chemical structures. PEGda has two acrylate moieties capable of crosslinking, whereas the PCL oligomer has four. In addition, the molar mass of PCL-o is greater, which also contributes to the greater weight percentage of PI needed for sufficient initiation. To ensure the compatibility of the prepolymer solutions with the laser wavelength range, absorbance characteristics of PCL-o-1 and PEGda-1 with and without initiator were determined using a UV-vis spectrofotometer. The measured absorbance of different photopolymer-initiator solutions is presented in Figure 10.5.

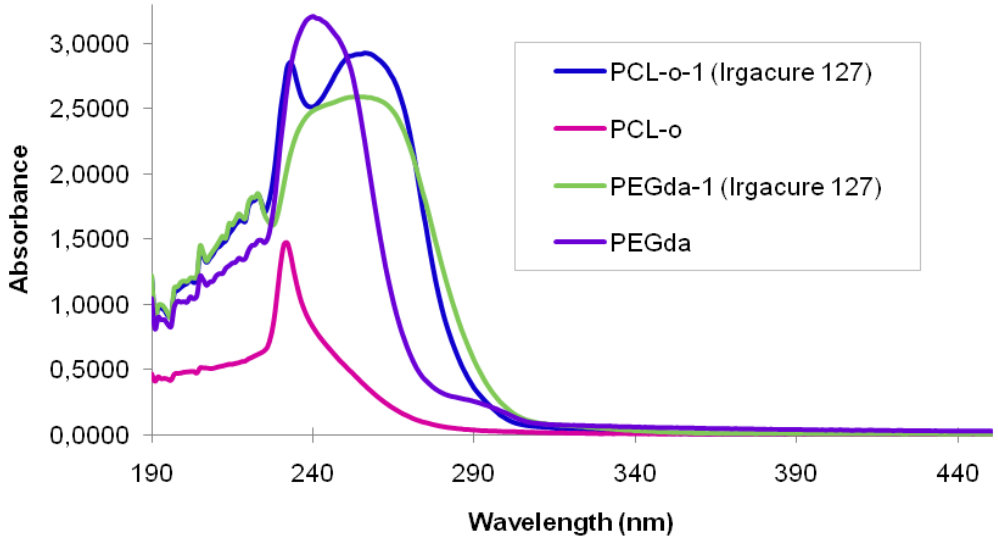

Figure 10.5. *Absorbance spectra of the photopolymer-initiator solutions used in the experiments.*

PCL-o measurements were done using dichloromethane as solvent, whereas water was used for PEGda; hence these spectrums are not entirely comparable to each other. An absorbance peak can be seen in the curves of both PCL-o and PEGda without initiator, indicating absorption at the double bonds. In the curve of the PCL-o-initiator solution, the individual peaks of PCL-o and the PI are clearly distinguishable at around 230 nm and 260 nm, respectively. The absorbance maximum in the PEGda/initiator

solutions is also around 260 nm. These results are in agreement with the absorbance spectrum of Irgacure® 127 provided by manufacturer (Figure 10.1).

10.3. Photocrosslinking reactions

So far in this chapter, the term *photopolymerization* has referred to 2PP of photocurable polymers. In the case of PCL-o and PEGda, however, the actual phenomenon should be discussed as photocrosslinking, as it only involves a light-induced reaction between the double bonds in the oligomers. Further on, the term photopolymerization will only be utilized to describe polymer solidification in a broader sense.

A hypothetical mechanism for the radical-initiated crosslinking of PCL-o is presented in Figure 10.6. In the first phase (1), a light-activated PI radical activates the double bond of one methacrylate moiety in the first oligomer. This is the initiation step. In the second phase (2), a covalent bond is formed between the PI and the oligomer, and the spare electron is localized at the α-carbon. The radicalized oligomer then reacts with another oligomer. This is the propagation step of the crosslinking reaction. In the final phase (3), termination takes place as two radicalized oligomers arms meet, react and end the reaction. It should be noted that the reaction scheme proposed in Figure 10.6 only involves one of the four arms of an oligomer, thus the same reaction can occur at all four arms simultaneously.

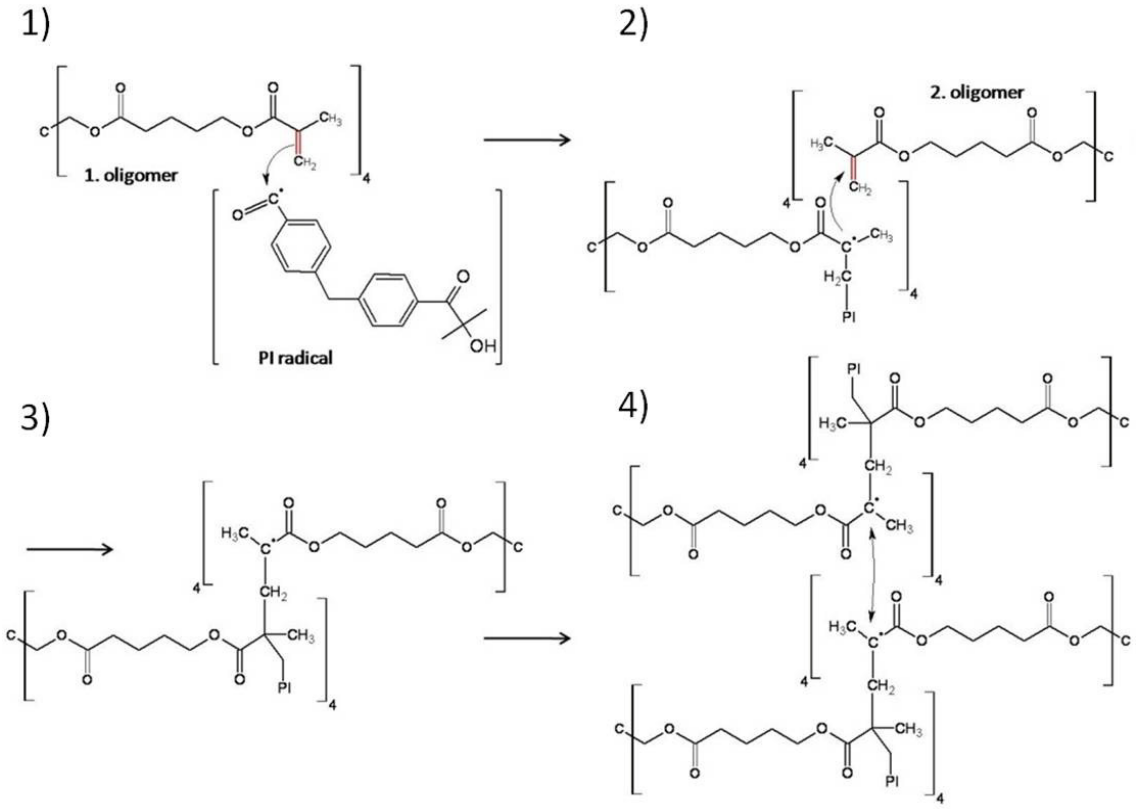

Figure 10.6. *A proposed mechanism for the crosslinking reaction of PCL-o with Irgacure® 127 as the photoinitiator.*

A hypothetical reaction mechanism for the photocrosslinking of PEGda is presented in Figure 10.7. The mechanism is similar to what was proposed for PCL-o. According to molecular simulations of hydrogel networks by Jang *et al.* [59], Wu *et al.* [160] proposed that in an ideally crosslinked network of PEGda, six oligomers form a unit cell, in which six chain ends meet and form a cyclododecane ring in the center of the unit cell. The structure of this network is presented in Figure 10.8.

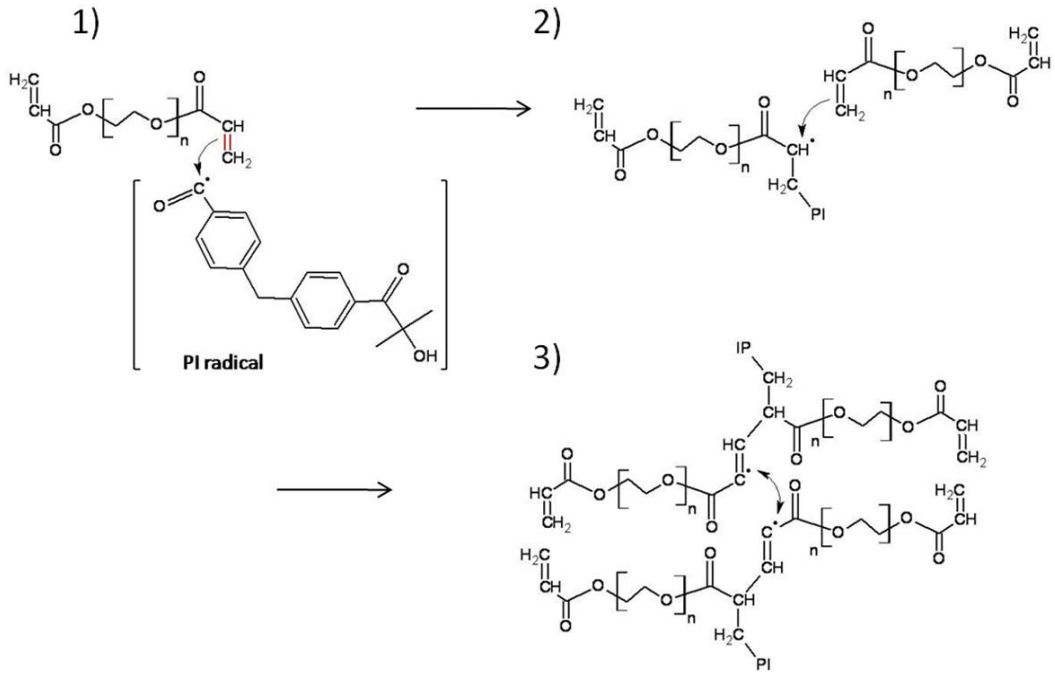

Figure 10.7. *A proposed mechanism for the crosslinking reaction of PEGda with Irgacure® 127 as the photoinitiator.*

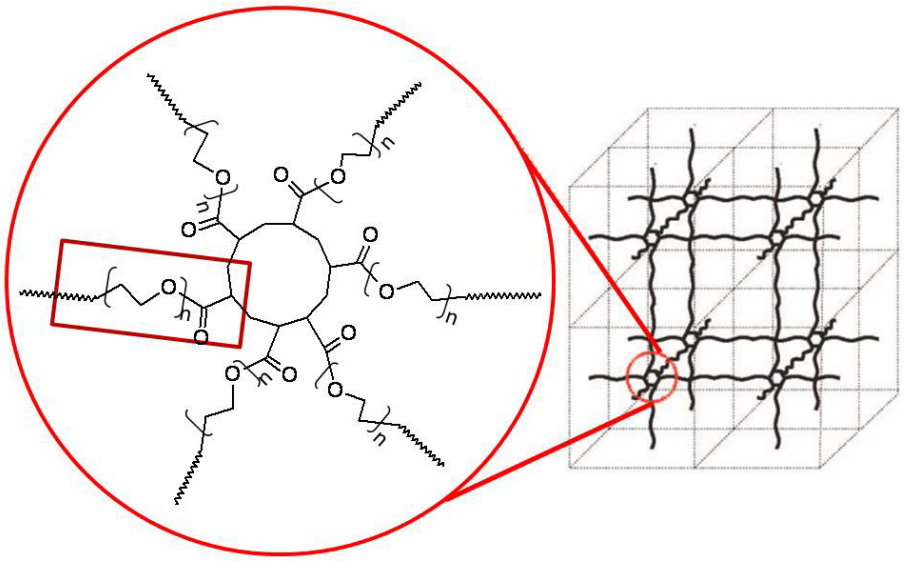

Figure 10.8. *Crosslinked network of six PEGda oligomers, which form a cyclododecane ring at the crosslinking point. Modified from [160].*

Due to the different chemical structures of PEGda and PCL-o, very different properties can be expected of the crosslinked networks. For example, for equal

crosslinking densities of PCL-o and PEGda, the PCL-o network is assumed to be denser and stiffer due to the greater amount of crosslinkable moieties in the star-shaped oligomer compared to the linear structure of PEGda.

On the other hand, the long linear molecule chains in the PEGda oligomer are supposed to introduce flexibility and expansibility to the crosslinked network. The flexibility of crosslinked PEGda was demonstrated also in practise when a polymerized sample was accidentally swept with something and the structure bent instead of breaking; an example of a distorted structure is shown in Figure 10.9.

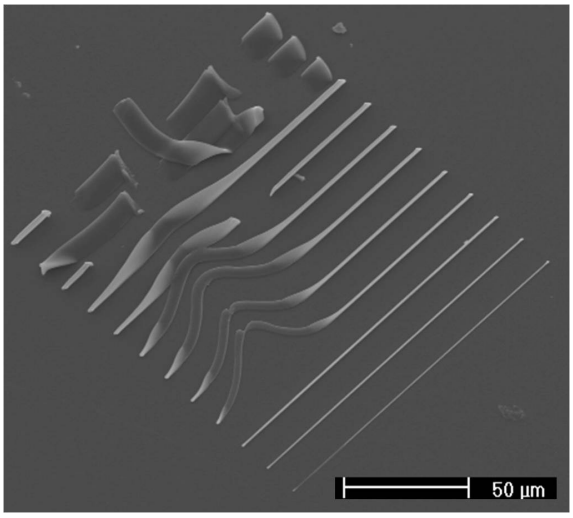

Figure 10.9. *A distorted array of PEGda-0.5 lines caused by contact with an unknown object.*

Polymerized PCL-o structures, on the other hand, exhibited high dimensional stability, and no distortion was observed during polymerization or after development. Moreover, the dimensions of the polymerized three-dimensional features corresponded well to those of the CAD models.

10.4. Optimizing of processing parameters

10.4.1. Laser power

In initial polymerization tests, the optimal laser-related processing parameters were studied in order to find out the suitable laser pulse power range and scanning speed. Using the WinPos software, simple lines and squares were fabricated for this purpose.

As noted earlier, the laser power had to be adjusted via the diode current, which was the only adjustable parameter. Due to the dependence of the pulse frequency on the diode current, all resolution and dimension calculations will be reported in graphs as function of the laser pulse energy, E. Commonly these graphs are plotted using the laser dose or the exposure time, as for example in references [75] and [76]. Unfortunately, the exposure time could not be quantitatively adjusted with the current laser system.

Furthermore, the laser power range had to be manually adjusted before fabrication by selection of a suitable mass attenuator, after which the average power can only be

fine-tuned by adjusting the diode current. Since it is unpractical to change the attenuator during the polymerization process, the number of data points for power-resolution plotting remains limited. The 25 % attenuator was found most suitable for both of the photopolymers and used in all polymerizations. The use of an attenuator of greater transmittance resulted in microboiling due to excess irradiation. As described earlier (Chapter 6.3.1 Process Characterization), microboiling is the formation of small gas bubbles in the polymerizable resin when the intensity of the laser beam is far above the polymerization threshold and causes thermal damage in the monomer molecules.

A slight problem occurred when handling the laser power via the diode current. The laser had a tendency to creep within the lower end of the range, which significantly complicated determination of the polymerization threshold. However, the 12.5 % attenuator could not be used to decrease the average power because the decrease would have been too massive. Therefore only rough estimations of the threshold behavior of the materials could be drawn, and no threshold values will be presented here.

10.4.2. Scanning speed

The xyz-stage scanning speed has a direct effect on polymerization, since it is directly related to the exposure time for each voxel. With scanning speed too fast, the production of initiator radicals is insufficient to propagate complete polymerization throughout the irradiated volume. On the other hand, scanning speed too slow will result in worsened resolution due to longer exposure time. To optimize the scanning speed for each prepolymer solution, simple two-dimensional structures were fabricated using different scanning speeds and visually estimating the properties of the resulting polymer during processing via the CCD camera system. To be precise, scanning speeds within the range of 1–150 μm/s were investigated.

A significant difference was observed in optimal scanning speed when comparing PCL-o to PEGda. With PCL-o, the scanning speed had to be at least ten times slower than with PEGda to achieve complete polymerization. Typical scanning speeds for PEGda samples varied from 20 to 100 μm/s whereas scanning speeds of 2–10 μm/s were used for PCL-o samples. Despite that no obvious explanations to this phenomenon were found, some speculations can be done. One possibility is that due to a more complicated chemical structure of the PCL-o having four crosslinkable moieties compared to the two in PEGda, more PI radicals are needed to propagate crosslinking around the whole monomer and a longer exposure time is required. Furthermore, the methacrylate moieties of the PCL-o are probably not as reactive as are the acrylate moieties of PEGda; in other words the energy transfer from the PI radical to the PCL double bonds may not be as effective as to the PEGda double bonds. A comprehensive kinetic polymerization study of the polymerization reactions including *in situ* characterization would be needed in order to fully understand the crosslinking phenomenon in these two materials.

Figure 10.10 presents SEM images of PCL-o-5 lattice-like microstructures polymerized with different scanning speeds. The scanning speed of 2 μm/s, image (a),

was found to be sufficient for polymerization. In image (b) the speed was 5 µm/s; some distortion is visible in the middle sections of the lattice. The scanning speed in image (c) was 10 µm/s, which was too fast for complete polymerization. In all the three lattices (a-c) the laser pulse energy was kept at 0.32 µJ.

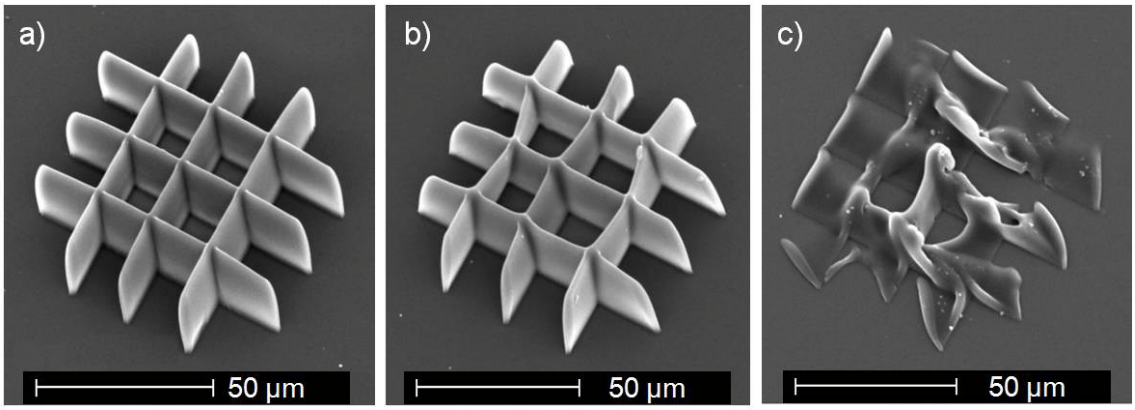

Figure 10.10. *SEM images of PCL-o-5 lattice structures polymerized with different scanning speeds; a) v=2 µm/s, b) v=5 µm/s and c) v=10 µm/s.*

A close-up of the lattice presented in Figure 10.10 (a) is shown in Figure 10.11 (a). The lattice has clean edges and intersections, wall width being approximately 3µm. For comparison, Figure 10.11 (b) presents a SEM image of a poorly polymerized PEGda-0.5 lattice fabricated with scanning speed of 100 um/s and laser pulse energy of 0.46 µJ. Individual voxels can be distinguished in the middle sections of the lattice, as emphasized in the close-up in the image. Only the ends of each line have been completely polymerized due to the slow acceleration of the xyz-stage.

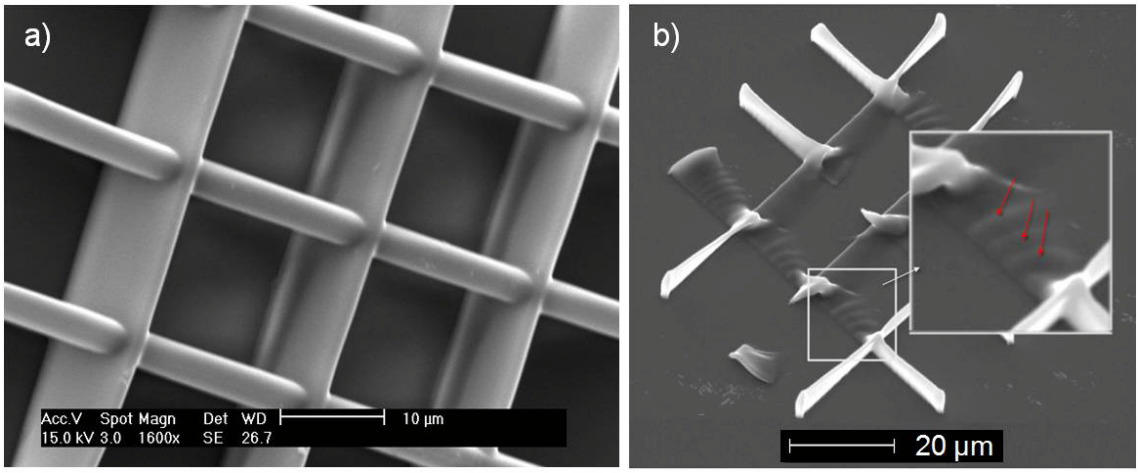

Figure 10.11. *Visual comparison between a) a well-polymerized PCL-o-5 lattice fabricated with scanning speed of 2µm/s and laser pulse energy of 0.32µJ and b) a poorly polymerized PEGda-0.5 lattice fabricated with scanning speed of 100 um/s and laser pulse energy of 0.46 µJ. The close-up in image (b) points out single voxels that have not been merged into a solid line.*

When three-dimensional microstructures are polymerized, faster scanning speeds can be utilized than for two-dimensional structures. Explanation for this originates from the contour scanning method, which will be discussed more in Chapter 10.6.

10.5. Determination of resolution

Resolution for our laser set-up and prepolymer solutions was studied by the SEM image analysis described earlier in Chapter 9.2.8. Unfortunately, the angle of view varied between almost every sample set of SEM images, the correct measurement angle had to be visually estimated for each image.

The fabrication equipment utilized in this study employed a Nd:YAG pulsed laser, which produces pulses of picoseconds in duration. This type of a laser is more affordable compared to the femtosecond Ti:sapphire lasers utilized in most of the reported 2PP studies, and thus is a reasonable choice for research purposes. Therefore a subsidiary motive of this study was to compare the gained resolution results to results reported with more expensive and sophisticated laser types.

10.5.1. Voxel arrays

Based on the mathematical models of 2PP, it is known that the voxel size is not linearly dependent on the laser power. When the laser power is increased after achieving the polymerization threshold, voxels start to grow gradually. Increase in voxel dimensions, especially in the longitudinal direction, continues nearly linearly. At a certain point the growth levels off and no further increase is observed in the voxel size. [7]

Figure 10.12 presents voxel length and voxel diameter as a function of the laser pulse energy. Three material samples containing different initiator concentrations of both PCL-o and PEGda were used; the goal was to find out the dependence of resolution on the photoinitiator concentration, and to compare the overall voxel size between the two photopolymers. PCL-o voxels are shown in the left graphs and PEGda voxels on the right.

Due to the limited power range available during fabrication, the curves do not completely characterize the resolution behavior of the system. If more data could have been gained from either end of the range, more accurate resolution values could have been drawn from these graphs. Furthermore, the margin of error for these length and diameter values is quite large, since the values are only based on visual image analysis. An average measurement error in the presented dimension values is approximately 0.5 µm. Another drawback is the variance in the data range between samples at the lower pulse energies; the difference is due to the incoherent threshold behavior of the sample materials and the creeping tendency of the laser.

However, all the curves in Figure 10.12 seem to correlate to the mathematical model, especially the length curves possessing first a slight increase, continuing with a phase of linear increase and then leveling off after a saturation point. Behavior of the diameter curves is not as clear, and more data points should have been measured at

higher energy values to unveil possible saturation. Further observation from the curves is that voxel dimensions increase along increase in the PI concentration, as expected. Interestingly for voxel length in both materials, the curves of two lowest concentrations seem to saturate almost at the same level, whereas the highest concentration curve follows a different trend at significantly longer voxels.

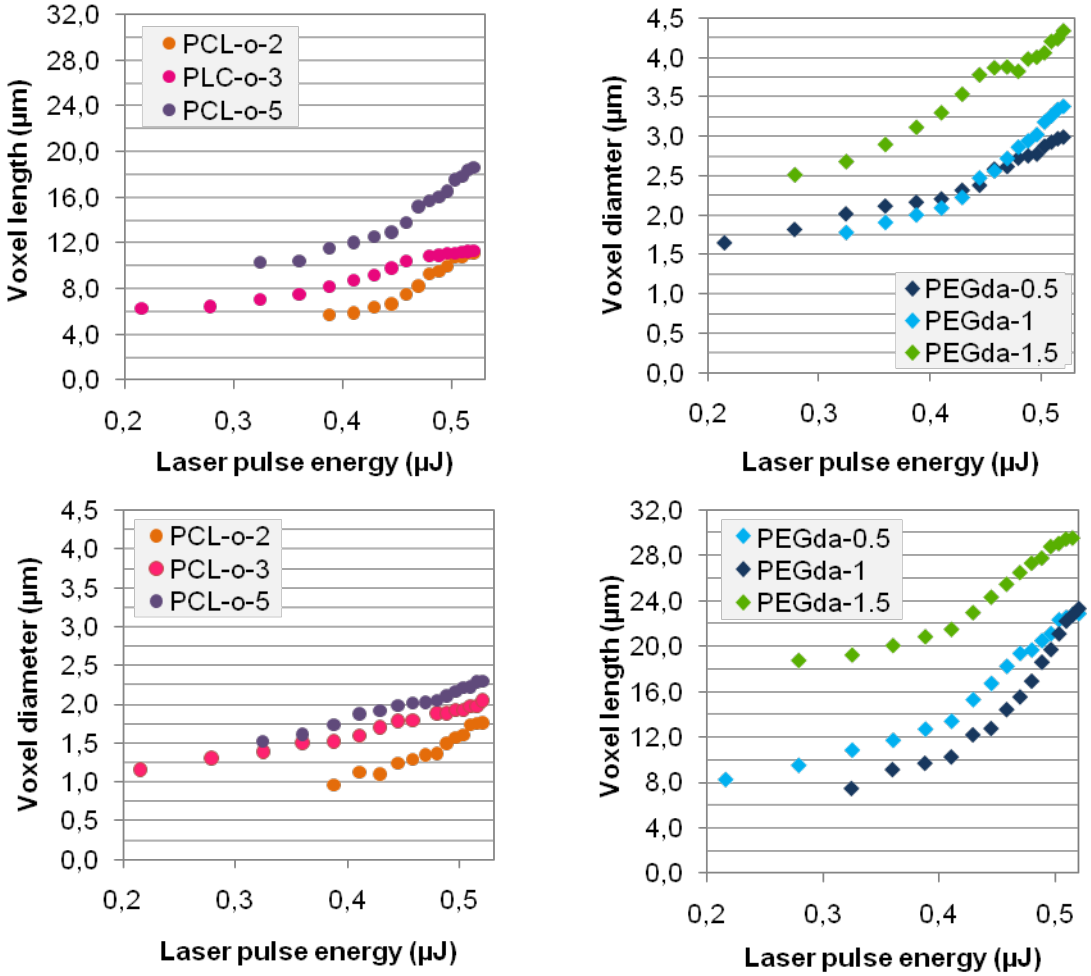

Figure 10.12. *The dependence of voxel dimensions on the laser pulse energy. Upper images present voxel length as a function of the laser pulse energy and the lower images present voxel diameter as a function of the laser pulse energy. Dimensions of PCL-o voxels are presented on the left graphs and PEGda voxels on the right.*

The most obvious conclusion from these curves is that the PCL-o produces smaller voxels than PEGda, and thus provides a better resolution. Assumingly, the larger size of the monomer and the significantly greater viscosity of PCL-o compared to those of PEGda contribute to the smaller size of the PCL-o voxels. More specifically, it can be presumed that PI radical diffusion is more restricted in PCL-o than in the low-viscosity PEGda, which results in a diminished voxel size.

Table 10.1 summarizes the highest achieved resolutions for both PEGda and PCL-o. The best overall resolution was achieved with PCL-o-2 with voxel diameter of 0.97 µm and voxel length of 5.74 µm.

Table 10.1. *Results from resolution studies for six prepolymer solutions, three for each material.*

voxel dimensions at best resolution	PCL-o-2	PCL-o-3	PCL-o-5	PEGda-0.5	PEGda-1	PEGda-1.5
voxel diameter	1.0 µm	1.2 µm	1.5 µm	1.6 µm	1.8 µm	2.7 µm
voxel length	5.7 µm	6.2 µm	10.3 µm	8.3 µm	7.5 µm	18.8 µm
voxel aspect ratio	6	5	7	5	4	7

Table 10.1 also lists the aspect ratios of the smallest voxels obtained. The voxel aspect ratio (the ratio of length to diameter) has a direct effect on resolution; therefore small values of aspect ratio are desirable when detailed submicron features are to be polymerized. Theoretically, the aspect ratio of a voxel is mainly affected by the numerical aperture (NA) of the objective lens used. Moreover, low values of laser power will produce voxels with low aspect ratio, thus providing increased resolution. With optimized fabrication set-up and low initiator concentration, aspect ratio near unity can be obtained. [7] In the current study, the average height to diameter ratio for PCL-o voxels was six, whereas for PEGda voxels it was five. These values indicate that the NA used (0.9) is not ideal and better resolution could be obtained using an objective with larger NA. These results also imply that the composition of the prepolymer solution does not have a significant effect on the ratio value, as similar ratios were obtained with both PCL-o and PEGda.

As discussed in the literature review, minimum feature sizes down to a few hundred nanometers have been reported in 2PP-related publications, yet these studies have employed expensive and sophisticated Ti:sapphire lasers and SU-8 as photoresist. However, in the paper by Clayessens *et al.* [24], which described 2PP with a novel biodegradable copolymer using a femtosecond laser, resolution of 4 µm was reported. This resolution is comparable to the results gained in the current study. Furthermore, as the current resolutions were gained with a picosecond laser and a non-optimized optics, significantly increased resolution could be expected of both PEGda and PCL-o when processed with a femtosecond laser system. Considering the quality of the fabrication system and the fact that these were the first 2PP studies with PCL-o, the obtained resolution values are more than satisfactory.

10.5.2. Two-dimensional microstructures

Two-dimensionally polymerized line arrays were used to study the combined effect of laser pulse energy and exposure time on resolution. A significant drawback of the SEM image analysis, especially for lines, is that practically no real measures can be derived from these dimension calculations. The height of each polymerized line depends on the objective focus height; usually the focus height was set so that only half of the focal

volume was observably polymerized on the substrate. This height adjustment was done to maximize the attachment surface area of the structure. Since the focus height could not be numerically adjusted, accurate comparison cannot be done between structure heights derived from images of different samples polymerized using different focus heights. Thus, only rough estimation of the real resolution–exposure time dependence can be drawn from the SEM images.

Figure 10.13 presents the SEM images of PEGda line arrays that have been used for height measurements. Images (a) and (b) presents lines polymerized of PEGda-1.5 whereas (c) and (d) present PEGda-1.

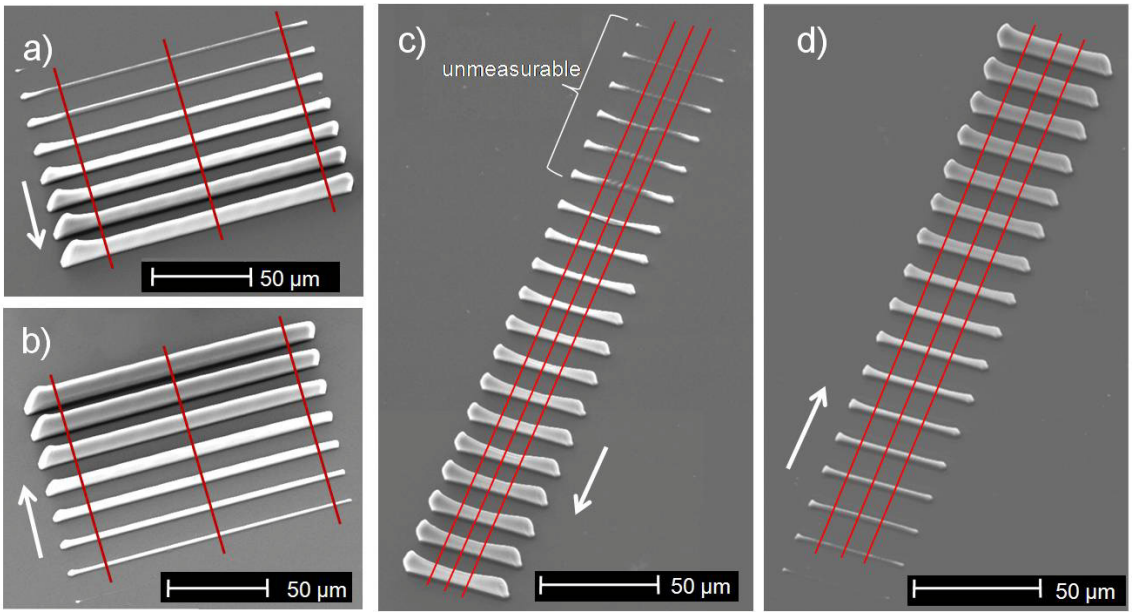

Figure 10.13. *PEGda lines polymerized with increasing laser pulse energy using different scanning speeds; a) PEGda-1.5, v=60 µm/s, b) PEGda-1.5, v= 30 µm/s, c) PEGda-1, v=100 µm/s and d) PEGda-1, v=50 µm/s. The red lines perpendicular to the polymerized lines mark the points of height measurement whereas the arrows point out the direction of increasing laser pulse energy. In image (c) the word 'unmeasurable' denotes lines that have not been completely polymerized and cannot be used for height measurements.*

As can be seen in the images, line height slightly increases at the end sections of the lines. This property originates from a practical problem. Polymerization is spatially controlled by the xyz-stage and some time is needed for the stage to reach the set scanning speed value. This acceleration behavior results in an increase in the exposure time at line ends. Longer exposure time leads to a bigger voxel size, which, in turn, can be observed as curvature at the line ends. Moreover, similar curvature is not observed at both of the line ends, but the ending end usually has more distinct curvature; deceleration of the xyz-stage is slower than acceleration.

The results from line height measurements are shown in Figure 10.14 in which only the relative increase in line height as a function of the laser pulse energy is presented due to the focus height problem. The percentage values have been calculated with the following equation:

$$relative\ increase\ as\ percentage = \frac{(x-y)}{y} \cdot 100\% \qquad (10.1)$$

in which x is line height at the smallest pulse energy (e.g. reference height) and y is line height at a certain pulse energy.

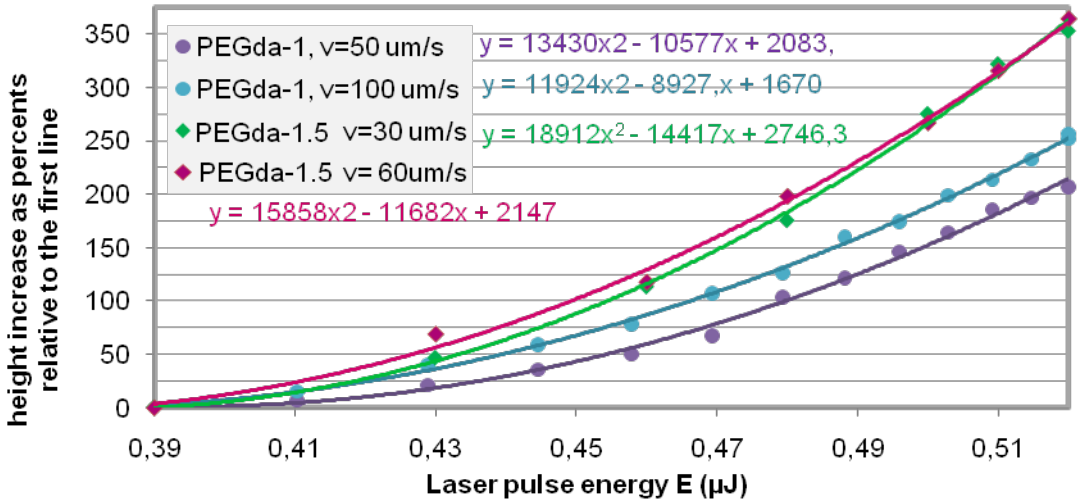

Figure 10.14. *Relative increase in line height as a function of the laser pulse energy. The graph shows the dependence of vertical resolution on the exposure time and on the PI concentration for PEGda-1 and PEGda-1.5.*

Theoretically, the curves presented in Figure 10.14 should follow the same trend as observed with voxel dimensions plotted against the pulse energy. However, second-order polynomial trendlines were found to fit the data of all samples, which points out the problem of limited data range, which occurred also in the resolution graphs presented earlier. Saturation in height increase, which is not shown in these curves, would be expected at higher pulse energies. Nevertheless Figure 10.14 shows that the relative height increase as a function of the laser pulse energy is more substantial at higher PI concentration.

The overall increase in line height as a function of the pulse energy is actually quite extensive. This phenomenon can be exploited during fabrication of more complex structures. For example, the laser focus height does not have to be meticulously adjusted when using higher pulse energies since the high-profile structure is likely to attach to the substrate even if the focus is not precisely at the substrate surface.

The effect of exposure time on line dimensions can interpreted through scanning speed values. As seen in Figure 10.14, lower scanning speed, meaning longer exposure time, results in slightly thicker lines. Furthermore, the curves in Figure 10.14 show that the relative increase in line height for slower scanning speed is not as considerable as for faster scanning. As a conclusion, longer exposure time leads to a diminished line aspect ratio, or more accurately, diminished aspect ratio of a voxel. This finding is coherent with the voxel scaling laws proposed by Sun *et al.* [146].

Unfortunately, robust and measurable line arrays could only be fabricated from PEGda-1.5 and PEGda-1. The problem with PEGda-0.5 and all PCL-o prepolymer

solutions was that lines collapsed immediately after polymerizing, even if scanning speed had been slow enough. The lateral resolution with these materials is quite high, for which the polymerized lines are very thin, and, apparently, do not have mechanical properties good enough to withstand the weight of the structure. Figure 10.15 presents examples of collapsed lines made of (a) PEGda-0.5 and (b) PCL-o-5.

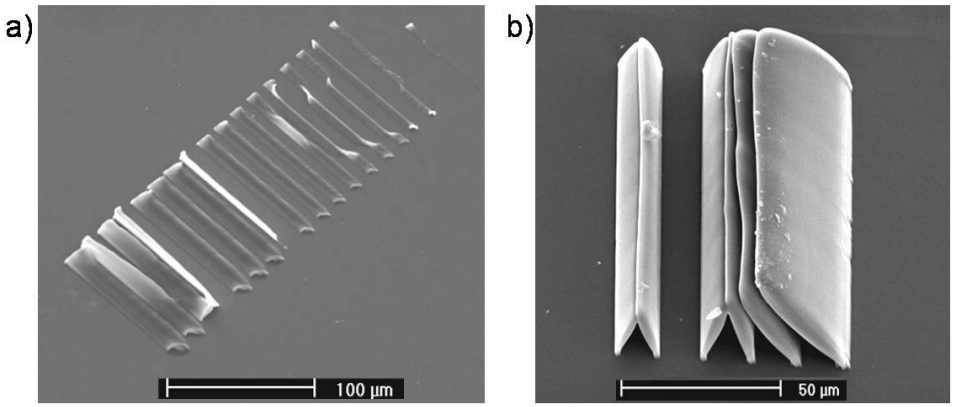

Figure 10.15. *SEM images of line arrays polymerized of a) PEGda-0.5 and b) PCL-o-5. These lines have collapsed after polymerization and could not be used for height measurements.*

As a solution to the problem of collapsed lines, lattice-like structures were used instead of simple lines. By measuring dimensions from these, the effect of exposure time on resolution could be estimated. Figure 10.16 represents illustrative images of the lattices used in the experiments. All these lattices were polymerized using simple two-dimensional WinPos codes.

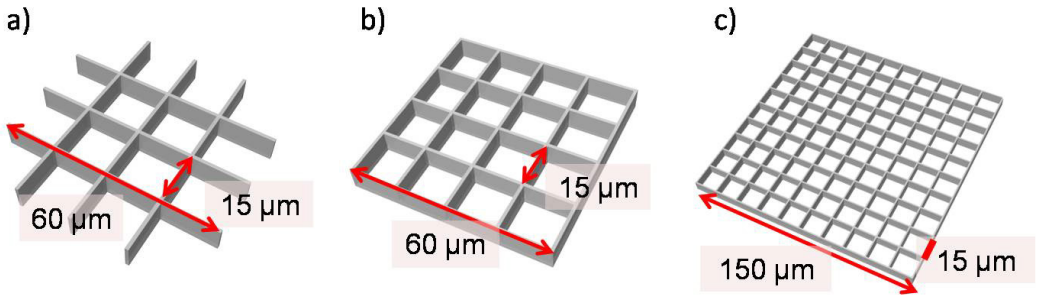

Figure 10.16. *Illustrations of the lattice codes used in polymerization experiments.*

The importance of the structural support provided by the lattice is seen in Figure 10.17, which presents a PCL-o-2 lattice polymerized according to the model presented in Figure 10.16 (c). Fabrication of the structure was manually interrupted, for which there are only four lines in the perpendicular direction. In the region of lines in only one direction the lines have fallen towards each other and the microstructure has been destructed.

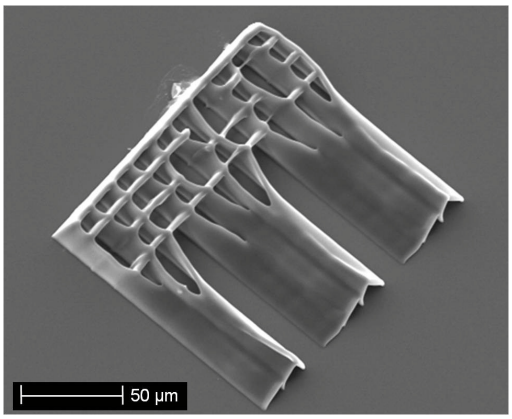

Figure 10.17. *PCL-o-2 lattice for which the fabrication process has been interrupted before completing the structure.*

By varying the laser pulse energy and scanning speed, lattices of different aspect ratios could be fabricated. In this case, aspect ratio describes the ratio of feature height to its width. Due to the resolution characteristics of our fabrication system, increase in the width of the lattice walls is quite modest when the pulse energy is increased, whereas the height of the walls increases substantially. Figure 10.18 presents SEM images of PEGda-0.5 lattices that were polymerized with three different laser pulse energy values. A similar set of SEM images for PCL-o-2 in seen in Figure 10.19.

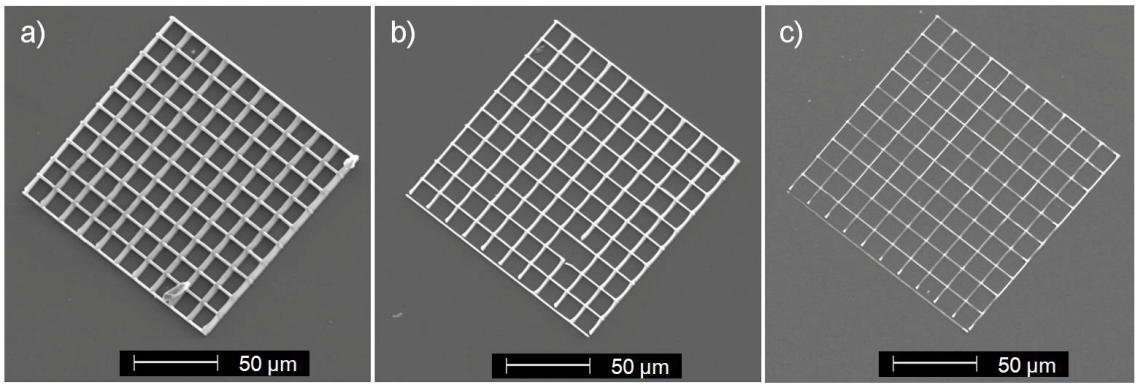

Figure 10.18. *PEGda-0.5 lattices polymerized with constant scanning speed of 30 µm/s using different laser pulse energies. In a) E= 0.51µJ, b)E= 0.46 µJ and c) e=0.43 µJ.*

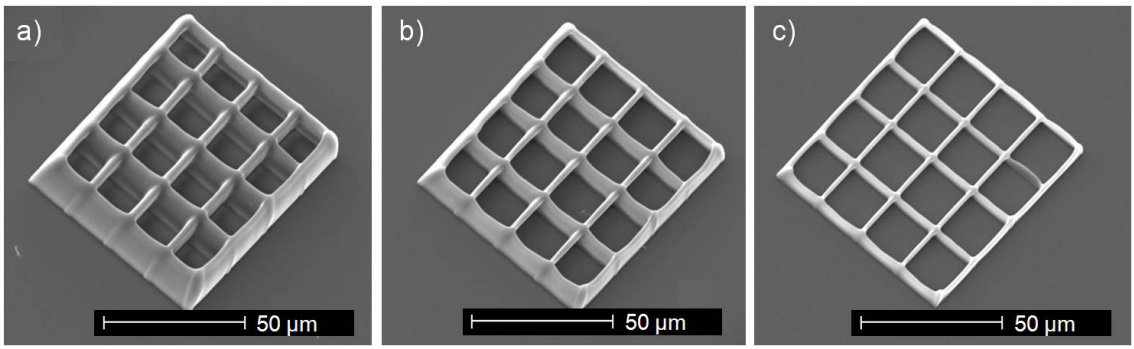

Figure 10.19. *PCL- lattices polymerized with constant scanning speed of 5 µm/s using different laser pulse energies. In a) E= 0.51µJ, b) E= 0.48 µJ and c) E=0.43 µJ.*

As can be visually estimated from Figure 10.19, the increase in feature height as a function of the laser pulse energy is substantial, whereas dimensional increase in the lateral direction is quite modest. This behavior is similar to what was observed with PEGda line arrays, thus it can be assumed not to be material-dependent but a consequence of the optical characteristics of the fabrication equipment.

The polymerization process for lattices presented in Figures 10.18 and 10.19 is fast, easy and readily variable. Fabrication of one such lattice takes only a couple of minutes. However, the exploitability of these one-layered features in practical applications remains unclear. More importantly, these simple lattices can be polymerized on top of each other to form truly three-dimensional scaffold-like structures. Furthermore, lattice dimensions can be individually adjusted for each layer to form, for example, microscaffolds with varying pore sizes.

10.6. Fabrication of three-dimensional microstructures

After optimizing the polymerization processing parameters, more complex structures were fabricated using the CorvusControl software with CAD models. As described earlier in Chapter 9.2.5, the three dimensional CAD models designed with Rhinoceros® were first sliced into horizontal layers by contour. With PCL-o, layer spacing of 0.5, 1, 2 and 4 µm were tested, whereas PEGda structures were fabricated with layer spacing varying from 0.35 µm to 2 µm.

As seen in the former chapter, PCL-o did not prove very suitable for polymerizing simple two-dimensional microstructures. Conversely, robust three-dimensional structures could be fabricated with the material, which was enabled by the contour scanning technique of layered CAD models. Because the layer spacing is much smaller than the vertical size of a voxel, illumination of one layer causes further polymerization in the layer below. If the model has several contours in the same contour plane, the distance of these is optimized to enable overlapping also in the lateral dimension. Figure 10.20 illustrates the overlapping phenomenon during contour scanning.

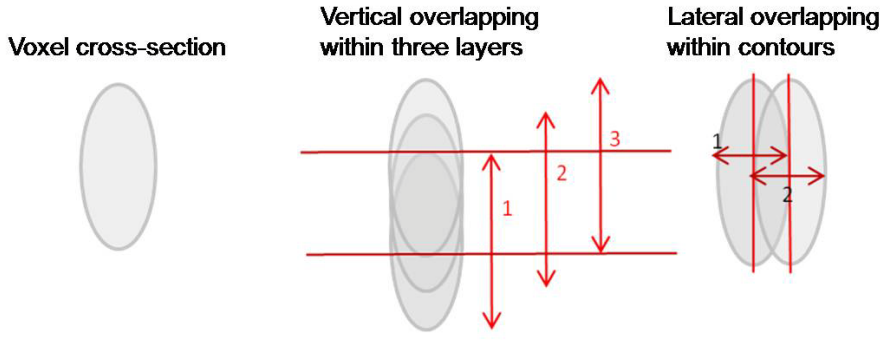

Figure 10.20. *Voxel overlapping during polymerization using the contour scanning technique.*

For PCL-o, scanning speed values within the range of 5–15 µm/s were used, whereas for PEGda, the tested scanning speed values were much higher, ranging from

30 to 100 µm/s. The higher values of suitable scanning speed used for three-dimensional structures than for simple lines also result from layer overlapping in contour scanning. As noted earlier, the scanning speed affects the resulting height of a polymerized layer, for which an optimal combination of layer spacing and scanning speed has to be studied in order to fabricate structures with optimized robustness and dimensional stability. If the CAD model is sliced densely, only thinly polymerized layers are needed, thus faster scanning can be used. This combination will result in good resolution and accurate repetition of the CAD model. On the other hand, if dense layer spacing is coupled with slow scanning speed, resolution will worsen but the resulting structure is likely to be robust and stable with thick contour walls.

Figure 10.21 presents two microcones made of PCL-o-5 and the respective CAD models. The layer spacings used were 2 µm and 4 µm. As can be seen in the SEM image, the cones have collapsed due to insufficient overlapping of contour layers. In this case, the combination of layer spacing and scanning speed was not ideal.

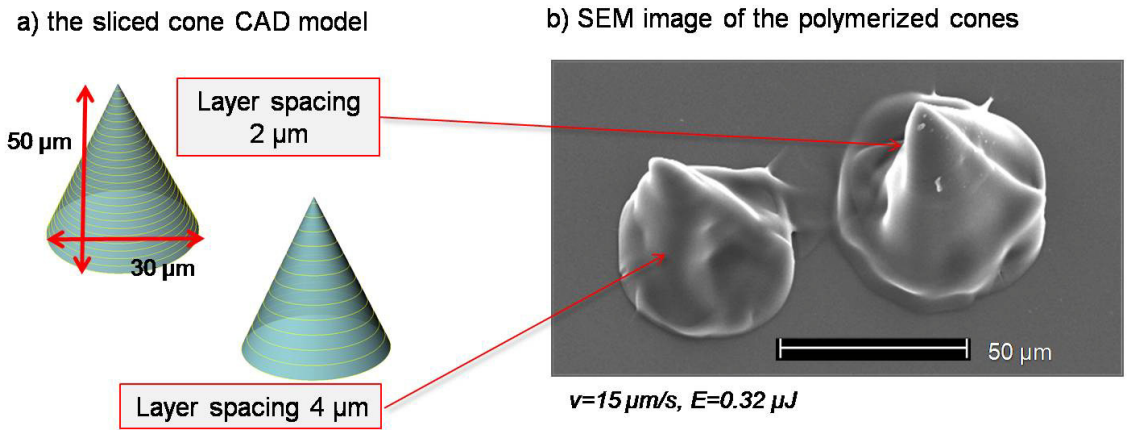

Figure 10.21. *CAD models of cones with layer spacing of 2 and 4 µm (a), and a SEM image of these cones polymerized of PCL-o-5. In both of the cones layer spacing has been too wide and insufficient overlapping between contour planes has resulted in collapsed structures.*

The resolution characteristics for our fabrication system became evident when more complicated structures were fabricated. In Figure 10.22 (c), a SEM image of a miniature cow polymerized of PCL-o-3 is presented with corresponding CAD images (a-b). The polymerized cow has distinctive features in the lateral direction, but vertically the structure seems as if it was extruded to the substrate surface from half way down.

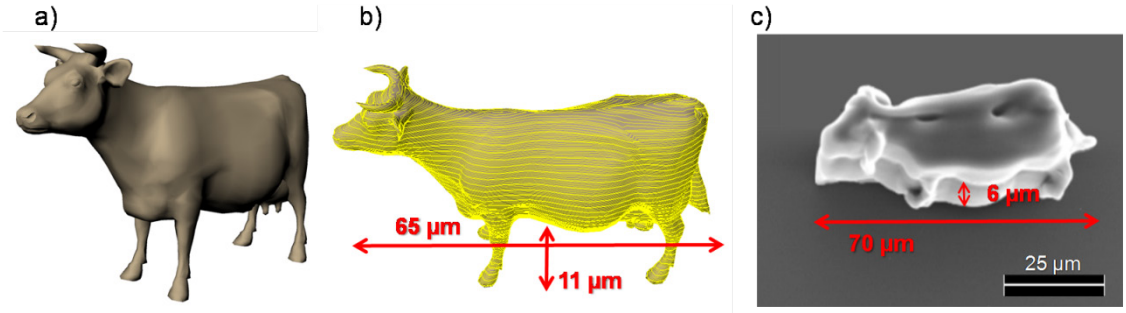

Figure 10.22. *A CAD image of a miniaturized cow (a),which is sliced into contours using layer spacing of 0.5 µm (b) and polymerized of PCL-o-3 using scanning speed of 25 µm/s and laser pulse energy of 0.36µJ (c).*

There are three possible reasons responsible for the insufficient CAD model replication observed in Figure 10.22. Firstly, the resolution in our system is not adequate for precise replication of features this small. Specifically, the aspect ratio of single voxels is too large to enable the high vertical resolution needed for this feature. Secondly, the material properties of the cured polymer are such that the floating parts will not keep their shape but will stretch and sink towards the substrate. Finally, the uncured prepolymer solution surrounding the structure is not viscous enough to support it mechanically.

In general, the problem with liquid prepolymer solutions is that any structure to be polymerized needs to be firmly attached to the substrate by its bottom. Liquid prepolymer solutions may flow during the polymerization process, which causes distortion to the polymerized structures. Furthermore, floating or separate structures will be rinsed away in the development process. However, it is possible to overcome some of the problems of liquid prepolymer solutions by careful model design.

Using PEGda-1 prepolymer solution and optimized processing parameters, a hollow bonfire-like microstructure was successfully fabricated; the CAD model and SEM images of polymerized structure are presented in Figure 10.23.

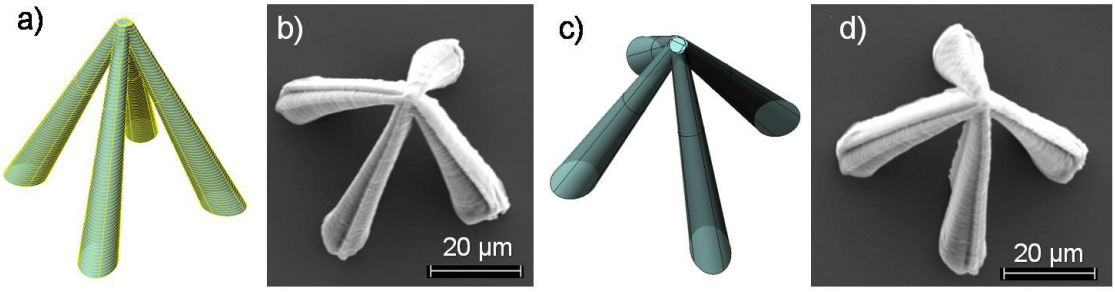

Figure 10.23. *A hollow bonfire-type microstructure as a) a sliced CAD model using layer spacing of 0.7 µm, b) SEM image of the polymerized structure, c) the CAD model from another view angle and c) the corresponding SEM image.*

Wall structures of different shapes, sizes and heights have been polymerized of both PCL-o and PEGda. These wall structures are designed to be used in cell culturing applications for guided cell growth, but in order to preserve the possible patentability of this application, no CAD or SEM images of the polymerized structures will be

presented in this thesis. The use of two-photon polymerized microstructures in cell culture applications will be discussed on a general level in Chapter 10.9.

In visual examination of the polymerized structures, those polymerized of PCL-o had a smooth surface whereas in PEGda structures the individually polymerized layers were still visible. This interesting difference between the two materials is presented in Figure 10.24.

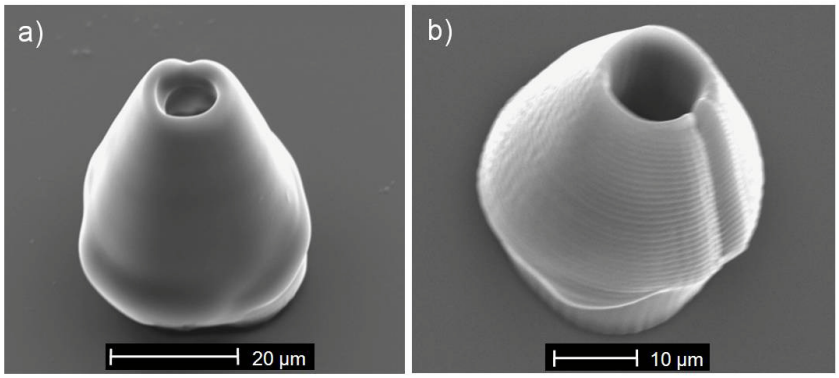

Figure 10.24. *PCL-o (a) and PEGda (b) cones polymerized using same CAD model with layer spacing of 1 µm and the same laser pulse energy of 0.43 µJ. Scanning speeds of 20 µm/s and 50 µm/s were used for cone (a) and (b), respectively.*

Although it is nearly impossible to draw any relevant conclusions of the molecular behavior from these micron-scale images without studying the reaction kinetics, some speculations can be done. It is possible, that the difference in the surface smoothness between PEGda and PCL-o objects is due to different organization of the crosslinked molecules on the surface. These reorganization reactions take place after light exposure to minimize the surface energy of the crosslinked network. It can be hypothesized that in PCL-o, the star-shaped oligomer structure offers more possible crosslinking points for the different polymerized layers to merge and form a continuous surface. In each polymerized layer of PEGda, on the other hand, the bifunctional monomers readily crosslink into an organized network with only a few dangling ends on the surfaces, and the next layer does not adhere to the former as tightly as in PCL-o. On possible network configuration for PEGda is the one proposed by Wu *et al.* [160] and shown in Figure 10.8. The observably faster polymerization rate of PEGda compared to PCL-o may also contribute to this phenomenon.

10.7. Comparison of processability

One of the main goals of this study was to evaluate and compare the overall processability of PCL-o and PEGda in 2PP microfabrication. One of the main factors contributing to processability is resolution, for which comparison between the two materials was done in Chapter 10.5. Besides resolution, other important aspects of processability include the ease of sample preparation and handling, toxicity of the solvents used in the fabrication process and sample shelf life.

Most of the differences between PEGda and PCL-o in terms of processability arise from the very different viscosity values of the monomer solutions. For preparation of the prepolymer solutions, similar procedures were used with both PCL-o and PEGda. Since the monomer solutions were directly measured and mixed with initiator powder, no solvents were needed in this step. However, dosage of the fluid PEGda monomer solution was slightly easier since it could be pipetted instead of employing the more complicated weighing procedure used with viscous PCL-o. The same problem occurred during sample preparation in polymerization experiments. PEGda samples could be proportioned quantitatively on the glass substrate using a pipette, whereas a less accurate dosing system had to be used for PCL-o samples.

As already noted, the PCL-o prepolymer solution exhibited crystallization behavior below temperature of 30°C. Therefore all PCL-o samples had to be slightly heated before polymerization to melt the crystallized oligomers in order make the solution to be light-transparent and polymerizable. This was an additional preparation step, which added to the total fabrication time.

On the other hand, despite the ease of dosing, the low viscosity of PEGda combined with the hydrophobic substrate surface caused the solution to sometimes escape from the sample well, which significantly complicated sample fabrication. Moreover, the higher viscosity of PCL-o effectively prevented flow in the unpolymerized solution, which was occasionally occurred in PEGda samples. Overall in practice, neither of the materials was superior to the other in terms of sample preparation or handling.

In 2PP experiments, one of the key parameters is the scanning speed. As already noted, scanning speed values one order higher could be used with PEGda compared to PCL-o. Scanning speed directly affects the rate of fabrication and therefore faster scanning speed is preferred if larger features are polymerized. Due to the slow scanning speed required by PCL-o, some of the more complicated and large structures polymerized of PEGda were not tested with PCL-o. To be able to reproducibly fabricate series of polymerized samples to cell culture experiments, for instance, the microfabrication process needs to be fast, reliable and effective. Therefore the problem of slow polymerization observed with PCL-o needs to be addressed before any larger and practically exploitable features could be fabricated.

The development procedure is a critical step in the fabrication process. For PEGda and PCL-o, similar procedures were used, but due to the very different solubility characteristics of these materials, different solvents were utilized. Uncrosslinked PEGda is water-soluble viscous liquid, thus water can be used for development of the polymerized structures. The use of water as solvent increases the biocompatibility of the overall process, since no toxic residues will be left in the polymer network. Furthermore, water is safe, cheap and easy to handle. Removal of uncrosslinked PCL-o, on the other hand, requires the use of organic solvents, since the uncrosslinked oligomers are non-soluble in water. In this study, dichloromethane and 2-propanol were used as solvents. Residues of these substances may cause cytotoxic effects that cannot be predicted before cell testing.

Despite the obvious superiority of water as development solvent, some problems occurred with PEGda samples. Firstly, the silane treatment of the microscope glasses used as substrates causes the glass surface to be hydrophobic, which resulted in difficulties during development. As water was apportioned on the polymerized sample, hydrophobicity of the surface caused the water droplets to roll over the surface without wetting it. Therefore careful rinsing with excess water had to be done multiple times to ensure all the uncrosslinked polymer had washed away. An example of a poorly developed PEGda lattice is presented in Figure 10.25, in which remnants of unpolymerized prepolymer solution can be seen at the bottom of the squares.

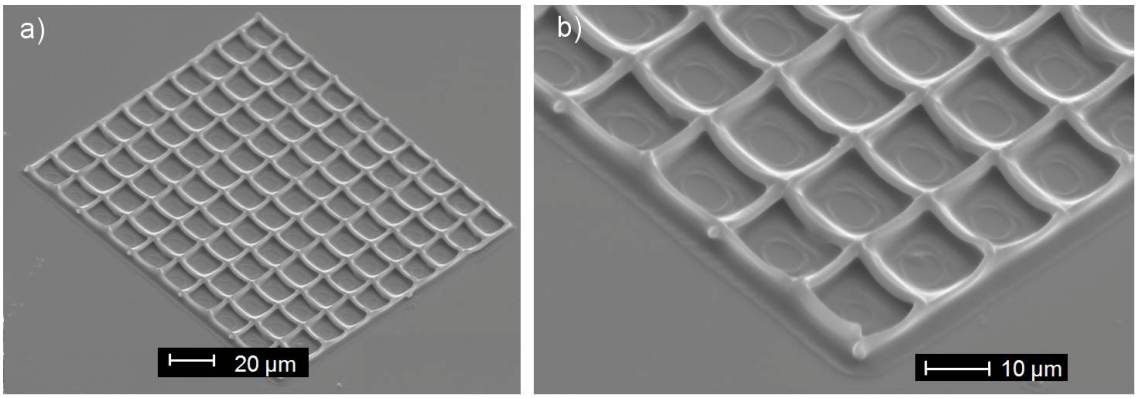

Figure 10.25. *a) An insufficiently developed PEGda-1 lattice and b) a close-up of the structure.*

There was also another problem caused by insufficient attachment of the polymerized structures coupled with heavy rinsing, which induced structures to detach from the substrate. It is possible, that some of the samples were fabricated on glass slides with a denaturized silane layer. Figure 10.26 shows examples of detached features; image (a) presents a PEGda-1 lattice that has been curved upwards from its two corners during development. A close-up of the same lattice is shown in image (b). It can be observed in these images that the lattice has bent without cracking, which is another indication of the flexibility of the crosslinked material. Figure 10.26 (c) presents distorted and partially detached PEGda-1.5 lattices. The reason why these lattices have kept the distorted shape is possibly the further solidifying effect of exposure to visible light after development.

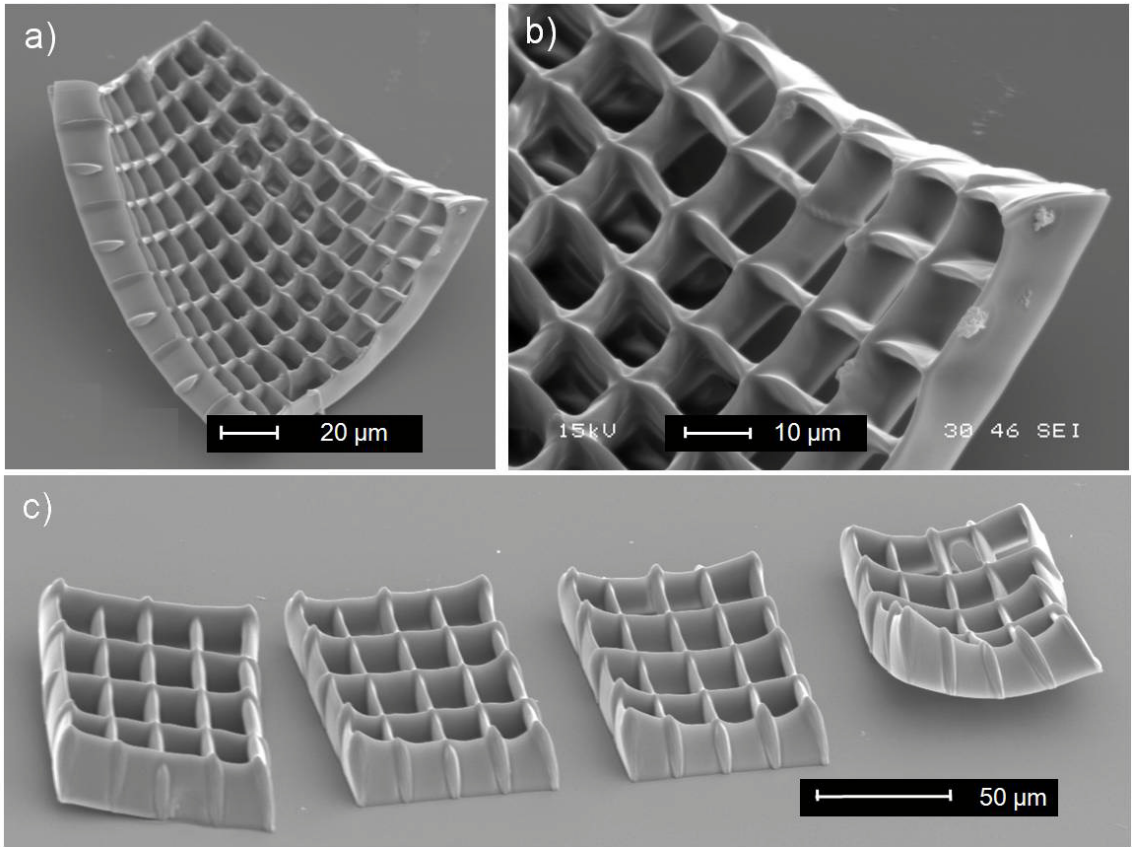

Figure 10.26. *Polymerized PEGda lattices, which have been partially detached from the substrate surface during development.*

After development, polymerized samples were stored for SEM imaging in a sealed, yet not airproof box. Time of storage varied from a few days to several weeks. Within this time scale, no visible changes in structure or dimensions were observed in the samples of either PEGda or PCL-o when imaged with an optical microscope. Consequently, the shelf life of the crosslinked structures made of both materials seems appropriate at least for research purposes.

10.8. Results of cytotoxicity testing

PEGda is a known biocompatible material used in different biomedical applications. PCL-o on the other hand, is a novel photopolymerizable material and no previous cell-based testing has been done with this material. However, PCL, the precursor material for PCL-o, is well known for its good biocompatibility [134]. To confirm the biocompatibility of PEGda and to investigate the possible cytotoxicity of PCL-o, initial cell culturing experiments were carried out. The testing was done using human derived neural stem cells, which are of special interest in other studies.

Similar results were attained with PEGda and PCL-o in cytotoxicity testing. With both materials, cell aggregates attached to the sample surface, but no outgrowth could be observed. Both live and dead cells were found in all samples. On the laminin control, on the other hand, extensive migration was observed on all sample surfaces, and the

morphology of the cells was neural-like. Images from the live-dead analysis are shown in Figure 10.27.

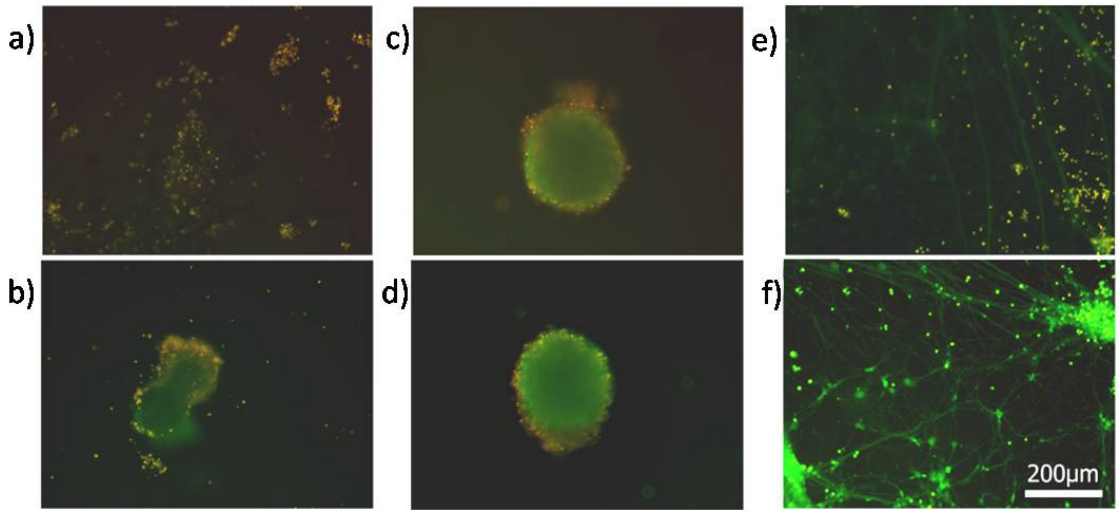

Figure 10.27. *The viability of neural cells on surfaces of PEGda (a-b), PCL-o (c-d) and laminin control (e-f). Dead cells are stained as red/yellow whereas live cells are green.*

As seen in Figure 10.27, majority of the cells on PEGda and PCL-o surfaces stayed alive, yet no neural-like behavior was observed. These results indicate that both of the materials are non-cytotoxic but do not promote cell migration at least in the case of neural cells.

10.9. Use of microstructures in guided cell growth

Spatial and topographical control over the microenvironment surrounding cells is essential in biomimetic cell culturing. Besides chemical cues, even subtle topographical cues can have a dramatic effect on cellular development of neurons via contact guidance. [64] The versatility and high resolution of 2PP makes it an excellent method for fabricating these guidance cues even in the third dimension.

Testing of different wall structures with varying heights and geometries would be overly complicated, time-consuming and expensive, if planar photolithographic methods were used, because several master molds would need to be fabricated first. With 2PP, one can quickly and easily vary design and fabrication parameters during polymerization. This enables the fabrication of arbitrary wall structures. It is important to notice that it is also possible to produce the same structures all over again, if for example parallel samples are needed.

Due to the attested non-cytotoxicity of PEGda and PCL-o with neuronal stem cells, two-photon polymerized microstructures fabricated from these materials exhibit a great potential to be used in contact guidance in neural cell culturing. As seen in the results of the cytoxicity tests, cell do not migrate on these materials. Especially if the substrate material is coated with cell-adhesive proteins, cells are likely to prefer migration on the

substrate rather than over the non-adhesive microwalls. Using this microwall approach, neural networks of high spatial order and low density could be cultured *in vitro*.

The obtained resolution in this study was in the order of one micrometer, which is an appropriate value for structures utilized in cell guidance applications. Furthermore, larger features up to a hundred microns in height could be fabricated using the same fabrication system. Therefore the current combination of biomaterials and microfabrication set-up seems highly suitable for the fabrication of microstructures for different cell-based applications.

11. CONCLUSIONS

Two-photon induced polymerization (2PP) is a photochemical phenomenon utilized in the microfabrication of photosensitive materials. In this experimental study, 2PP of two photocrosslinkable materials was compared in terms of resolution and processability. The studied materials were a diacrylated PEG-based photosensitive hydrogel (PEGda) and a novel methacrylated PCL-based photosensitive oligomer (PCL-o). For the latter, these were the first 2PP studies ever. A commercial UV photoinitiator, Irgacure® 127 was added to the prepolymer solutions to initiate the crosslinking reaction.

The polymerization tests were done using a custom-built Nd:YAG pulsed laser setup, which is an affordable and thus reasonable choice for basic material research. 2PP of PEGda using this type of a laser has not been previously reported in literature which also emphasizes the originality of the current study.

Two- and three-dimensional microstructures were polymerized on glass substrates as process parameters such as the laser pulse energy and scanning speed were varied. Characterization of the polymerized structures was performed with scanning electron microscope. In addition to polymerization studies, the applicability of the fabricated microstructures to applications of guided cell growth was evaluated by cytotoxicity testing, which was done by culturing human derived embryonic stem cells on UV-polymerized thin films of both PEGda and PCL-o.

In the polymerization experiments, 2PP of both PEGda and PCL-o was successfully demonstrated establishing the suitability of a Nd:YAG laser for the research and microfabrication of novel biomaterial microstructures. To determine resolution for the current fabrication set-up, voxel arrays were fabricated with an ascending scan method varying the laser pulse energy. Moreover, the effect of PI concentration on resolution was tested with both materials. Smallest voxels, with diameter of 1.0 μm and length of 5.7 μm, were achieved with PCL-o using the lowest photoinitiator concentration, 2 wt-%. Voxel size grew as the initiator concentration increased in both PEGda and PCL-o. As expected, increase in the voxel size as a function of the laser pulse energy exhibited non-linear behavior.

A significant difference was observed in optimal scanning speed when comparing the two materials. For PCL-o, suitable scanning speed (2–10 μm/s) was ten times slower than for PEGda (20–100 μm/s). This difference could be explained by the chemical structures of the photosensitive oligomers. However, faster scanning could be used for both PEGda and PCL-o in 3D object fabrication due to voxel overlapping between adjacent layers, which strengthened the polymerized structure.

The overall processability of PEGda and PCL-o was evaluated by taking account the whole fabrication process. Table 11.1 presents the different factors utilized for assessment and the corresponding ratings for both materials.

Table 11.1. *An overall comparison between PEGda and PCL-o in terms of different processability factors. The factors have been rated using the following system: (++) good, (+) satisfactory, (–) needs for improvement and (– –) unacceptable.*

Factor of processability	**PEGda**	**PCL-o**
Sample preparation	++	+
Resolution	+	++
Fabrication rate*	+	–
Non-cytotoxicity	+	+
Biocompatibility of the fabrication process	++	–
Suitability for 3D fabrication	+	++
Shelf life	+	+

** related to suitable scanning speed*

The major differences between PEGda and PCL-o originated from their different viscosity and solubility properties. The PEGda prepolymer solution is a water-soluble liquid with relatively low viscosity. The uncrosslinked, highly viscous PCL-o, on the other hand, only dissolves in organic solvents such as dichloromethane. Some problems occurred with PEGda during polymerization and sample development due to its mechanical and viscosity properties. However, the overall microfabrication process for PEGda was found more biocompatible because of the use of water as solvent. In terms of sample preparation and handling, neither of the materials proved superior.

On the whole, this study demonstrated the applicability of two photosensitive biomaterials for microfabrication by means of two-photon induced polymerization. Considering the lack of suitable biocompatible photoresist materials for biomedical applications of 2PP, the outcome of this study was a success, as a whole new photosensitive non-cytotoxic material, PCL-o, was successfully introduced to 2PP fabrication. Furthermore, the study was done with an affordable laser type, which established the fact that the use of an expensive femtosecond laser is not essential for innovative and scientifically relevant research.

12. SUGGESTIONS FOR FUTURE STUDIES

The positive results achieved in the experimental study presented in this thesis suggest that more research should be focused on to broaden the selection of suitable photopolymerizable biomaterials for 2PP applications. In the future, collaboration with the TKK Laboratory of Polymer Technology should be continued for this purpose. An important theme for research would be to understand the effect of chemical structure on polymerization properties in a 2PP system. Hence, 2PP with a few similar oligomers with a slightly different molecular structure should be studied. Besides testing the polymerization of individual oligomers, it would be interesting to fabricate blends and copolymers of the novel oligomers in order to adjust the polymerization characteristics and the mechanical properties of the resulting microstructures. Additionally, novel oligomers could be blended with commercial photosensitive materials such as PEGda.

In addition to material-related developments, some improvements are needed in the fabrication process as well, in order to make it more versatile and practical. First, a central theme in future studies should be the optimization of the photoinitiation system. The currently used PI, Irgacure® 127, does obviously not have ideal two-photon absorption properties. Moreover, the biocompatibility of the molecule has not been proven. Therefore photoinitiators with better absorption characteristics and biological properties should be explored and tested. If the current initiator will, however, be used in future as well, a more systematic study on suitable initiator concentration should be carried out with the novel PCL oligomer.

Secondly, in order to develop the resolution characteristics of the current fabrication set-up, an objective lens with larger numerical aperture should be used. In addition, the laser power handling system should be improved in order to gain reliable and accurate resolution data from a wider power range. In fact, after finishing the polymerization experiments included in this thesis, the fabrication equipment has been upgraded and better resolution can be expected in future studies. Third, when it comes to sample characterization, atomic force microscopy (AFM) should be employed in order to gain reliable, quantitative data on the surface topography of the polymerized microstructures. Furthermore, AFM could be used in the measurement of voxel dimensions as well.

To study and exploit the technology in practice, cell culturing on different microstructures of varying sizes and architectures should be experimented. For this purpose, one of the main goals for future studies would be to find an optimal sterilization method for the polymerized microstructures. A comparison between gamma-irradiation, ethylene oxide sterilization, cold plasma sterilization and disinfection with ethanol should be made to determine the least damaging method.

REFERENCES

1. Aguilar, C., Lu, Y., Mao, S. & Chen, S. *Direct micro-patterning of biodegradable polymers using ultraviolet and femtosecond lasers.* Biomaterials 26(2005)36, pp. 7642–7649.
2. Ahola, N., Veiranto, M., Efimov, A. & Kellomäki, M. 2009. *Hydrolytic degradation of poly(lactide-co-E-caprolactone) 70/30.* 22nd European Conference on Biomaterials, 7.–11.9.2009, Lausanne, Switzerland. 1 p.
3. Allen, R., Nielson, R., Wise, D. & Shear, J. *Catalytic Three-Dimensional Protein Architectures.* Analytical Chemistry 77(2005)16, pp. 5089–5095.
4. Andersson, H. & Berga, A. *Microfabrication and microfluidics for tissue engineering: state of the art and future opportunities.* Lab on a Chip 4(2004)2, pp. 98–103.
5. Anseth, K.S., Metters, A.T, Bryant, S.J., Martens, P.J., Elisseeff, J.H. & Bowman, C.N. *In situ forming degradable networks and their application in tissue engineering and drug delivery.* Journal of Controlled Release 78(2002)1-3, pp. 199–209.
6. Arcaute, K., Mann, B. & Wicker, R. *Stereolithography of Three-Dimensional Bioactive Poly(Ethylene Glycol) Constructs with Encapsulated Cells.* Annals of Biomedical Engineering 34(2006)9, p. 1429–1441.
7. Bąk, T. *Two Photon Microstereolithography of Polymers for Tissue Engineering.* Dissertation. Twente, the Netherlands, 2009. University of Twente, Institute for Biomedical Technology and Technical Medicine, Faculty of Science and Technology. 168 p.
8. Baroli, B. *Photopolymerization of biomaterials: issues and potentialities in drug delivery, tissue engineering, and cell encapsulation applications.* Journal of Chemical Technology and Biotechnology 81(2006)4, pp. 491–499.
9. Bártolo, P. & Bidanda, B. *Bio-materials and prototyping applications in medicine.* 2008, Springer Science + Business Media, LLC. 216 p.
10. Basu, S., Cunningham, L.P., Pins, G.D., Bush, K.A., Taboada, R., Howell, A.R., Wang, J. & Campagnola, P.J. *Multiphoton Excited Fabrication of Collagen Matrixes Cross-Linked by a Modified Benzophenone Dimer: Bioactivity and Enzymatic Degradation.* Biomacromolecules 6(2005)3, pp. 1465–1474.
11. Bettinger, C., Weinberg, E., Kulig, K., Vacanti, J., Wang, Y., Borenstein, J. & Langer, R. *Three-Dimensional Microfluidic Tissue-Engineering Scaffolds Using a Flexible Biodegradable Polymer.* Advanced Materials 18(2005)2, pp. 165–169.
12. Borenstein, J. *Tissue Engineering.* In: Gianchandani, Y., Tabata, O. & Zappe, H., editors. Comprehensive Microsystems. Volume 2, chapter 2.15. 2007, Elsevier. 2100 p.
13. Branch, D., Corey, J., Weyhenmeyer, J., Brewer, G., & Wheeler, C. *Microstamp patterns of biomolecules for high-resolution neuronal networks.* Medical and Biological Engineering and Computing 36(1998)1, pp. 135–141.

14. Burdick, J., Khademhosseini, A. & Langer, R. *Fabrication of Gradient Hydrogels Using a Microfluidics/Photopolymerization Process.* Langmuir 20(2004)13, pp. 5153–5156.

15. Cabodi, M., Choi, N., Gleghorn, J. & Lee, C. *A Microfluidic Biomaterial.* Journal of American Chemical Society 127(2005)40, pp. 13788–13789.

16. Chan-Park, M., Yan, Y., Neo, W., Zhou, W., Zhang, J. & Yue, C. *Fabrication of High Aspect Ratio Poly(ethyleneglycol)-Containing Microstructures by UV Embossing.* Langmuir 19(2003)10, pp. 4371–4380.

17. Chan-Park, M.B. & Neo, W. K. *Ultraviolet embossing for patterning high aspect ratio polymeric microstructures.* Microsystem Technologies 9 (2003)6-7, pp. 501–506.

18. Chaterji, S., Kwon, I. & Park, K. *Smart polymeric gels: Redefining the limits of biomedical devices.* Progress in Polymer Science 32(2007)8–9, pp.1083–1122.

19. Chen, S., Kancharla, V. & Lu, Y. *Laser-based microscale patterning of biodegradable polymers for biomedical applications.* International Journal of Materials and Product Technology 18(2003)4/5/6, pp. 457–468.

20. Chen, Y., Ferracane, J. & Prahl, S. *Quantum yield of conversion of the photoinitiator camphorquinone.* Dental Materials 23(2007)6, pp. 655–664.

21. Choi, N.W., Cabodi, M., Held, B., Gleghorn, J.P., Bonassar, L.J. & Stroock, A.D. *Microfluidic scaffolds for tissue engineering.* Nature Materials 6(2007)11, pp. 908–915.

22. *Ciba® IRGACURE 127.* [WWW] Ciba Specialty Chemicals. [Cited: 7.8.2009] Available: http://www.ciba.com/irgacure_127-2.htm.

23. Cimetta, E., Figallo, E., Cannizzaro, C. & Elvassore, N. *Micro-bioreactor arrays for controlling cellular environments: Design principles for human embryonic stem cell applications.* Methods 47(2009)2, pp. 81–89.

24. Claeyssens, F., Hasan, E., Gaidukeviciute, A., Demetra, A., Ranella, A., Reinhardt, C., Ovsianikov, A., Shizhou, X., Fotakis, C., Vamvakaki, M., Chichkov, B., Farsari, M. *Three-Dimensional Biodegradable Structures Fabricated by Two-Photon Polymerization.* Langmuir 25(2009)5, pp. 3219–3223.

25. Corey, J. & Feldman, E. *Substrate patterning: an emerging technology for the study of neuronal behavior.* Experimental Neurology 184(2003)S1, pp. 89–96.

26. Corey, J., Wheeler, B. & Brewer, G. *Compliance of hippocampal neurons to patterned substrate networks.* Journal of Neuroscience Research 30(1991)2, pp. 300–307.

27. Cunningham, L.P., Veilleux, MP. & Campagnola, PJ. *Freeform multiphoton excited microfabrication for biological applications using a rapid prototyping CAD-based approach.* Optics Express 14(2006)19, pp. 8613–8621.

28. Davidson, R.S. *Radiation Curing.* 2001, iSmithers Rapra Publishing. 132 p.

29. Davis, K., Burdick, J. & Anseth, K. *Photoinitiated crosslinked degradable copolymer networks for tissue engineering applications.* Biomaterials 24(2003)14, pp. 2485–2495.

30. Decker, C. *Photoinitiated Crosslinking Polymerization.* Progress in Polymer Science 21(1996)4, pp. 593–650.

31. Delamarche, E., Schmid, H., Michel, B. & Biebuyck, H. *Stability of molded polydimethylsiloxane microstructures.* Advanced Materials 9(1997)9, pp. 741–746.

32. Dertinger, S., Jiang, X., Li, Z., Murthy, V. & Whitesides, G. *Gradients of substrate-bound laminin orient axonal specification of neurons.* Proceedings in the National Academy of Science of the United States of America 99(2002)20, pp. 12542–12547.

33. Diakoumakos, C., Douvas, A., Raptis, I., Kakabakos, S., Dimotikalli, D., Terzoudi, G. & Argitis, P. *Dilute aqueous base developable resists for environmentally friendly and biocompatible processes.* Microelectronic Engineering 61–62(2002), pp. 819–827.

34. Dietlin, C., Lalevee, J., Allonas, X., Fouassier, J.P, Visconti, M., Bassi, G. & Norcini, G. *Reactivity and Effciency of Difunctional Radical Photoinitiators.* Journal of Applied Polymer Science 107(2008)1, pp. 246–252.

35. Doraiswamy, A., Jin, C., Narayan, R.J., Mageswaran, P., Mente, P., Modi, R., Auyeung, R., Chrisey, D.B., Ovsianikov, A. & Chichkov, B. *Two photon induced polymerization of organic–inorganic hybrid biomaterials for microstructured medical devices.* Acta Biomaterialia 2(2006)3, pp. 267–275.

36. Douvas, A., Argitis, P., Misiakos, K., Dimotikali, D., Petrou, P. &Kakabakos, S. *Biocompatible photolithographic process for the patterning of biomolecules.* Biosensors & Bioelectronics 17(2002)4, pp. 269–278.

37. Eddington, D. & Beebe, D. *Flow control with hydrogels.* Advanced Drug Delivery Reviews 56(2004)2, pp. 199–210.

38. El-Ali, J., Sorger, P. & Jensen, K. *Cells on chips.* Nature 442(2006)7101, pp. 403–411.

39. Elisseeff, J., McIntosh, W., Fu, K., Blunk, T. & Langer, R. *Controlled-release of IGF-I and TGF-1 in a photopolymerizing hydrogel for cartilage tissue engineering.* Journal of Orthopaedic Research 19(2001)6, pp. 1098–1104.

40. Erickson, D. & Li, D. *Integrated microfluidic devices.* Analytica Chimica Acta 507(2004)1, pp. 11–26.

41. Fedorovich, N., Oudshoorn, M., Geemen, D. & Hennink, W. *The effect of photopolymerization on stem cells embedded in hydrogels.* Biomaterials 30(2009)3, pp. 344–353.

42. Fidkowski, C., Kaazempur-Mofrad, M., Borenstein, J., Vacanti, J., Langer, R. & Wang, Y. *Endothelialized Microvasculature Based on a Biodegradable Elastomer.* Tissue Engineering 11(2005)1-2, pp. 302–309.

43. Fried, J. L. *Polymer Science and Technology.* Second edition. New Jersey, USA 2003, Prentice Hall. 582 p.

44. *GIMP - The GNU Image Manipulation Program* [WWW]. The GIMP Team. [Cited 15.2.2010]. Available: http://www.gimp.org/.

45. Gomez-Sjöberg, R., Leyrat, A., Pirone, D., Chen, C. & Quake, S. *Versatile, Fully Automated, Microfluidic Cell Culture System.* Analytical Chemistry 79(2007), pp. 8557–8563.

46. Gonsalves, K., Halberstadt, G., Laurencin, C. & Lakshmi, N. *Biomedical Nanostructures. Part 1: Nanostructure Fabrication.* 2008, John Wiley & Sons. 525 p.

47. Grijpma, D.W., Hou, Q. & Feijen, J. *Preparation of biodegradable networks by photo-crosslinking lactide, ε-caprolactone and trimethylene carbonate-based oligomers functionalized with fumaric acid monoethyl ester.* Biomaterials 26)2005)16, pp. 2795–2802.

48. Haas, K-H. & Wolter, H. *Synthesis, properties and applications of inorganic–organic copolymers (ORMOCER®s).* Current Opinion in Solid State and Materials Science 4(1999)6, pp. 571–580.

49. Haeberle, S. & Zengerle, R. *Microfluidic for Lab-on-a-Chip.* In: Gianchandani, Y., Tabata, O. & Zappe, H., editors. Comprehensive Microsystems. Volume 2, chapter 2.13. 2007, Elsevier. 2100 p.

50. Hahn, M., Miller, J. & West, J. *Three-Dimensional Biochemical and Biomechanical Patterning of Hydrogels for Guiding Cell Behavior.* Advanced Materials 18(2006)20, pp. 2679–2684.

51. He, D., Susanto, H. & Ulbricht, M. *Photo-irradiation for preparation, modification and stimulation of polymeric membranes.* Progress in Polymer Science 34(2009)1, pp. 62–98.

52. He, W., Halberstadt, C. & Gonsalves, K. *Lithography application of a novel photoresist for patterning of cells.* Biomaterials 25(2004)11, pp. 2055–2063.

53. Helminen, A., Korhonen, H. & Seppälä, J. *Cross-Linked Poly(ε-caprolactone/D,L-lactide) Copolymers with Elastic Properties.* Macromolecular Chemistry and Physics 203(2003)18, pp. 2630–2639.

54. Helminen, A., Korhonen, H. & Seppälä, S. *Structure modification and crosslinking of methacrylated polylactide oligomers.* Journal of Applied Polymer Science 86(2002)14, pp. 3616–3624.

55. Hutchison, J., Haraldsson, K., Good, B., Sebra, R., Luo, N., Anseth, K. & Bowman, C. *Robust polymer microfluidic device fabrication via contact liquid photolithographic polymerization (CLiPP).* Lab on a chip 4(2004)6, pp. 658–662.

56. Huttunen, A., Ellä, V. & Hackspik, M. *Laser micromachining of biomaterials.* LCC Finland Newsletter December, 2006. p. 4.

57. Huttunen, A., Laakso, P., Ellä, V., Heikkilä, R. & Kellomäki, M. *Picosecond laser micromachining of biomedical materials.* 3rd Marie Curie Cutting-Edge conference in Funchal, Madeira, Portugal, 4.–8.6.2007. 1 p.

58. Huttunen, A., Laakso, P., O´Connell, C., Williams, G., Huttunen, M., Niiranen, H., Ellä, V., Kellomäki, M. & Sherlock, R. *Nano-, pico- and femtosecond laser machining of biomedical composites.* Proceedings of the 5th Tampere Tissue Engineering Symposium.

59. Jang, S., Goddard, W. & Kalani, M.Y. *Mechanical and Transport Properties of the Poly(ethylene oxide)-Poly(acrylic acid) Double Network Hydrogel from Molecular Dynamic Simulations.* Journal of Physical Chemistry B 111(2007)7, pp. 1729–1737.

60. Jariwala, S., Tan, B. & Venkatakrishnan, K. *Micro-fluidic channel fabrication via two-photon absorption (TPA) polymerization assisted ablation.* Journal of Micromechanics and Microengineering 19(2009)11, p. 115023.

61. Jockusch, S., Landis, M., Freiermuth, B. & Turro, N. *Photochemistry and Photophysics of R-Hydroxy Ketones.* Macromolecules 34(2001)6, pp. 1619–1626.

62. Jon, S., Seong, J., Khademhosseini, A., Tran, T-N., Laibinis, P.E. & Langer, R. *Construction of Nonbiofouling Surfaces by Polymeric Self-Assembled Monolayers.* Langmuir 19(2003)24, pp. 9989–9993.

63. Kaehr, B. & Shear, J. *Multiphoton fabrication of chemically responsive protein hydrogels for microactuation.* Proceedings in the National Academy of Sciences of United States of America 105(2008)26, pp. 8850–8854.

64. Kaehr, B., Allen, R., Javier, D., Currie, J. & Shear, J. *Guiding neuronal development with in situ microfabrication.* Proceedings of the National Academy of Sciences of the United Stated of America 101(2004)46, pp. 16104–16108.

65. Kaehr, B., Ertas, n., Nielson, R., Allen, R., Hill, R.T., Plenert, M. & Shear, J. *Direct-Write Fabrication of Functional Protein Matrixes Using a Low-Cost Q-Switched Laser.* Analytical chemistry 78(2006)9, pp. 3198–3202.

66. Kane, B.J., Zinner, M.J., Yarmush, M.L. & Toner, M. *Liver-specific functional studies in a microfluidic array of primary mammalian hepatocytes.* Analytical Chemistry 78(2006)13, pp. 4291–4298.

67. Khademhosseini, A. & Langer, R. *Microengineered hydrogels for tissue engineering.* Biomaterials 28(2007)34, pp. 5087–5092.

68. Khademhosseini, A., Suh, K., Jon, S., Eng, G., Yeh, J., Chen, G-J. & Langer, R. A *Soft Lithographic Approach To Fabricate Patterned Microfluidic Channels.* Analytical Chemistry 76(2004)13, pp. 3675–3681.

69. King, K., Wang, C., Kaazempur-Mofrad, M., Vacanti, J. & Borenstein, J. *Biodegradable Microfluidics.* Advanced Materials 16(2004)22, pp. 2007–2012.

70. Kizilel, S., Pérez-Luna, V.H. & Teymour, F. *Photopolymerization of poly(ethylene glycol) diacrylate on eosin-functionalized surfaces.* Langmuir 20(2004)20, pp. 8652–8658.

71. Krsko, P. & Libera, M. *Biointeractive Hydrogels.* Materials Today 8(2005)12, pp. 36–44.

72. Kuhn, W. & Hargitay, B. *Reversible Dilation and Contraction by Changing the State of Ionization of High-Polymer Acid Networks.* Nature 165(1950)4196, pp. 514–516.

73. LaFratta, C., Fourkas, J., Baldacchini, T. & Farrer, R. *Multiphoton Fabrication.* Angewandte Chemie International Edition 46(2007)33, pp. 6238–6258.

74. *Laser (instrument).* [WWW] Encyclopædia Britannica Online. [Cited: 28.7.2009] Available: http://www.britannica.com/EBchecked/topic/330874/laser.

75. Lee, K., Yang, D., Park, S. H. & Kim, R. H. *Recent developments in the use of two-photon polymerization in precise 2D and 3D microfabrications.* Polymers for Advanced Technologies 17(2006)2, pp. 72–82.

76. Lee, K-W., Kim, R.H., Yang, D-Y. & Park, S.H. *Advances in 3D nano/microfabrication using two-photon initiated polymerization.* Progress in Polymer Science 33(2008)6, pp. 631–681.

77. Lee, L.J. *Nanoscale Polymer Fabrication for Biomedical Applications.* In: Ferrari, M., Lee, A. & Lee, L.J. BioMEMS and Biomedical Nanotechnology. Volume 1. 2006, Springer US. pp. 51–96.

78. Lee, S., Eddington, D., Kim, Y., Kim, W., Beebe, D. *Control Mechanism of an Organic Self-Regulating Microfluidic System.* Journal of Microelectromechanical Systems 12(2003)6, pp. 848–854.

79. Lee, S.J. & Lee, S.Y. *Micro total analysis system (μ-TAS) in biotechnology.* Applied Microbiology and Biotechnology 64(2004)3, pp. 289–299.

80. Li, N., Tourovskaia, A. & Folch, A. *Biology on a Chip: Microfabrication for Studying the Behavior of Cultured Cells.* Critical Reviews™ in Biomedical Engineering, 31(2003)5-6, pp. 423–488.

81. Li, P. *Fundamentals of Microfluidics and Lab on a Chip for Biological Analysis and Discovery.* 2010, CRC Press. 352 p.

82. Li, P. *Microfluidic Lab-on-a-Chip for Chemical and Biological Analysis and Discovery*. 2005, CRC Press. 528 p.

83. Li, Q., Williams, C., Sun, D., Wang, J., Leong, K. & Elisseeff, J. *Photocrosslinkable polysaccharides based on chondroitin sulfate.* Journal of Biomedical Materials Research Part A 68A(2003)1, pp. 28–33.

84. Liu, V. & Bhatia, S. *Three-Dimensional Photopatterning of Hydrogels Containing Living Cells.* Biomedical Microdevices 4(2002)4, pp. 257–266.

85. Liu, Y., Pyrak-Nolte, L.J & Nolte, D.D. *Large-Scale 3D Microporous Structures by Two-photon Laser Machining.* Conference on Lasers and Electro-Optics/Quantum Electronics and Laser Science Conference and Photonic Applications Systems Technologies, San Jose, California 4.5.2008. 2008, Optical Society of America. Paper CTuG7.

86. Liu, Y., Pyrak-Nolte, L.J & Nolte, D.D. *Toward 3D Microfluidic Structures Fabricated with Two-photon Laser Machining.* Photonic Applications Systems Technologies Conference (PhAST), Baltimore, Maryland, 8.5.2007. 2007, Optical Society of America. Paper JThD98.

87. Lorenz, H., Despont, M., Fahrni, N., LaBianca, N., Renaud, P. & Vettiger, P. *SU-8: a low-cost negative resist for MEMS.* Journal of Micromechanical Microengineering 7(1997)3, pp. 121–124.

88. Lu, Y. & Chen, S.C. *Micro and nano-fabrication of biodegradable polymers for drug delivery.* Advanced Drug Delivery Reviews 56(2004)11, pp. 1621– 1633.

89. Luo, Y. & Shoichet, M. *A photolabile hydrogel for guided three-dimensional cell growth and migration*. Nature Materials 3(2004)4, pp. 249–253.

90. Mahoney, M. & Anseth, K. *Three-dimensional growth and function of neural tissue in degradable polyethylene glycol hydrogels.* Biomaterials 27(2006)10, pp. 2265–2274.

91. Malek, C. *Laser processing for bio-microfluidics applications (part I).* Analytical and Bioanalytical Chemistry 385(2006)8, pp. 1351–1361.

92. Maruo, S., Nakamura, O. & Kawata, S. *Three-dimensional microfabrication with two-photon-absorbed photopolymerization.* Optics Letters 22(1997)2, pp. 132–134.

93. Matsuda, T. & Mizutani, M. *Molecular design of photocurable liquid biodegradable copolymers. 2. Synthesis of coumarin-derivatized oligo(methacrylate)s and photocuring.* Macromolecules 33(2000)3, pp.791–794.

94. Matsuda, T., Mizutani, M. & Arnold, S.C. *Molecular Design of Photocurable Liquid Biodegradable Copolymers. 1. Synthesis and Photocuring Characteristics.* Macromolecules 33(2000)3, pp. 795–800.

95. McDonald, J., Duffy, D., Anderson, J., Chiu, D., Wu, H., Schueller, O. & Whitesides, G. *Fabrication of microfluidic systems in poly(dimethylsiloxane).* Electrophoresis 21(1999)1, pp. 27–40.

96. Melchels, F., Feijen, J. & Grijpma, D.W. *A poly(d,l-lactide) resin for the preparation of tissue engineering scaffolds by stereolithography.* Biomaterials 30(2009)23-24, pp. 3801–3809.

97. Metz, S., Holzer, R. & Renaud, P. *Polyimide-based microfluidic devices.* Lab on a Chip 1(2001)1, pp. 29–34.

98. Mills, C.A., Martinez, E., Bessuielle, F., Villanueva, G., Bausells, J., Samitier, J. & Errachid, A. *Production of structures for microfluidics using p olymer imprint techniques.* Microelectronic Engineering 78–79(2005), pp. 695–700.

99. Mills, C.A., Martínez, E., Errachid, A., Gomila, G., Samsó, A. & Samitier, J. *Small scale structures: the fabrication of polymeric nanostructures for biomedical applications using pattern replication techniques.* Contributions to Science3(2005)1, pp. 47–56.

100. Mizutani, M. & Matsuda, T. *Photocurable liquid biodegradable copolymers: in vitro hydrolytic degradation behaviors of photocured films of coumarin-end-capped poly(e-caprolactone-co-trimethylene*. Biomacromolecules 3(2002)2, pp. 249–255.

101. Mizutani, M., Arnold, S.C. & Matsuda, T. *Liquid phenylazide-endcapped copolymers of e-caprolactone and trimethylene carbonate: preparation, photocuring characteristics and surface layering.* Biomacromolecules 3(2002)4, pp. 668–675.

102. Musoke-Zawedde, P. & Shoichet, M.S. *Anisotropic three-dimensional peptide channels guide neurite outgrowth within a biodegradable hydrogel matrix.* Biomedical Materials 1(2006)3, pp. 162–169.

103. Naka, Y., Eda, A., Takei, H. & Shimizu, N. *Neurite outgrowths of neurons on patterned self-assembled monolayers.* Journal of Bioscience and Bioengineering 94(2002)5, pp. 434–439.

104. Namba, R., Cole, A., Bjugstad, K. & Mahoney, M. *Development of porous PEG hydrogels that enable efficient, uniform cell-seeding and permit early neural process extension.* Acta Biomateria 5(2009)6, pp. 61884–1897.

105. Newman, J., Zengerle, R., Ernst, H., Messner, S., Andrieux, G., Provence, M. *FlowMap: Microfluidics Roadmap for the Life Sciences.* 2004, Books on Demand. 200 p.

106. Nguyen, K. & West, J. *Photopolymerizable hydrogels for tissue engineering applications.* Biomaterials 23(2002)22, pp. 4307–4314.

107. Nikkola, L., Viitanen, P. & Ashammakhi, N. *Temporal control of drug release from biodegradable polymer: Multicomponent diclofenac sodium releasing PLGA 80/20 rod.* Journal of Biomedical Materials Research, Part B, Applied Biomaterials 89B(2009)2, pp. 518–526.

108. *Ormocomp — UV Curable Hybrid Polymer for Moulding.* [WWW] Germany, Micro Resist Technology GmbH. [Cited: 5.1.2010] Available: http://www.microresist.de/products/ormocers/pdf/pi_ormocomp_en_07062201_ls_neu.pdf.

109. Ostendorf, A. & Chichkov, B. *Two-photon polymerization: a new approach to micromachining.* Photonics Spectra 40(2006)10, pp. 72–80.

110. Ovsianikov, A. & Chichkov, B. *Two-Photon Polymerization – High Resolution 3D Laser Technology and Its Applications.* In: Korkin, A. & Rosei, F. Nanoelectronics and Photonics. Part 2. 2008, Springer New York. 477 p.

111. Ovsianikov, A., Chichkov, B., Adunkab, O., Pillsbury, H., Doraiswamy, A. & Narayan, R.J. *Rapid prototyping of ossicular replacement prostheses.* Applied Surface Science 253(2007)15, pp. 6603–6607.

112. Ovsianikov, A., Doraiswamy, A., Narayan, R. & Chichkov, B. *Study of Polymeric Microneedle Arrays for Drug Delivery.* Material Research Society Symposium Proceedings 950(2007). 0950-D14-05.

113. Ovsianikov, A., Ostendorf, A. & Chichkov B. *Three-dimensional photofabrication with femtosecond lasers for applications in photonics and biomedicine.* Applied Surface Science 253(2007)15, pp. 6599–6602.

114. Ovsianikov, A., Passinger, S., Houbertz, S. & Chichkov, B. *Three dimensional material processing with femtosecond lasers.* In: Laser Ablation and its Applications. 2007, Springer. pp. 123-159.

115. Ovsianikov, A., Schlie, S., Ngezahayo, A., Haverich, A. & Chichkov, B. *Two-photon polymerization technique for microfabrication of CAD-designed 3D scaffolds from commercially available photosensitive materials.* Journal of Tissue Engineering and Regenerative Medicine 1(2007)6, pp. 443–449.

116. Paakinaho, K., Ellä, V., Syrjälä, S. & Kellomäki, M. 2009. *Melt spinning of poly(L/D)lactide 96/4: Effects of molecular weight and melt processing on hydrolytic degradation.* Polymer Degradation and Stability 94 3, pp. 438–442.

117. Paguirigan, A. & Beebe, J.D. *Gelatin based microfluidic devices for cell culture.* Lab on a Chip 6(2006)3, pp. 407–413.

118. Park, Y., Tirelli, N. & Hubbell, J. *Photopolymerized hyaluronic acid-based hydrogels and interpenetrating networks.* Biomaterials Volume 24(2003)6, pp. 893–900.

119. Pat. WO 097533. *Photoresists processable under biocompatible conditions for multi-biomolecule patterning.* Demokritos National Center for Scientific research, Greece. (Argitis, P., Misiakos, K., Kakabakos, S., Douvas, A. & Diakoumakos, C.). App. no. PCT/GR2002/000033, 30.05.2002. (5.12.2002).

120. Peltola, S., Kellomäki, M. & Viitanen, J. 2008. *Two-photon polymerization of protein patterns with nd:yag pulsed laser.* Icaleo, 27th International Congress on Applications of Lasers & Electro-Optics, 20.–23.10.2008, Temecula, CA, USA pp. 93–98.

121. Peppas, N., Hilt, Z., Khademhosseini, A. & Langer, R. *Hydrogels in Biology and Medicine: From Molecular Principles to Bionanotechnology.* Advanced Materials 18(2006)11, pp. 1345–1360.

122. Pihl, J., Sinclair, J., Karlsson, M. & Orwar, O. *Microfluidics for Cell-based Assays.* MaterialsToday 8(2005)12, pp. 46–51.

123. Pitts, J., Campagnola, P., Epling, G. & Goodman, S. *Submicron Multiphoton Free-Form Fabrication of Proteins and Polymers: Studies of Reaction Efficiencies and Applications in Sustained Release.* Macromolecules 33(2000)5, pp. 1514–1523.

124. Pitts, j., Howell, A., Taboada, R., Banerjee, I., Wang, J., Goodman, S. & Campagnola, P. *New Photoactivators for Multiphoton Excited Three-dimensional Submicron Cross-linking of Proteins: Bovine Serum Albumin and Type 1 Collagen.* Photochemistry and Photobiology 76(2002)2, pp. 135–144.

125. Powers, M, Janigian, D., Wack, K., Baker, C., Stolz, D. & Griffith, L. *Functional Behavior of Primary Rat Liver Cells in a Three-Dimensional Perfused Microarray Bioreactor.* Tissue Engineering 8(2002)3, pp. 499–513.

126. Ravenscroft, M., Bateman, K., Shaffer, K,. Schessler, H., Jung, D., Schneider, T., Montgomery, C., Custer, T., Schaffner, A., Liu, Q., Li, Y., Barker, J. & Hickman, J. *Developmental Neurobiology Implications from Fabrication and Analysis of Hippocampal Neuronal Networks on Patterned Silane-Modified Surfaces.* Journal of American Chenmical Society 120(1998)47, pp. 12169–12177.

127. Rich, J., Korhonen, H., Hakala, R., Korventausta, J., Elomaa, L. & Seppälä, J. *Porous biodegradable scaffold: predetermined porosity by dissolution of poly(ester-anhydride) fibers from polyester matrix.* Macromolecular Bioscience 9(2009)7, pp. 654–660.

128. Sarig-Nadir, O., Livnat, O., Zajdman, R., Shoham, S. & Seliktar, D. *Laser Photoablation of Guidance Microchannels into Hydrogels Directs Cell Growth in Three Dimensions.* Biophysical Journal 96(2009)11, pp. 4743–4752.

129. Sawhney, A., Pathak, C & Hubbell, J. *Bioerodible hydrogels based on photopolymerized poly(ethylene glycol)-co-poly(α-hydroxy acid) diacrylate macromers.* Macromolecules 26(1993)4, pp. 581–587.

130. Schlie, S., Ngezahayo, A., Ovsianikov, A., Fabian, T., Kolb, H.A., Haferkamp, H., Chichkov B.N. *Three-dimensional cell growth on structures fabricated from ORMOCER by two-photon polymerization technique.* Journal of Biomaterials Applications 22(2007)3, pp. 275–287.

131. Schmedlen, R, Masters, K. & West, J. *Photocrosslinkable polyvinyl alcohol hydrogels that can be modified with cell adhesion peptides for use in tissue engineering.* Biomaterials 23(2002)22, pp. 4325–4332.

132. Sebra, R., Anseth, K. & Bowman, C. *Integrated Surface Modification of Fully Polymeric Microfluidic Devices Using Living Radical Photopolymerization Chemistry.* Journal of Polymer Science: Part A: Polymer Chemistry 44(2006)4, pp. 1404–1413.

133. Seidlits, S., Schmidt, C. & Shear, J. *High-Resolution Patterning of Hydrogels in Three Dimensions using Direct-Write Photofabrication for Cell Guidance.* Advanced Functional Materials 19(2009)22, pp. 3543–3551.

134. Selvaganapathy, P.R. *Polymers.* In: Gianchandani, Y., Tabata, O. & Zappe, H., editors. Comprehensive Microsystems. Volume 1, chapter 1.04. 2007, Elsevier, 2100 p.

135. Serbin, J., Egbert, A., Ostendorf, A. & Chichkov, B. *Femtosecond laser-induced two-photon polymerization of inorganic–organic hybrid materials for applications in photonics.* Optics Letters 28(2003)5, pp. 301–303.

136. Sia, S. & Whitesides, G. *Microfluidic devices fabricated in poly(dimethylsiloxane) for biological studies.* Electrophoresis 24(2003)21, pp. 3563–3576.

137. Simms, H., Bowman, C. & Anseth, K. *Using living radical polymerization to enable facile incorporation of materials in microfluidic cell culture devices.* Biomaterials 29(2008)14, pp. 2228–2236.

138. Situma, C., Hashimoto, M. & Soper, S. *Merging microfluidics with microarray-based bioassays.* Biomolecular Engineering 23(2006)5, pp. 213–231.

139. Sorribas, H., Padeste, C. & Tiefenauer, L. *Photolithographic generation of protein micropatterns for neuron culture applications.* Biomaterials 23(2002)3, pp. 893–900.

140. Stenger, D., Pike, C., Hickman, J. & Cotman, C. *Surface determinants of neuronal survival and growth on self-assembled monolayers in culture.* Brain Research 630(1993)1-2, pp. 136–147.

141. Stenger, D.,Hickman, J., Bateman, K., Ravenscroft, M., Ma, W., Pancrazio, J., Shaffer, K., Schaffner, A., Cribbs, D. & Cotman, C. *Microlithographic determination of axonal/dendritic polarity in cultured hippocampal neurons*. Journal of Neuroscience Methods 82(1998)2, pp. 167–173.

142. Stratakis, E., Ranella, A., Farsari, M. & Fotakis, C. *Laser-based micro/nano-engineering for biological applications.* Progress in Quantum Electronics 33(2009)5, pp. 127–163.

143. Stroock, A. & Cabodi, M. *Microfluidic Biomaterials.* MRS Bulletin 31(2006)2, pp. 114–119.

144. Suggs, L. Kao, E., Palombo, L., Krishnan, R., Widmer, M. Mikos, A. *Preparation and characterization of poly(propylene fumarate-co-ethylene glycol) hydrogels.* Journal of Biomaterial Science, Polymer Edition 9(1998)7, pp. 653–66.

145. Suggs, L., Krishnan, R,. Garcia, C. Peter, S., Anderson, J. & Mikos, A. *In vitro and in vivo degradation of poly(propylene fumarate-co-ethylene glycol) hydrogels.* Journal of Biomedical Materials Research 42A(1998)2, pp. 312–320.

146. Sun, H., Takada, K., Kim, M., Lee, K. & Kawata, S. *Scaling laws of voxels in two-photon photopolymerization nanofabrication.* Applied Physics Letters 83(2003)6, id. 1104.

147. Sun, H-B. & Kawata, S. *Two-Photon Laser Precision Microfabrication and Its Applications to Micro–Nano Devices and Systems.* Journal of Lightwave Technology 21(2003)3, pp. 624–633.

148. Terry, S.C., Jerman, J.H. & Angell, J.B. *A gas chromatographic air analyzer fabricated on a silicon wafer.* IEEE Transactions on Electron Devices 26(1979)12, pp. 1880–1886.

149. Tibbitt, M. & Anseth, K. *Hydrogels as extracellular matrix mimics for 3D cell culture.* Biotechnology and Bioengineering 103(2009)4, pp. 655–663. .

150. Weibel, D. & Whitesides, G. *Applications of microfluidics in chemical biology.* Current Opinion in Chemical Biology 10(2006)6, pp. 584–591.

151. Weiss, T., Hildebrand, G., Schade, R. & Liefeith, K. *Two-Photon polymerization for microfabrication of three-dimensional scaffolds for tissue engineering application.* Engineering in Life Sciences 9(2009)5, pp. 384–390.

152. Velve-Casquillas, G., Le Berrea, M., Piel, M. & Tran, P.T. *Microfluidic tools for cell biological research.* Nano Today 5(2010)1, pp. 28–47.

153. Venkatakrishnan, K., Jariwala, S. & Tan, B. *Maskless fabrication of nano-fluidic channels by two-photon absorption (TPA) polymerization of SU-8 on glass substrate.* Optics Express 17(2009)4, pp. 2756–2762.

154. Whitesides, G. & Xia, Y. *Soft Lithography.* Annual Review of Materials Science 28(1998), pp. 153–184.

155. Whitesides, George M. *The origins and the future of microfluidics.* Nature 442(2006)27, pp. 368–373.

156. Williams, C.G., Malika, A.N., Kima, T.K., Manson, P.N. & Elisseeff, J.H. *Variable cytocompatibility of six cell lines with photoinitiators used for polymerizing hydrogels and cell encapsulation.* Biomaterials 26(2005)11, pp. 1211–1218.

157. Vogt, A., Wrobel, G., Meyer, W., Knoll, W. & Offenhäusser, A. *Synaptic plasticity in micropatterned neuronal networks.* Biomaterials 26(2005)15, pp. 2549–2557.

158. Wosnick, J. & Shoichet, M. *Three-dimensional Chemical Patterning of Transparent Hydrogels.* Chemistry of Materials 20(2008)1, pp. 55–60.

159. Wu, S., Serbin, J. & Gu, M. *Two-photon polymerisation for three-dimensional micro-fabrication. Journal* of Photochemistry and Photobiology A: Chemistry 181(2006)1, pp. 1–11.

160. Wu, Y, Joseph, S. & Aluru, R.N. *Effect of Cross-Linking on the Diffusion of Water, Ions, and Small Molecules in Hydrogels.* Journal of Physical Chemistry B 113(2009)11, pp. 3512–3520.

161. Wylie, R. & Shoichet, M. *Two-photon micropatterning of amines within an agarose hydrogel.* Journal of Materials Chemistry 18(2008)23, pp. 2716–2721.

162. Yi, C., Li, C-W., Ji, S. & Yang, M. *Microfluidics technology for manipulation and analysis of biological cells.* Analytica Chimica Acta 560(2006)1–2, pp. 1–23.

163. Yu, L.M.Y., Leipzig, N.D. & Shoichet, M.S. *Promoting neuron adhesion and growth.* Materials Today 11(2008)5, pp. 36–43.

164. Zhang, X. & Haswell, S.J. *Materials Matter in Microfluidic Devices.* MRS Bulletin 31(2006)2, pp. 95–99.

165. Ziaie, B. *Hard and soft micromachining for BioMEMS: review of techniques and examples of applications in microfluidics and drug delivery.* Advanced Drug Delivery Reviews 56(2004)2, pp. 145–172.

APPENDIX 1: SILANIZATION OF THE MICROSCOPE GLASS SLIDES

The microscope glasses used in the polymerization experiments were prepared for use by treatment with a coupling agent. The chemical used was 3-(trimethoxysilyl)propyl methacrylate (or 3-methacryloxypropyltrimethoxysilane, MAPTMS) from Sigma-Aldrich (Steinheim, Germany). The silanization treatment was carried out using the following protocol.

Preparation

The following recipe is sufficient for treatment of 10 microscope glasses (75mm x 25mm). Note, that the ethanol-MAPTMS solution is preserved for one day. All procedures must be done in a fume hood.

Reagents

MAPTMS (Sigma-Aldrich)
Ethanol (Etax Aa)
Acetic acid 1:10 (10 ml H2O + 1 ml acetic acid)

Equipment

10 pcs. microscope glass slides and a suitable container
400 ml decanter
300 ml measuring glass
automatic pipette of 10–1000 µl and suitable tips
automatic pipette of 2–20 ml and suitable tips
watch
magnetic stirrer and a stirring rod
parafilm

1. Wash the glass slides carefully with Deconex detergent, rinse with deionized water and ethanol. Place the glass slides in the container and let ethanol evaporate for 15 minutes in a fume hood.
2. Pipette 1 ml of MAPTMS to the decanter, in which you have measured 200 ml of ethanol (Etax Aa). Cover the decanter with parafilm and mix the solution with the magnetic stirrer for a couple of minutes.

3. Make sure that all the ethanol has evaporated from the glass slides. Add 6 ml of the diluted 1:10 acetic acid to the ethanol-MAPTMS solution. Stir the solution for a couple of more minutes. Then pour the solution on the glass slides in the container. Let the solution to take effect for 3 minutes.
4. Pour the silanization solution out of the container. Rinse the glass slides with ethanol for a few times to minimize the amount of residual reagents. Let the slides dry in the fume hood.
5. When the glass slides have dried, store them in nitrogen atmosphere in a vacuum desiccator.